

Czech Technical University in Prague
Faculty of Electrical Engineering

Habilitation thesis

**Self-lubricating nanostructured coatings based on
transition metal dichalcogenides alloyed with carbon**

by

Tomáš Polcar

Contents

Preface	i-ii
1. Introduction and motivation	6
2. Transition metal dichalcogenides and their friction reducing material role	8
2.1 Fundamental properties of transition metal dichalcogenides	8
2.2 Superlubricity of sputtered TMD	9
2.3 TMD solid lubricant drawbacks	10
2.4 TMD doped with elements and compounds	11
2.5 TMD doped with non-metallic elements	12
3. New concept of coating microstructure based on TMD-C system	15
3.1 Approach	15
3.2 How to deposit the coatings with required microstructure?	16
3.3 Tribological performance	17
3.4 Evidence of the sliding mechanism	19
3.5 Industrial applications of new coating design	21
References	23
Annex: Collected papers	26
T. Kubart, T. Polcar , L. Kopecký, R. Novák and D. Nováková, Temperature dependence of tribological properties of MoS ₂ and MoSe ₂ coatings, <i>Surface and Coatings Technology</i> 193 (2005), Pages 230-233	A1
T. Polcar , A. Nossa, M. Evaristo and A. Cavaleiro, Nanocomposite coatings of C-based and TMD phases: a review, <i>Reviews on Advanced Materials Science</i> , 15 (2007) 118-126	A5
T. Polcar , M. Evaristo and A. Cavaleiro, Friction of self-lubricating W-S-C sputtered coatings sliding under increasing load, <i>Plasma Processes & Polymers</i> , 2007, 4, S541-S546	A12
T. Polcar , A. Nossa, M. Evaristo and A. Cavaleiro, Nanocomposite coatings of C-based and TMD phases: a review, <i>Reviews on Advanced Materials Science</i> , 15 (2007) 118-126	A16
T. Polcar , M. Evaristo and A. Cavaleiro, Friction of self-lubricating W-S-C sputtered coatings sliding under increasing load, <i>Plasma Processes & Polymers</i> , 2007, 4, S541-S546	A25
T. Polcar , M. Evaristo, M. Stueber, A. Cavaleiro, Synthesis and structural properties of Mo-Se-C sputtered coatings, <i>Surface and Coatings Technology</i> 202 (2008) 2418-2422	A31
C. Silviu Sandu, T. Polcar , A. Cavaleiro, TEM investigation of MoSeC films, <i>Microscopy and Microanalysis</i> 14 supp 3 (2008) 7-10	A36
T. Polcar , M. Evaristo, M. Stueber, A. Cavaleiro, Mechanical and tribological properties of sputtered Mo-Se-C coatings, <i>Wear</i> 266 (2009) 393-397	A40
T. Polcar , M. Evaristo, A. Cavaleiro, Comparative study of the tribological behaviour of self-lubricating W-S-C and Mo-Se-C sputtered coatings, <i>Wear</i> 266 (2009) 388-392	A45
M. Evaristo, T. Polcar , A. Cavaleiro, Synthesis and properties of W-Se-C coatings deposited by PVD in reactive and non-reactive processes, <i>Vacuum</i> 83 (2009) 1262-1265	A50
M. Evaristo, T. Polcar , A. Cavaleiro, Can W-Se-C coatings be competitive to W-S-C ones?, <i>Plasma Processes & Polymers</i> , 2009, 6, S92-S95	A54
T. Polcar , M. Evaristo and A. Cavaleiro, Self-lubricating W-S-C nanocomposite coatings, <i>Plasma Processes & Polymers</i> , 2009, 6, 417-424	A58
T. Polcar , M. Evaristo, R. Colaço, C. Silviu Sandu, A. Cavaleiro, Nanoscale triboactivity: Response of Mo-Se-C coatings to sliding, <i>Acta Materialia</i> 56 (2008) 5101-5111	A66

Preface

Some people might think I am a scientist. Honestly, I am not. I admire science, I admire scientists, but I am sound enough to know that I am not one of them. I will never make any breakthrough - but I can live with that provide I am satisfied with my work. And I am...

As a boy, I wanted work as a garbage collector in orange waistcoat. Splendid job - they were riding on the dust carts, moving dustbins with one hand and using words completely unknown to me. Then, I wanted to be doctor of medicine, particularly during my long hospital experience. Later, astronaut was high on the list of potential occupations, so does the mariner. Work in science? Never...

I was a very bad college student with a very low rating showing a minimal interest in compulsory subjects. On the other hand, I had a lot of time to touch history and philosophy and I started to stockpile my small private library. One can not read about French Revolution at age 14 without dreaming of revolution - particularly when one lives in communist Czechoslovakia. I was conditionally expelled from the college just before revolution - and it came in time to save me.

I was playing with an extraordinary idea at age 16 - to leave college and work as the lowest worker in order to understand working class. I missed that opportunity, but the French Foreign Legion was another tempting option. My parents pressed me to continue studies at university - I declined. Eventually, I agreed to try and went to one they selected: Czech Technical University in Prague, Faculty of Mechanical Engineering. Well, I am engineer.

I spent a significant part of the studies in bed reading history books. I liked that life-style and PhD seemed as a nice prolongation. I designed 10MW hot-water boiler as my MSc. thesis - a monster thirty meters high. One centimeter makes no difference in such construction... so I started PhD study at Physics Department dealing with thin films, where every nanometer counts.

Lovely years... I traveled every winter to explore South America, I read huge amount of books, played soccer every weekend - and, from time to time, stayed overnight in the lab trying to crack tribological issues at elevated temperature. Moreover, I became husband and father. Amazingly, I have been awarded by PhD title for that.

When the thesis was submitted, I started looking for a position in Spain. I was communicating with several Spanish companies when I got a mail from Portugal offering a PostDoc position at Coimbra. I had never heard about Coimbra before... but I thought Portugal had to be like

Spain (I know I can not say it loudly in Portugal). I replied and I was accepted - the best luck in my life. My supervisor Albano Cavaleiro turned out to be the best guy one can meet. He gave me only one order: "Do what you want and I will support you as much as I can". Thanks to my PostDoc in Portugal, I could join the scientific community - and Albano opened the door pushing me in.

Portugal was beautiful, work was great, salary more then sufficient, beaches nearby with hot sun, my family was happy there including the new member, my second daughter: why did I return? There were several reasons to do so. Firstly, Michael Šebek, chief of the very progressive Department of Control Engineering, offered me a splendid position: fully independent researcher. Secondly, I believe that my Alma Mater could grow quickly to be one of the best technical universities in Europe - and second to none in Central Europe (well, after many major and painful improvements). Lastly, I have never left Portugal for long time - I still work there several months a year (by coincidence mostly in summer).

Typical preface ends with thanks to many people. I am obliged to many, but I prefer to express my gratitude personally. Unfortunately, I can not do so in case of my grandfather, who deserves it most. He taught me to read, to write, and to play soccer, and I thank him for everything.

Tomáš Polcar

1. Introduction and motivation

Many environmental issues we face today are related with energy production. It produces detrimental effects such as release of greenhouse gases, destruction of countryside or irrecoverable loss of valuable raw material. Recent actions trying to slow down the increasing consumption of combustibles led to minimal success considering money and effort; moreover, side effects of such eco-behavior very often lead to destruction of unexpected part of sensitive ecosystems. Use of bio-oil, for example, destroys large part of tropical forests in developing countries. In developed ones, the situation is similar - corn use for ethanol production in USA will quickly dry all water sources [1]. Large solar plants change surrounding habitat, not to mention huge energy demand for silicon cutting. Nuclear energy and eventually nuclear fusion would solve many problems; unfortunately, the first is not politically attractive (and, again, not a long term solution) and the latter is still in an early stage of development. Fortunately, there is a complementary way to environment-friendly energy production - to increase the efficiency of energy use or, in other words, to fight energy losses.

About 25% of the energy used in the world is wasted on overcoming friction [2] and losses due to wear of materials have been estimated by various sources to be 1.3 to 1.6% of the GNP of an industrialized country. The cost of friction, wear and lubrication (including reduced life time, repair and maintenance costs) is estimated at 350×10^9 Euro/year. Breaking this down by activity sectors, the maximum cost are associated with Surface Transport (46.6%), Industrial manufacturing and processing (33%), Energy suppliers (6.8%), Aeronautic (2.8%) and Household (0.5%). Other sectors complete the remaining 10.3%.

Reduction of friction in mechanical and other systems might significantly lower energy demands - and save money. For example, the effective coefficient of friction at the gear teeth in oil lubricated gearboxes generally lies in the range 0.04 to 0.08, with a resulting power loss in the range of 0.3% to 1.5% of the transmitted power. Considering the case of automotive gearboxes, if a coating could reduce the coefficient of friction by 20%, it could reduce the mesh friction loss in a typical automotive gearbox from 0.8% to 0.64%. This would mean a cost saving of 26×10^9 Euro/year [3], only in the Surface transport Sector. A lot of money - provide it is used wisely.

Tribology is the science and technology of interacting surfaces in relative motion. Friction reduction is a typical area of tribology. The history of the subject dates back to the studies of

friction by Thermistius about 350 BC who found that the friction for sliding is greater than that for rolling – in modern terms that the static friction coefficient is greater than the kinetic coefficient of friction. Leonardo da Vinci first noted in the 1500's that friction is proportional to load and independent of the area of sliding surfaces. This fundamental law was rediscovered by Amontons in 1699, verified by Euler in 1750 and Coulomb in 1781. Interestingly, the word tribology was first used in England in the 1960's and comes from the Greek word 'tribos' meaning 'to rub'. As referred to above, potential savings through tribology are huge [4].

The objective of this work is to offer small contribution to a wide effort to save energy by friction reduction.

2. Transition metal dichalcogenides and their friction reducing material role

2.1 Fundamental properties of transition metal dichalcogenides

The lamellar crystal structure is found in many chemical substances, and several of these have lubricating properties, such as naturally occurring micas, talc and graphite or synthetically prepared compounds. However, many of them were found to be unsatisfactory in friction applications and many of successful ones can not be applied directly as solid lubricants.

Transition metal dichalcogenides (TMD) are, in many ways, gift of nature to mechanical engineers looking for friction reduction. They exist in two crystal forms, hexagonal and rhombohedral. We will only deal here with the hexagonal structure, which is the most common and important for low-friction applications. The hexagonal crystal structure with six-fold symmetry, two molecules per unit cell, and a laminar, or layer-lattice structure, is shown in Fig. 1. Each atom is equidistant from three metal atoms, and each metal atom is equidistant from six dichalcogenide atoms. Attraction between metal and dichalcogenide atoms is powerful covalent bonding; however, there is only weak Van der Waals attraction between lattice layers [5]. TMD family consists of molybdenum, tungsten and niobium disulphides and diselenides.^a

To reduce friction, TMD is often used as oil additive or coating. Latter could be prepared as a thick film (e.g. burnished [6], films prepared by electrochemical processes [7], etc.) or a thin film deposited mainly by Physical Vapour Deposition (PVD) [5]. TMD could be formed as well during sliding process on the surfaces in the contact by tribochemical reactions [8].

Recently, attention has been paid to

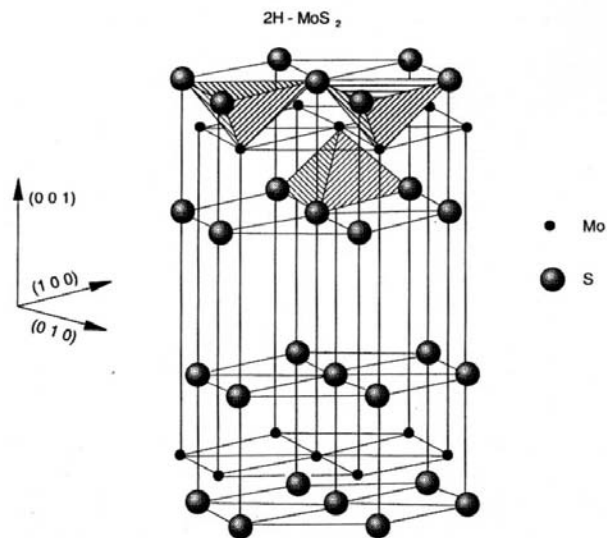


Fig. 1 Hexagonal structure of MoS₂ (Adapted from [5])

^a Tellurides (TeS₂ and TeSe₂) are, technically speaking, members of TMD family as well, but their low-friction behaviour is questionable. For more details, see e.g. E. Bermann et al, Tribology International 14 (1981) 329.

fullerene-like TMD [9,10,11] and TMD nanotubes [12,13,14], both as additives and films. However, despite several successful laboratory tests, the industrial applicability is still very limited.

2.2 Superlubricity of sputtered TMD

Thanks to unique highly anisotropic crystal structure, TMD could behave as solid superlubricant, i.e. material with friction lower than 0.01. Martin et al [15] reported superlubricity of MoS₂ film deposited and tested in UHV conditions with friction coefficient as low as 0.001. In fact, they observed "loss" of friction in several cases, which was attributed to a superlubric state confirming theoretical prediction [16] of frictional anisotropy of friction-oriented sulphur basal planes of MoS₂ grains [15].

To achieve such tribological properties, three fundamental conditions must be fulfilled:

I. Absence of contaminants

Presence of contaminants either in the TMD material (i.e. elements from residual atmosphere) or in surrounding atmosphere is detrimental. Crystal lattice could be modified by presence of oxygen or carbon. Water could significantly hinder easy shear between basal planes. Sputtering and immediate testing in ultra-high vacuum conditions are therefore required to achieve superlubricity. Testing at low vacuum or inert gas exhibits higher friction [17,18].

II. Formation of well adhered TMD transfer film on the counterpart

TMD adhere readily to most substrates. As a result, in sliding process with a solid surface the adhesion and junction growth take place and TMD transfer layer is progressively formed on counterpart. Adhesive forces between MoS₂ and solid substrates are usually much higher than the weak attractive forces between lamellae; consequently, the slip occurs preferentially between lamellae and friction coefficient is very low [19].

III. Reorientation of the (0001) basal planes of TMD grains

Friction and resulting shear stress reorient basal planes in the interface (either in the transferred layer, the tribolayer or the film itself).

2.3 TMD solid lubricant drawbacks

Superlubricity is not necessary for mechanical applications; even low-friction material would be sufficient. Why is it so difficult to use pure TMD films deposited by conventional (i.e. not UHV) magnetron sputtering in terrestrial atmosphere?

1. Deposition of TMD by magnetron sputtering inevitably leads to disordered structure. Low-friction prominent orientation, (0002), can not be achieved except for a very thin film not exceeding tens of nanometers [5].

2. TMD films are extremely sensitive to environmental attacks. When sliding in air, a very likely reaction is oxidation producing metal oxides. Presence of WO_{3-x} and MO_{3-x} oxides increases friction, although there is still controversy in estimation how detrimental such oxides are [21,22,23,24]. Nevertheless, the reactive prismatic edges on the (1120) face are more prone to chemical attack than the inert (0002) van der Waals basal plane [25]. Therefore, well oriented TMD with basal planes parallel to surface resist to oxidation. Another issue related with environment is storage of films. It has been documented that TMD deteriorate when stored in presence of oxygen and, particularly, water [26].

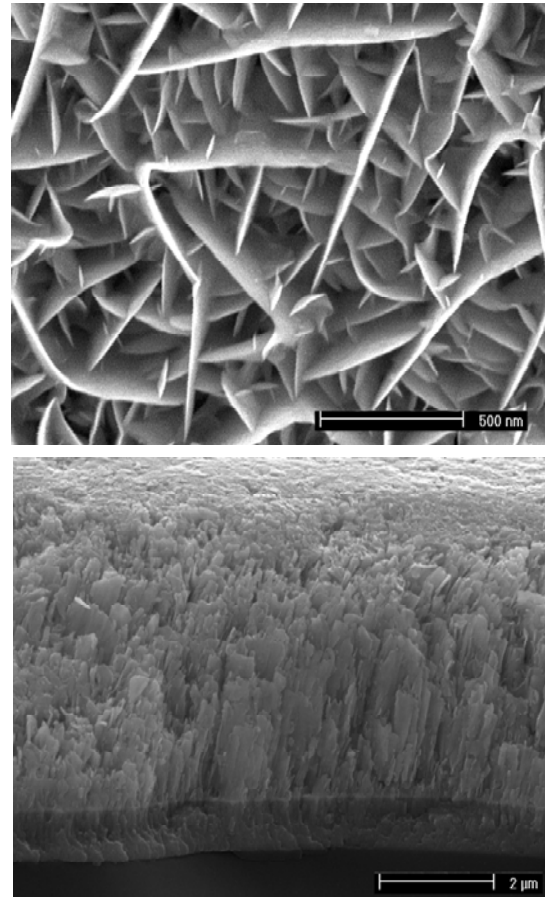


Fig. 2 SEM micrographs of porous and columnar sputtered WS₂ film [20]

3. TMD films are very porous (partially due to columnar morphology), as demonstrated in Fig. 2. Oxygen, water and other reactive species could easily penetrate the film and intensify film transformation (see above).

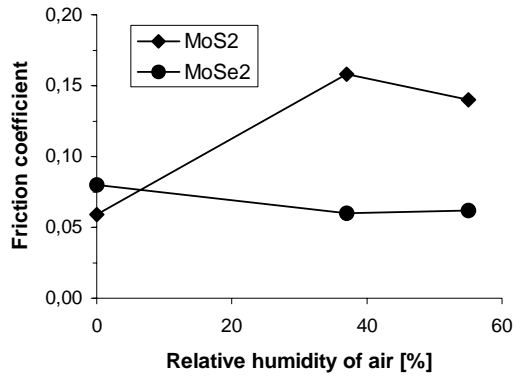


Fig. 3 Comparison of MoS₂ and MoSe₂ friction as a function of relative air humidity [27]

4. Hardness of TMD is very low compared to competitive low-friction coatings, such as diamond-like carbon (DLC). It is typically in range from 0.3 to 2 GPa depending on stoichiometry, morphology, and deposition conditions.

5. Adhesion on steel substrates is not adequate. However, it can be improved by thin metallic interlayer, typically Ti or Cr.

6. Diselenides are less sensitive to water and oxygen (Fig. 3); however, they are not environmentally friendly [5, 27].

7. Thanks to morphology and low adhesion, the load-bearing capacity is very low. TMD are peeled off the substrate under high contact pressures.

8. Material transfer to counterbody could be limiting factor in many applications. In general, solid lubricants can be used only in closed friction systems, where the contact between surfaces is repetitive.

Various countermeasures have been applied to remedy above referred limitations. Reduction of water in residual chamber atmosphere to diminish oxygen content in the film [28], variation of deposition temperature [29] or gas pressure [29,30] and others approaches slightly improved TMD tribological behavior. However, the main issues remained and pure sputtered TMD are restricted to vacuum applications [31].

2.4 TMD doped with elements and compounds

First attempts to dope TMD films were aimed at increase of density and consequent reduction of porosity, improved adhesion and significant increase of hardness. In general, the aims have been achieved. Among many metal dopants (Ti [24,32,33,34,35], Al [36], Au [37,38], Pb [39,40], Ni [37,41,42]), Cr [43,44] titanium was probably the most successful from commercial point of view (MOST® by Teer, Ltd., i.e. MoS₂ doped by Ti). The improvement of mechanical properties was evident; however, it could explain the increase in the wear resistance and load-bearing capacity but not the fact that low friction was observed. It has

been speculated that Ti reduces oxidation of TMD films by i) getter effect during deposition and ii) preferential oxidation in the film compared to TMD [32]. However, new results do not support such hypothesis [24]. Moreover, the doping with "inert" metals such Au resulted in similar sliding properties.

Non-metallic elements and compounds, such as ZnO [45], Sb₂O₃ [46,47], or PbO [47,48], were analyzed in 90's; however, the benefit of doping with such compounds was negligible compared to that of metals.

All films referred above shows two general features: prevalence of TMD phase (maximum content of dopants is about 20 at.%) and limited interaction between TMD phase and dopants or between TMD elements and dopants (contamination of oxygen and carbon from residual atmosphere during sputtering process is not considered here as doping).

2.5 TMD doped with non-metallic elements

Compared to previous section, the TMD coatings alloyed with non-metallic elements usually show higher non-TMD content; moreover, doping elements might react either with transition metals or dichalcogenides. Typical example is nitrogen forming tungsten nitride [49,50], niobium forming NbS₂ [51,52], or carbon producing tungsten carbides [49,50, 53,54,55,56,57]. We will focus here mainly on the most analyzed TMD film alloyed with carbon.

In late nineties, a new concept of coatings based on the alloying of transition metal dichalcogenides (TMD) with carbon started to attract the attention of several scientific groups. The original idea was to join the excellent frictional behavior of TMDs in vacuum and dry air with the tribological properties of DLC coatings. Moreover, an increase in the coatings compactness in relation to TMD and an improvement of the mechanical properties, particularly the hardness, was expected. Zabinski et al [53] prepared W-S-C coatings either by magnetron-assisted pulsed laser deposition (MSPLD – target WS₂) or by laser ablation of a composite target made of graphite and WS₂ sectors. The friction coefficient in dry air was lower than the one measured in humid air (0.02 and 0.15, respectively), and the so-called “chameleon behaviour” observed during environmental cycling was considered as the most interesting feature. The low friction in dry air increased in the presence of humid air and fell down when the atmosphere was dried again.

W-S-C coatings prepared by magnetron sputtering have been intensively studied by Cavaleiro et al, concerning: the structure [58], the mechanical properties [59] and the tribological

performance [49,60]. In a first set of studies, W-S-C films were deposited by sputtering from a WS₂ target in a CH₄-containing reactive atmosphere. The flow of CH₄ and the target power were varied to prepare a large range of chemical compositions from pure WS₂ to W-S-C with carbon contents up to 70 at.%; the S/W ratio was about 1.2. Fig. 4a clearly shows that the main disadvantage of TMD films, the detrimental effect of the humid air, was not overcome and the friction in these conditions was relatively high whatever the carbon content was [59,61]. However, the rapid film failure typical of pure tungsten disulphide was not observed and the coating wear rate was quite low (Fig. 4b), result attributed to the significant increase of the hardness, from 0.5 GPa (WS₂) to ~10 GPa, achieved with the C incorporation.

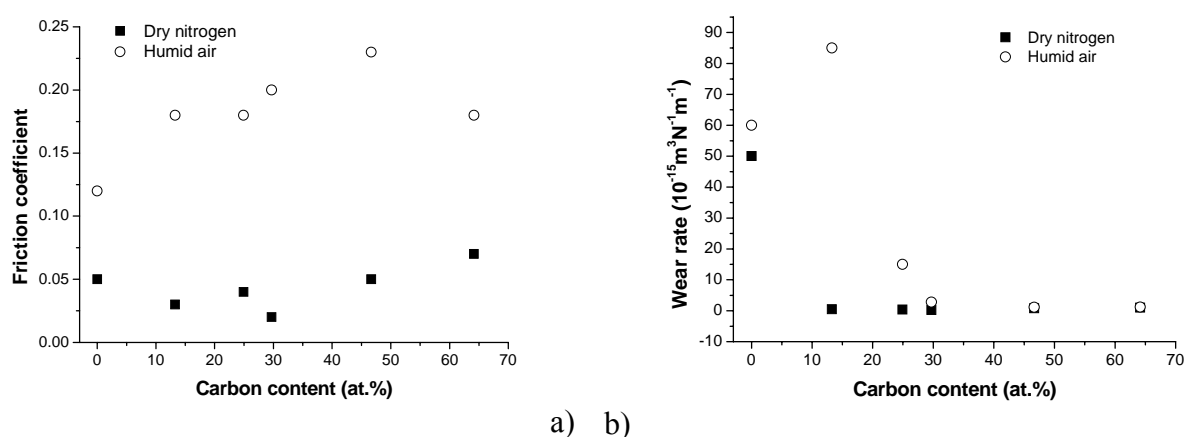


Fig. 4 Friction, a), and wear, b), coefficients of W-S-C reactive deposited sputtered coatings as a function of the C content when tested in humid air and dry N₂ (load 5N).

The analysis of the microstructure of the reactive deposited W-S-C coatings [20] allowed to conclude that, for high carbon content, they were formed by a mixture of nanocrystals of WS₂ phase side by side with nanocrystals of W-C phases and small C-based amorphous zones (see example in Fig. 5), or just by WS₂ nanograins dispersed in an amorphous carbon matrix (low carbon content). A similar behavior was observed elsewhere for WS₂/DLC/WC coatings showing a huge friction coefficient difference when sliding in humid or dry air [54,55,56]; the friction behavior was attributed to the alternative formation of a WS₂-rich or a C-rich layer during the cyclic change of the environment from dry to humid, respectively. Another concept presented in literature for the TMD+C composite coatings deals with nanolayered structured coatings [62], where tungsten disulphide and carbon layers form a “super-lattice” film (the thickness of layers is in nanometer scale). The performance of such films was only moderate.

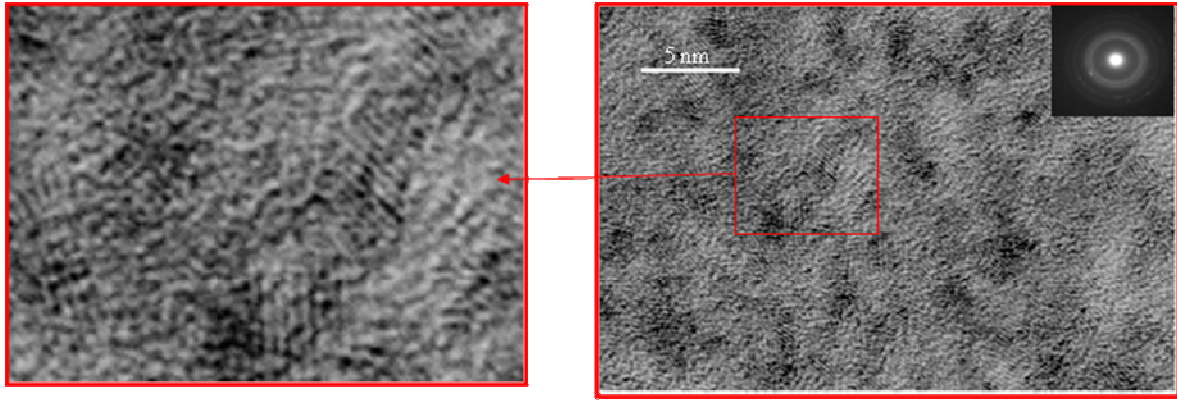


Fig. 5 TEM micrographs of the reactive sputtered $W_{17}S_{15}C_{68}$ [20,50].

All these three different coating microstructures schematically shown in Fig. 6 proved to be unsatisfactory for reducing the friction coefficient in humid air sliding conditions. The multilayer films are vulnerable to cohesion damage, since interlayers sliding can occur in the bulk of the film where the shear stresses are larger than at the surface. This problem can be partially solved by thinning of layers down to units of nanometers; however, such a superlattice structure is difficult to be achieved on typical industrial substrates with standard surface roughness.

On the other hand, the other two microstructures cannot guarantee simultaneously that either the TMD nanocrystals could be re-oriented with the basal planes parallel to the sliding distance or the oxidation of the dangling bonds should not occur. In fact, during the re-orientation process the extremities of the grains will enter directly in contact with the atmosphere being immediately oxidized.

It was obvious that a new concept is required for modern low-friction universal coating exhibiting high wear resistance, load-bearing capacity and, particularly, low friction in various sliding environments (vacuum/dry air or nitrogen/humid air; elevated temperature, etc.).

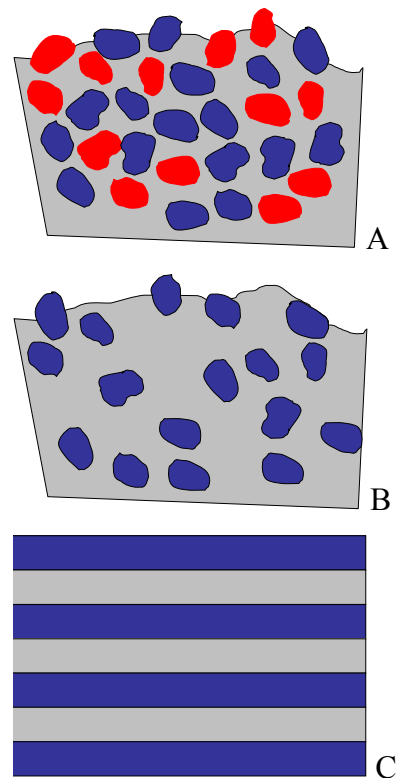


Fig. 6 Schematic view of previous W-S-C films designs:

A Nanocomposite coatings with hard WC nanoparticles embedded together with WS_2 nanograins in an amorphous carbon matrix (top);
 B nanograins of WS_2 in a C-matrix (center);
 C super-lattice WS_2 +C layers film (bottom)

3. New concept of coating microstructure based on TMD-C system

3.1 Approach

The basis for the achievement of a low friction coating in a great variety of environments could be envisaged by a micro(nano)structure where TMD nanocrystals could be deposited completely enrobed in a protective C-rich matrix. If possible, these nanocrystals should have shapes that allow an easy reorientation of the basal planes parallel to the sliding direction. Carbon matrix will contribute for improving the hardness and the compactness of the coatings as well as for protecting the TMD against the oxidation until the moment that they are completely aligned and arise to the contact surface. By their side, TMD should assure the low friction coefficients, due to the easy sliding of the basal planes, and only a few amounts of strong bonds, promoted by the oxygen, should exist. In parallel with this approach, the use of other types of TMDs with less sensibility to the oxidation than tungsten and molybdenum disulphides, such as MoSe_2 [5,27], should also be envisaged, since carbon matrix could improve their very low hardness and mechanical properties.

During sliding in pin-on-disk testing, strong shear stresses occur which could contribute for the re-orientation of the TMD crystals in the C-based amorphous matrix. However, during the alignment of the TMD nanocrystals parallel to the sliding direction, their contact with the atmosphere gives rise to the reaction of the dangling bonds of the end plans with oxygen with the consequent increase of the friction. In pure TMD coatings this phenomenon was not observed due to the porous structure and very low hardness giving rise to very high wear rate. Therefore, as generally accepted in the wear models it is expected that TMD material is worn out and then adheres on both surfaces in the contact. Such tribolayer is very thin (nanometer scale) with highly oriented TMD phase, mainly with the basal plans parallel to film surface [5,63].

The problems referred to above could be avoided if the crystals were already aligned in the material, since in this case almost no dangling bonds would be available for reaction [25]. Recently, it was possible to prove that nanocrystals of a compound, such as TiC , could be re-arranged through the C-matrix where they were embedded, during the mechanical deformation of the material by indentation [64]. It might be possible that TMD-C films, where nanograins of TMD are embedded in an amorphous carbon matrix, exhibit similar behavior. Nevertheless, the re-orientation of TMD crystals in a carbon matrix has not been studied yet.

Thus, it was decided to prepare TMD-C films with very small nanograins of the TMD phase (reduced, if possible, to one cell of TMD), since small grain size could promote more easily the re-orientation of the TMD phase inside the carbon matrix.

3.2 How to deposit the coatings with required microstructure?

In order to deposit coatings containing simultaneously C and the TMD phase with a new microstructure, the deposition by co-sputtering from TMD and C sources, either from separate targets or by a puzzled target with both materials (Fig. 7), can be an alternative.

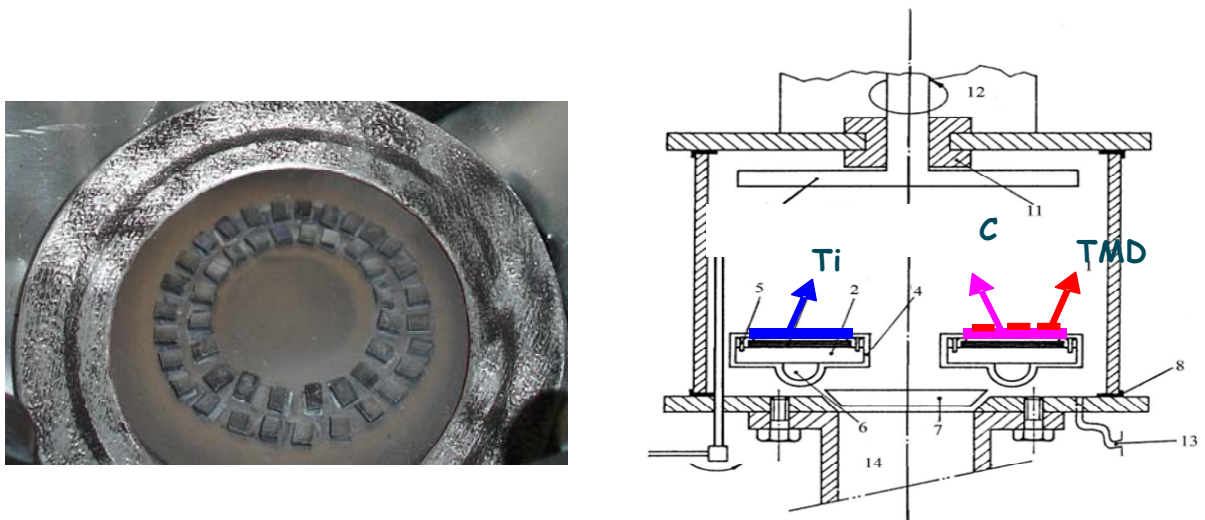


Fig. 7 Schema of the deposition chamber with two electrodes and picture of the puzzled target. For separate target deposition the Ti target is replaced by a TMD one whereas in the other electrode only a C target is attached.

With this geometry, microstructures such as those shown in Fig. 8 for Mo-Se-C and W-S-C films with ~50 at.% of carbon can be deposited [65,66]. The TMD phase is under a platelet shape with only a couple of stacked basal planes. The platelets are completely enrobed by the C-matrix. X-ray diffraction and Raman spectroscopy undoubtedly confirmed the presence of the TMD and the C phases [67,68,69]. The hardness was about 3 and 10 GPa for Mo-Se-C and W-S-C, respectively, compared to the <0.5 GPa of the pure TMD films sputtered under identical conditions from the TMD target.

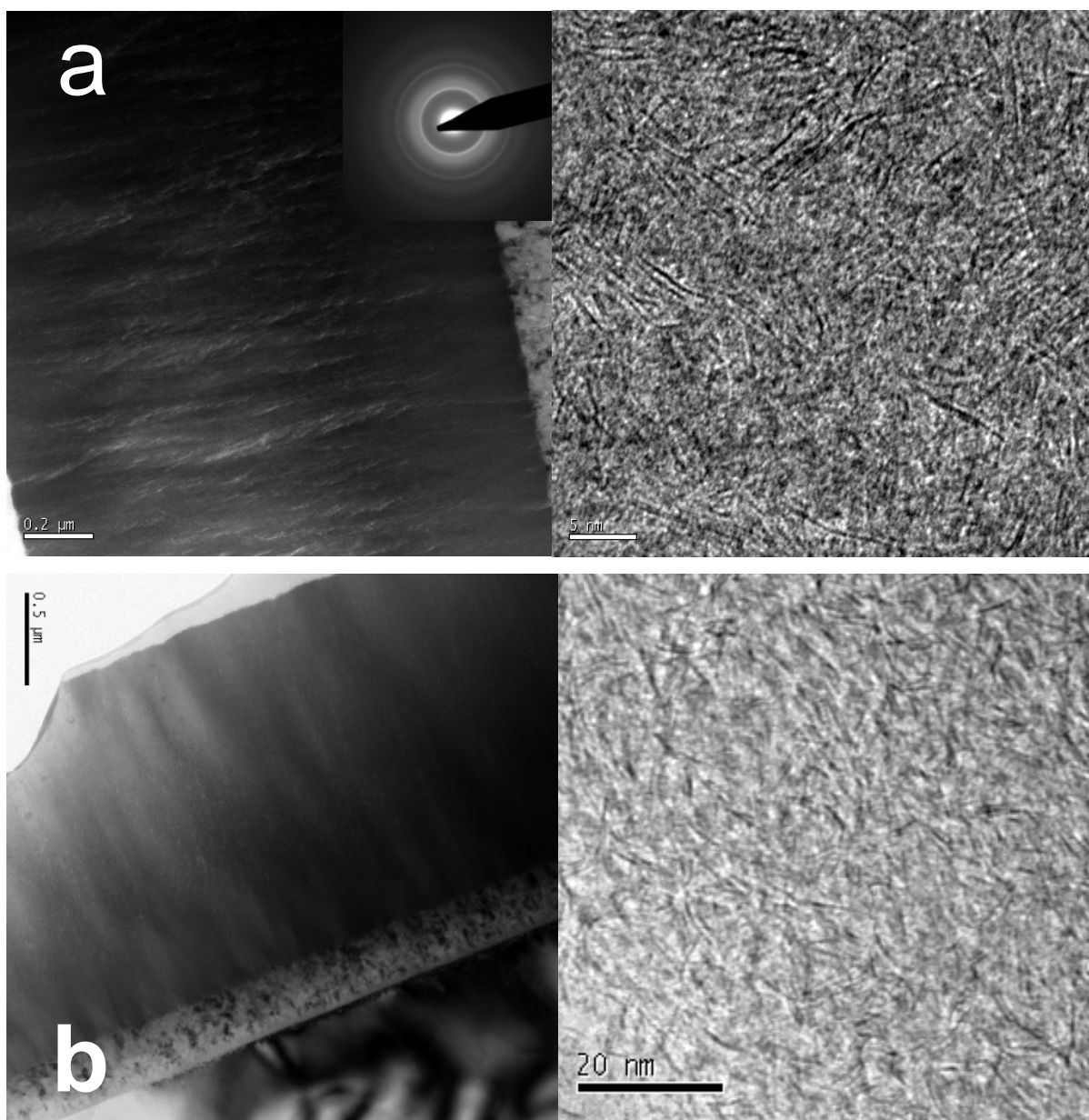


Fig. 8 TEM images of W-S-C (a) and Mo-Se-C (b) co-sputtered films deposited with ~ 50 at.% C. Note the dense structure (left) and the separated TMD platelets (right).

3.3 Friction performance

The W-S-C and Mo-Se-C coatings with carbon content from 25 to 70 at.% were tested under different conditions, such as relative air humidity (from dry air to 90%) [70,71], load (pin-on-disc: 5 to 48 N; reciprocating ball-on-disc: 20 to 1000 N) [68,73], sliding speed (from 10 to 1000 $\text{mm}\cdot\text{s}^{-1}$) [65], temperature (room temperature to 500 °C) [67,71], and test duration (several cycles to one million) [66]. Typical behavior of newly developed TMD-C films could be summarized as follows:

- I. Friction in dry air is very low (<0.05)
- II. For short test duration, the friction is humidity-dependent. However, the running-in process of TMD-C films is extremely long and final steady state value of friction in humid air is close to that of dry air or nitrogen.
- III. At elevated temperature, the friction is slightly lower than in dry air
- IV. Functional temperature limit is $400\text{ }^{\circ}\text{C}$ for W-S-C and $250\text{ }^{\circ}\text{C}$ for Mo-Se-C films, respectively.
- V. Friction decreases with load.
- VI. Whatever the sliding conditions are, the medium carbon content (close to 50 at.%) films exhibits the best tribological properties.

To analyze coating functional limits, a new series with carbon content ~ 50 at.% have been deposited and tested. Fig. 9 shows the friction coefficient obtained in a sliding reciprocating ball-on-plate test (frequency - 20 Hz; stroke length - 1 mm). Two facts are evident: (i) in humid conditions Mo-Se-C coatings show slightly better friction performance than W-S-C ones; (ii) in some loading conditions (very high applied loads) the friction coefficient in humid air approaches that in dry conditions.

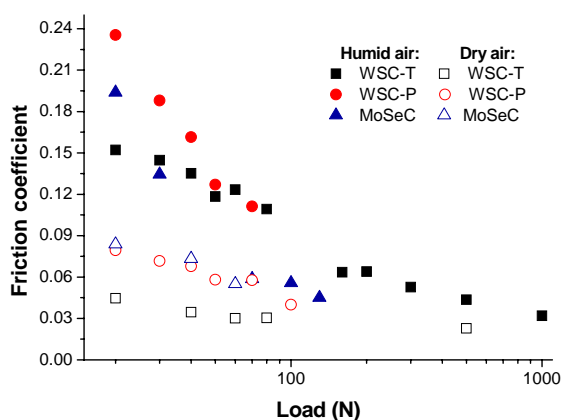


Fig. 9 Friction coefficient of TMD coatings as a function of the applied load in dry and humid conditions (WSC-T was deposited from two target, WSC-P from composite target). Note logarithmic load scale.

coatings exhibit a slight increase of the friction with load [65]. It is also important to remark that a similar behavior is found in dry conditions although with a starting value much lower (~ 0.08 against ~ 0.20 for a 20 N load).

This last result gives strong evidence that the scope of re-orientation of the TMD nanocrystals, in conditions of oxidation protection, could be achieved. However, significant amount of mechanical energy have to be used to allow the correct reorientation in the envisaged conditions. The progressive decrease of the friction coefficient with increasing applied load suggests that the sliding process is driven by the TMD phases in the contact (such decrease is typical of TMD [72]), since pure carbon films identical to the amorphous carbon matrix of these

Fig. 10 shows the average friction coefficient obtained in tests with increasing duration times when a low load (5 N) is applied to the ball. As can be confirmed, there is a steep decrease of the friction coefficient in the first thousands of cycles being possible to reach a steady state value (~ 0.05) close to 100,000 cycles, which is not far from the lowest value showed in Fig. 9. **Chyba!** **Nenalezen zdroj odkazů.** for

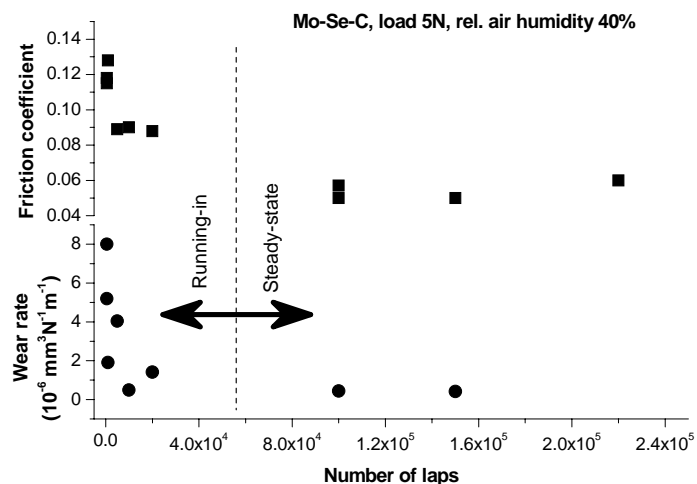


Fig. 10 Evolution of the friction coefficient and the wear rate after tests with different duration of a Mo-Se-C coating sliding under room conditions with an applied load of 5 N (pin-on-disc, 100Cr6 ball with a diameter of 6 mm). The steady state wear regime was reached after long running-in.

these coatings when tested with much higher loads. Such observation is supported by the evolution of the friction coefficient as a function of the number of cycles for a W-S-C coating tested by changing the humidity in the atmosphere every 10,000 cycles [73]. Besides the progressive approach between the friction values in both, dry and humid, environments with increasing test duration, also in both cases a decreasing trend in each step can be observed. In conclusion, in sliding tests of TMD-C coatings, low friction coefficients can be achieved in any environment providing that sufficient contact pressure or test duration are used.

3.4 Evidence of the sliding mechanism

The progressive way how the formation of the TMD tribolayer occurs can be demonstrated experimentally by the analysis of the top surface of the sliding track after wear testing. Fig. 11 shows the Raman spectra of TMD-C films obtained after tribological tests carried out with either the same number of cycles but different loads or the same load but different number of cycles. It is clear that the increase in the load and/or the number of cycles gives rise to a more intense signal of the bands assigned to the TMD phase in comparison to those of the C-based material (G and D bands). This result confirms an increasing agglomeration of TMD material close to the contact zone.

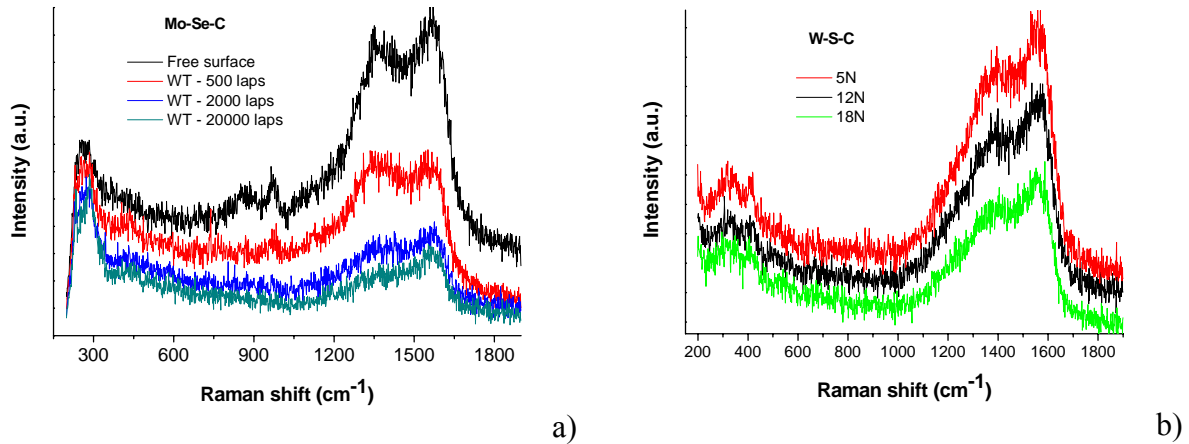


Fig. 11 Raman spectra taken from the center of the wear track as a function of the test duration (a) and applied load (b).

Auger spectroscopy (AES) chemical depth profiles show the thickening of the surface TMD tribolayer when contact pressure and/or number of laps (i.e. test duration) is increased [65,66]. Absence of the C-signal on the top layer suggests that it is formed almost exclusively by TMD phase. However, the agglomeration of the TMD material in the contact zone should only lead to the reduction of the friction coefficient providing that its basal planes are aligned parallel to the surface and no abundant oxidation occurs that can lead to strong bonding between them. It is therefore also important to remark the absence of O in this top layer (compare to the residual signal of the material underneath) stating that the formation of the tribolayer is achieved in a protective way, without the oxidation of the dangling bonds of the original short TMD platelets.

The microstructural observation of the cross section of the top layer of the wear track by HR-TEM (high-resolution transmission electron microscopy) reveals platelets of TMD aligned parallel to the surface covering the most part of the zones which were analyzed, see Fig. 12. Furthermore, the same micrograph shows that as the analysis is being moved to the interior of the film, the alignment is less and less evident. The observation of a great number of micrographs of different zones of the wear track [66] permitted concluding that the reorientation of the TMD platelets is made progressively from some tens of nanometers until the track surface. Almost no other orientations but parallel to the surface are encountered in the first 5 nm top layer. Moreover, the platelets were re-oriented even in the depth of the coating; on the other hand, the number of well oriented platelets with basal planes parallel to surface decreases with increasing distance from surface.

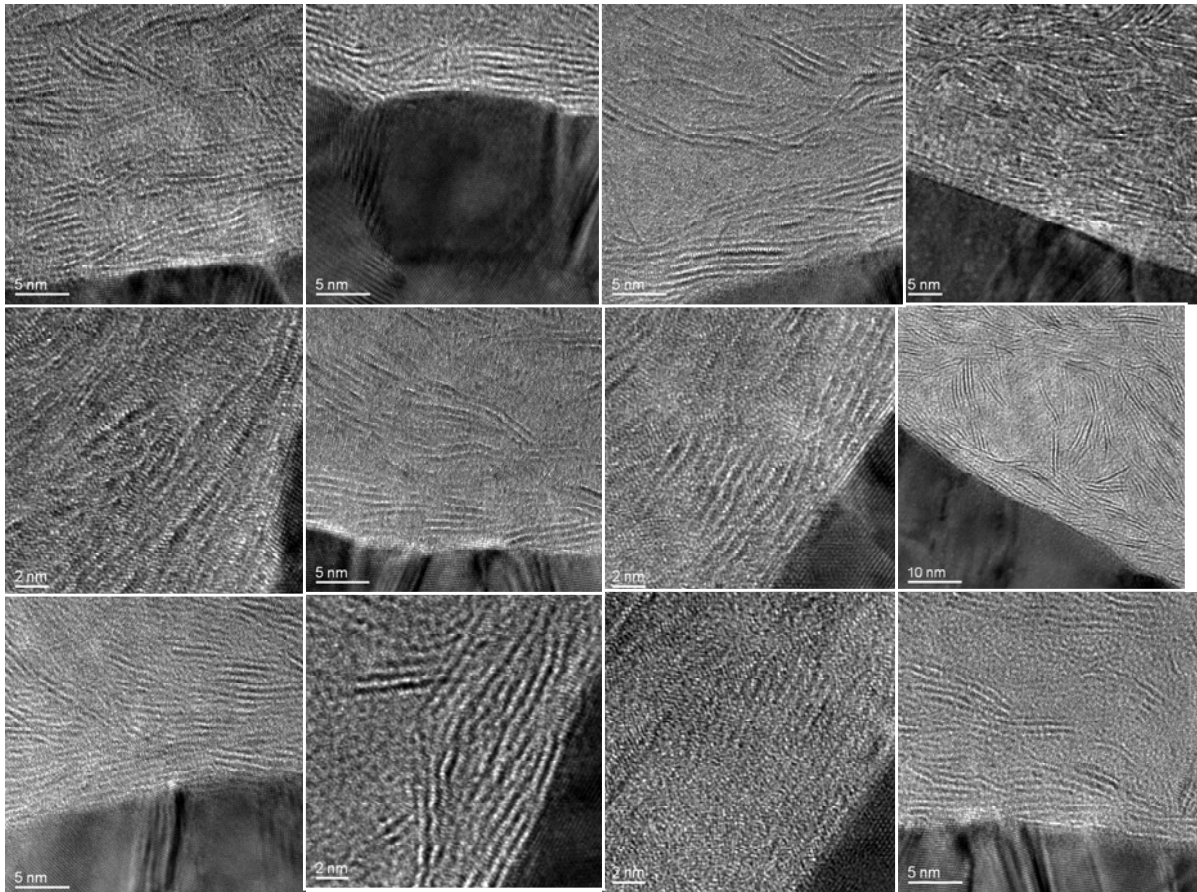


Fig. 12 HR-TEM images of the cross-section of the wear tracks prepared by the Focused Ion Beam. The black part of the images is the protective gold layer sputtered over the wear track after sliding test. The preferential orientation of the TMD platelets is clearly visible contrasting to as-deposited state shown in Fig. 8.

3.5 Industrial applications of new coating design

Based on structural, mechanical and tribological analysis, we can draw a roadmap for TMD-C coatings (Tab. 1). In general, the coating should exhibit the following features:

- Thickness of the adhesion tribolayer: ~ 300 nm
- Thickness of the coating: 2-3 μm
- Carbon content: ~ 50 at.%
- chalcogenide to metal ratio: higher than 1.5 (i.e. close to stoichiometry)

Typical application conditions						
TMD-C coating	Vacuum/dry air	Humid air	Elevated temperature	High contact pressure	Changing atmosphere humidity	Presence of abrasive particles
W-S-C	+++	++	+++	+++	++	-
Mo-S-C	+++	+	?	?	++	---
W-Se-C	+++	+	---	++	+	---
Mo-Se-C	+++	+++	-	+++	+++	---

Tab.1 Roadmap of TMD-C tribological behavior at different sliding conditions.

Selected TMD-C coatings (W-S-C and Mo-Se-C) have been successfully deposited on various parts provided by automotive industry, see Fig. 13. The coated parts are being intensively tested in field applications.

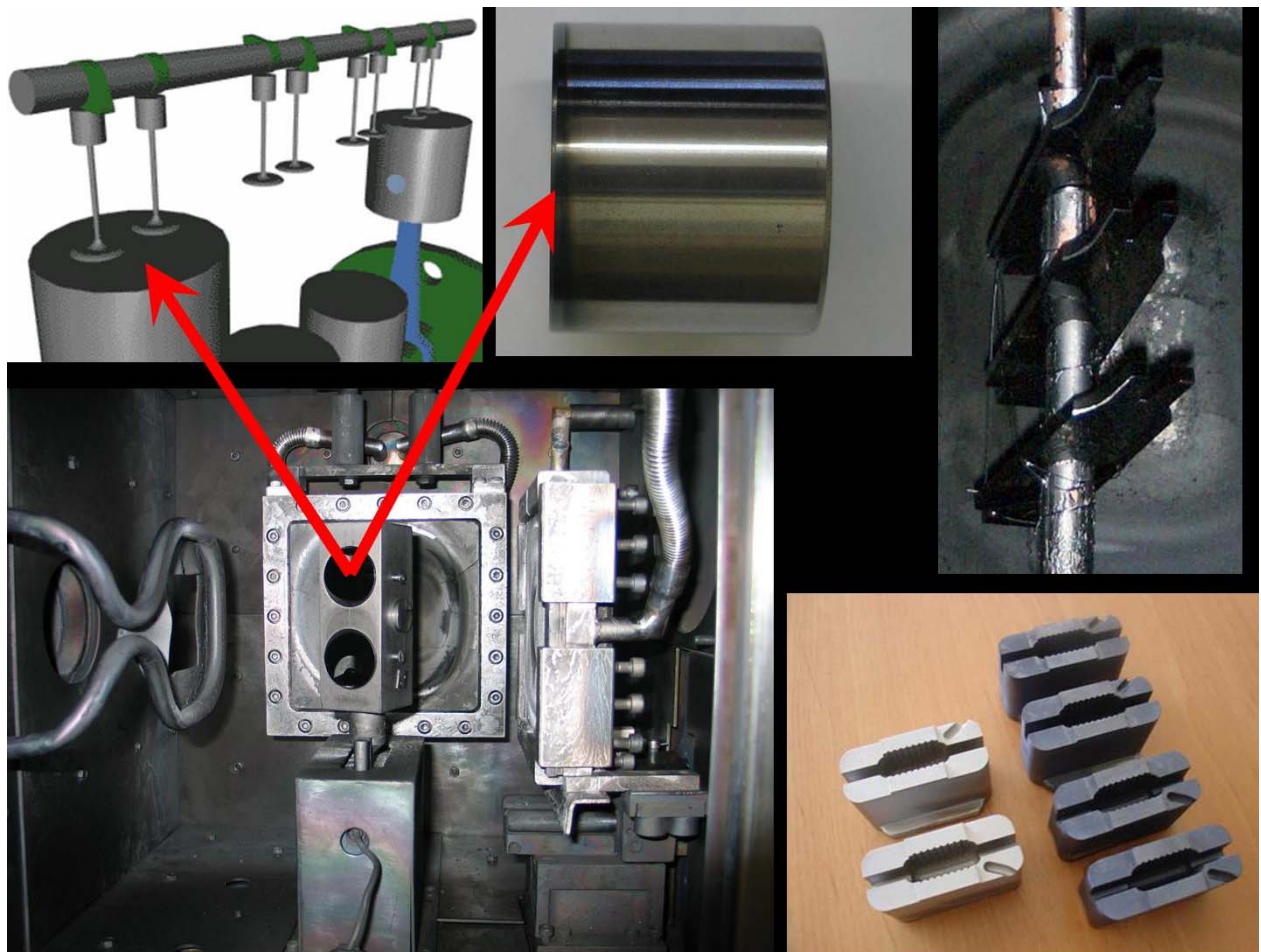


Fig. 13 Coated parts for automotive industry.

References

- [1] R.F. Service, *Science* 326 (2009) 516
- [2] Oakridge National Laboratory, USA
- [3] Eurostat, report DK28157, 2005
- [4] J. A. Tichy, D. M. Meyer, *International Journal of Solids and Structures* 37 (2000) 391-400
- [5] A.R. Lansdown, *Molybdenum Disulphide Lubrication*, Elsevier, 1999
- [6] H. Waghray, T.-S. Lee, B. Tatarchuk, *Surf. Coat. Technol.* 76-77 (1995) 415
- [7] M.F. Cardinal, P.A. Castro, J. Baxi, H. Liang, F.J. Williams, *Surf. Coat. Technol.* 204 (2009) 85
- [8] C. Grossiord, K. Varlot, J. -M. Martin, Th. Le Mogne, C. Esnouf, K. Inoue, *Trib. Int.* 31 (1998) 737
- [9] L. Rapoport, Y. Bilik, Y. Feldman, M. Homyonfer, S.R. Cohen, R. Tenne, *Nature* 387 (1997) 791
- [10] M. Chhowalla, G.A.J. Amaratunga, *Nature* 407 (2000) 164-167
- [11] Y. Golan, C. Drummond, M. Homyonfer, Y. Feldman, R. Tenne, J. Israelachvili, *Adv. Mater.* 11 (1999) 934
- [12] M. Remskar, A. Mrzel, Z. Skraba, A. Jesih, M. Ceh, J. Demsar, P. Stadelmann, F. Levy, D. Mihailovic, *Science* 292 (2001) 479
- [13] M. Remskar, *Adv. Mater.* 16 (2004) 1497
- [14] M. Akbulut, N. Belman, Y. Golan, J. Israelachvili, *Adv. Mater.* 18 (2006) 2589
- [15] J.M. Martin, C. Donnet, Th. Le Monge, Th. Epicier, *Phys Rev* 48 (1993) 10583
- [16] M. Hirato, K. Shinjo, R. Kaneko, Y. Murato, *Phys. Rev. Lett.* 67 (1991), 2634
- [17] D.R. Wheeler, *Thin Solid Films* 223 (1993) 78
- [18] J. Moser, F. Levy, *J. Mater. Res.* 8 (1993) 206
- [19] Weise, G., Mattern, N., Hermann, H., *Thin Solid Films*, 298 (1997)
- [20] A. Nossa, A. Cavaleiro, *J. Mater. Res.* 19 (2004) 2367
- [21] Steinmann et al., *Tribol. Int.* 37 (2004) 879
- [22] Lauwerens et al., *Surf. Coat. Technol.* 131 (2000) 216
- [23] Hirvonen et al., *Surf. Coat. Technol.* 80 (1996) 139
- [24] T.W. Scharf, A. Rajendran, R. Banerjee, F. Sequeda, *Thin Solid Films* 517 (2009) 5666
- [25] G. Salitra, G. Hodes, E. Klein, R. Tenne, *Thin Solid Films* 245 (1994) 180
- [26] Takanori Takeno, Shingo Abe, Koshi Adachi, Hiroyuki Miki, Toshiyuki Takagi, *Diamond and Related Materials*, doi:10.1016/j.diamond.2009.10.028
- [27] T. Kubart, T. Polcar, L. Kopecký, R. Novák, D. Nováková, *Surf. Coat. Technol.* 193 (2005) 230
- [28] V. Buck, *Wear* 114 (1987) 263
- [29] F. Lévy and J. Moser, *Surf. Coat. Technol.* 69-68 (1994) 433

-
- [30] M. Regula, C. Ballif, J. H. Moser, F. Lévy, *Thin Solid Films* 280 (1996) 67
- [31] <http://www.osti.gov/bridge/purl.cover.jsp;jsessionid=64689C7DE3D03F885E809AA479ABA>
BA8?purl=/884665-QtPaGD/
- [32] D.G. Teer, *Wear* 251 (2001) 1068.
- [33] A. Savan, M.C. Simmonds, Y. Huang, C.P. Constable, S. Creasey, Y. Gerbig, H. Haefke, D.B. Lewis, *Thin Solid Films* 489 (2005) 137.
- [34] N.M. Renevier, V.C. Fox, D.G. Teer, J. Hampshire, *Surf. Coat. Technol.* 127 (2000) 24.
- [35] N.M. Renevier, J. Hampshire, V.C. Fox, J. Witts, T. Allen, D.G. Teer, *Surf. Coat. Technol.* 142–144 (2001) 67
- [36] J.D. Holbery, E. Pflueger, A. Savan, Y. Gerbig, Q. Luo, D.B. Lewis, W.-D. Munz, *Surf. Coat. Technol.* 169–170 (2003) 716.
- [37] S. Mikhailov, A. Savan, E. Pflueger, L. Knoblauch, R. Hauert, M. Simmonds, H. Van Swygenhoven, *Surf. Coat. Technol.* 105 (1998) 175.
- [38] J.R. Lince, *Trib. Lett.* 17 (2004) 419.
- [39] K.J. Wahl, L.E. Seitzman, R.N. Bolster, I.L. Singer, *Surf. Coat. Technol.* 73 (1995) 152.
- [40] K.J. Wahl, D.N. Dunn, I.L. Singer, *Wear* 230 (1999) 175.
- [41] J.R. Lince, M.R. Hilton, A.S. Bommannavar, *J. Mater. Res.* 10 (1995) 2091
- [42] M.R. Hilton, G. Jayaram, L.D. Marks, *J. Mater. Res.* 13 (1998) 1022.
- [43] Su YL, Kao WH. *Tribol Int* 36 (2003) 11.
- [44] Simmonds MC, Savan A, Pfluger E, Van Swygenhoven H. *Surf Coat Technol* 126 (2000) 15.
- [45] S.V. Prasad, N.T. McDevitt, J.S. Zabinski, *Wear* 237 (2000) 186.
- [46] J.S. Zabinski, M.S. Donley, N.T. McDevitt, *Wear* 165 (1993) 103.
- [47] J.S. Zabinski, M.S. Donley, S.D. Walck, T.R. Schneider, N.T. McDevitt, *Trib. Trans.* 38 (1995) 894.
- [48] J.S. Zabinski, M.S. Donley, V.J. Dyhouse, N.T. McDevitt, *Thin Solid Films* 214 (1992) 156.
- [49] A. Nossa, A. Cavaleiro, *Surf. Coat. Technol.* 163–164 (2003) 552.
- [50] A. Nossa, A. Cavaleiro, N.J.M. Carvalho, B.J. Kooi, J.Th.M. De Hosson, *Thin Solid Films* 484 (2005) 389.
- [51] Ihsan Efeoglu, Özlem Baran, Fatih Yetim, Sabri Altıntaş, *Surf. Coat. Technol.* 203 (2008) 766
- [52] Ersin Arslan, Özlem Baran, Ihsan Efeoglu, Yasar Totik, *Surf. Coat. Technol.* 202 (2008) 234
- [53] A.A. Voevodin, J.S. Zabinski, *Thin Solid Films* 370 (2000) 223
- [54] A. A. Voevodin, J. P. O’Neill and J. S. Zabinski, *Surf. Coat. Technol.* 116-119 (1999) 36.
- [55] J. -H. Wu, M. Sanghavi, J. H. Sanders, A. A. Voevodin, J. S. Zabinski and D. A. Rigney, *Wear* 255 (2003) 859.
- [56] J.-H. Wu, D. A. Rigney, M. L. Falk, J. H. Sanders, A. A. Voevodin and J. S. Zabinski, *Surf. Coat. Technol.* 188-189 (2004) 605

-
- [57] A. A. Voevodin and J. S. Zabinski, *Comp. Sci. and Technol.* 65 (2005) 741.
- [58] A. Nossa, A. Cavaleiro, *J. Mater. Res.* 19 (2004) 2356
- [59] M. Evaristo, A. Nossa and A. Cavaleiro, *Surf. Coat. Technol.* 200 (2005) 1076
- [60] A. Nossa, A. Cavaleiro, *Surf. Coat. Technol.* 142-144 (2001) 984
- [61] A. Nossa, A. Cavaleiro, *Tribology Letters* 28 (2007) 59
- [62] J. Noshiro, S. Watanabe, T. Sakurai, S. Miyake, *Surf. Coat. Technol.* 200 (2006) 5849
- [63] J. Moser, F. Lèvy, *Thin Solid Films* 228 (1993) 257
- [64] C.Q. Chen, Y.T. Pei, K.P. Shaka, J.M.T. De Hosson, *Appl. Phys. Lett.* 92 (2008) 241913
- [65] T. Polcar, M. Evaristo and A. Cavaleiro, *Plasma Processes & Polymers*, 2009, 6, 417-424
- [66] T. Polcar, M. Evaristo, R. Colaço, C. Silviu Sandu, A. Cavaleiro, *Acta Mater* 56 (2008) 5101
- [67] T. Polcar, M. Evaristo, A. Cavaleiro, *Vacuum*, 81 (2007) 1439
- [68] T. Polcar, M. Evaristo and A. Cavaleiro, *Plasma Processes & Polymers*, 2007, 4, S541
- [69] T. Polcar, M. Evaristo, M. Stueber, A. Cavaleiro, *Surf. Coat. Technol.* 202 (2008) 2418
- [70] M. Evaristo, T. Polcar, A. Cavaleiro, *Int. J. Mech. Mat. Design* 4 (2008) 137
- [71] T. Polcar, M. Evaristo, M. Stueber, A. Cavaleiro, *Wear* 266 (2009) 393-397
- [72] I. L. Singer, R. N. Bolster, J. Wegand, S. Fayeulle, B. C. Stupp, *Appl. Phys. Lett.* 1990, 57, 995
- [73] T. Polcar, M. Evaristo, A. Cavaleiro, *Wear* 266 (2009) 388

Annex: Author's papers dealing with TMD and TMD-C coatings

- T. Kubart, **T. Polcar**, L. Kopecký, R. Novák and D. Nováková, Temperature dependence of tribological properties of MoS₂ and MoSe₂ coatings, *Surface and Coatings Technology* 193 (2005), Pages 230-233 A1
- T. Polcar**, A. Nossa, M. Evaristo and A. Cavaleiro, Nanocomposite coatings of C-based and TMD phases: a review, *Reviews on Advanced Materials Science*, 15 (2007) 118-126 A5
- T. Polcar**, M. Evaristo and A. Cavaleiro, Friction of self-lubricating W-S-C sputtered coatings sliding under increasing load, *Plasma Processes & Polymers*, 2007, 4, S541-S546 A12
- T. Polcar**, A. Nossa, M. Evaristo and A. Cavaleiro, Nanocomposite coatings of C-based and TMD phases: a review, *Reviews on Advanced Materials Science*, 15 (2007) 118-126 A16
- T. Polcar**, M. Evaristo and A. Cavaleiro, Friction of self-lubricating W-S-C sputtered coatings sliding under increasing load, *Plasma Processes & Polymers*, 2007, 4, S541-S546 A25
- T. Polcar**, M. Evaristo, M. Stueber, A. Cavaleiro, Synthesis and structural properties of Mo-Se-C sputtered coatings, *Surface and Coatings Technology* 202 (2008) 2418-2422 A31
- C. Silviu Sandu, **T. Polcar**, A. Cavaleiro, TEM investigation of MoSeC films, *Microscopy and Microanalysis* 14 supp 3 (2008) 7-10 A36
- T. Polcar**, M. Evaristo, M. Stueber, A. Cavaleiro, Mechanical and tribological properties of sputtered Mo-Se-C coatings, *Wear* 266 (2009) 393-397 A40
- T. Polcar**, M. Evaristo, A. Cavaleiro, Comparative study of the tribological behaviour of self-lubricating W-S-C and Mo-Se-C sputtered coatings, *Wear* 266 (2009) 388-392 A45
- M. Evaristo, **T. Polcar**, A. Cavaleiro, Synthesis and properties of W-Se-C coatings deposited by PVD in reactive and non-reactive processes, *Vacuum* 83 (2009) 1262-1265 A50
- M. Evaristo, **T. Polcar**, A. Cavaleiro, Can W-Se-C coatings be competitive to W-S-C ones?, *Plasma Processes & Polymers*, 2009, 6, S92-S95 A54
- T. Polcar**, M. Evaristo and A. Cavaleiro, Self-lubricating W-S-C nanocomposite coatings, *Plasma Processes & Polymers*, 2009, 6, 417-424 A58
- T. Polcar**, M. Evaristo, R. Colaço, C. Silviu Sandu, A. Cavaleiro, Nanoscale triboactivity: Response of Mo-Se-C coatings to sliding, *Acta Materialia* 56 (2008) 5101-5111 A66

Temperature dependence of tribological properties of MoS₂ and MoSe₂ coatings

T. Kubart^{a,*}, T. Polcar^c, L. Kopecký^b, R. Novák^a, D. Nováková^c

^aDepartment of Physics, Faculty of Mechanical Engineering, Technická 4, CTU Prague, 160 07, Czech Republic

^bDepartment of Structural Mechanics, Faculty of Civil Engineering, CTU Prague, Thákurova 7, 160 07, Czech Republic

^cDepartment of Applied Mathematics, Faculty of Transportation Sciences, Na Florenci 25, CTU Prague, 11000, Czech Republic

Available online 19 September 2004

Abstract

Transition metal dichalcogenides are well known for their lubricating properties. MoS₂ is the most popular member of this family and it is widely used as a solid lubricant in vacuum and inert gases. However, the lubricating properties of MoS₂ are deteriorated in humid air. It is known that molybdenum diselenide (MoSe₂) has the same crystal structure and also exhibits suitable lubricating properties, but their dependence on air humidity has not been studied yet in details.

This paper is aimed to the comparison of tribological properties of MoS₂ and MoSe₂ coatings measured in air of different humidity and at elevated temperatures. Both coatings were prepared by non-reactive DC magnetron sputtering and tested with ball-on-disc high temperature tribometer. The results of measurements of friction coefficient and wear rate vs. tribometer revolutions and the resulting dependencies of friction coefficient and wear rate on ambient air relative humidity are presented.

These results show that the friction coefficient of MoSe₂ was not influenced by air humidity. Wear rate of MoSe₂ in dry air was substantially higher than that of MoS₂; in humid air, the MoS₂ wear rate increased rapidly while wear rate of MoSe₂ remained unchanged. The operating temperature of both coatings was limited to 350 °C.

© 2004 Elsevier B.V. All rights reserved.

Keywords: Friction; MoSe₂; MoS₂; Solid lubricant coatings

1. Introduction

Transition metal dichalcogenides (sulfides, selenides or tellurides of tungsten, molybdenum and niobium) are well known for their lubricating property [1]. Low friction coefficient is caused by the special layered crystal structure. These structures consist of stack of layers in which a layer of metal is surrounded with layers of chalcogen atoms. The attraction between molybdenum and chalcogen is strong covalent bonding while there is only weak van der Waals attraction between sandwich layers. Therefore a slip between lamellae takes place when friction occurs and it results in low coefficient of friction and other tribological

phenomena, e.g. the transfer of coating material to opposing surface is possible.

MoS₂ is the most popular member of the above-mentioned family and it is widely used as a solid lubricant in vacuum and inert gases. Modern method of application is a magnetron sputtering, which improved tribological properties and provided the modification of chemical composition and crystal structure [2,3]. The main problem of MoS₂ used as a lubricant is the strong influence of humidity on the coating properties. Numbers of investigation have been done on that issue and a lot of different ways for solving the problem were shown [4,5].

There is lack of information on behavior of other dichalcogenides in humid air [6]. This paper is a contribution to comparison of the friction properties of the molybdenum disulfide (MoS₂) and molybdenum diselenide (MoSe₂) measured in the air of different humidity and at elevated temperatures. The comparatively high resistance of

* Corresponding author.

E-mail address: Tomas.Kubart@fs.cvut.cz (T. Kubart).

Table 1
Chemical composition of used materials (wt.%)

	Fe	C	Cr	Mn	Ni	P	S	Si
100Cr6	1	1.5	0.4	max 0.3	max 0.027	max 0.03	0.2	
Substrate	2	12	0.3	max 0.5	max 0.03	max 0.035	0.35	

MoSe₂ coatings to the ambient air relative humidity is presented.

2. Experimental details

The examined coatings were sputtered on substrates in the shape of discs 20 mm in diameter and 4 mm thick made from tool steel processed to the hardness of 60 HRC. The substrate chemical composition is in Table 1. The substrate surface was polished with diamond pastes to the roughness of Ra<30 nm using standard metallographic procedures. The samples were coated by DC magnetron sputtering in Ar atmosphere using planar cylindrical magnetron. The sputtering targets were MoS₂ resp. MoSe₂ (purity 99%) circular, 96 mm in diameter. Prior to deposition the apparatus was evacuated to 5×10⁻⁴ Pa and the deposition process was carried out at argon atmosphere of the pressure of 0.2 Pa. The relatively long target–substrate distance about 120 mm was chosen in order to achieve uniform film thickness on substrates. The samples were on earth potential during deposition.

The tribological tests were carried out with a high temperature ball-on-disc tribometer (CSM Instrument). This device allowed measurements of the friction coefficient continuously during sliding test at elevated temperatures from room temperature (RT) up to 800 °C in a controlled atmosphere. The counterparts used in these measurements were 100Cr6 bearing steel balls with 6 mm diameter. All measurements were provided with a load of 5 N and a sliding speed of 4 cm · s⁻¹ on radius in the range from 3 to 6 mm. Because of the variable diameter, the time dependence of the friction coefficient was evaluated on the number of cycles instead of the sliding distance. Number of cycles was 2000 unless stated otherwise. Measurements were performed in both dry nitrogen and humid air with relative humidity 35% and 50%. The declared values of relative humidity were measured at room temperature.

The worn volume was evaluated by means of the wear track width measurement. Since there was no significant ball wear, the wear track was assumed to be circular-shaped and its area was evaluated from measured width and known ball diameter. The coating wear rate w was determined from the cross-section area A of the wear track, loading force F and number of cycles n as

$$w = \frac{A}{nF}. \quad (1)$$

The wear track width was measured by optical microscope.

3. Results and discussion

3.1. Coatings properties

The stoichiometry of the MoSe₂ film determined by means of EDX was 1:1.91. X-ray diffraction showed hexagonal structure. In the case of MoS₂, the structure was a mixture of rhomboidal and hexagonal ones. The value of critical force at the scratch test was 60 N for MoS₂ and 50 N for MoSe₂ coatings.

3.2. Friction tests

Fig. 1 shows the typical dependence of MoS₂ friction coefficient as a function of the number of loading cycles at two different temperatures. It could be clearly seen that the temperature effect on friction properties of MoS₂. In comparison with the results measured at room temperature, the value of the friction coefficient was three times lower at 100 °C and the curve turned to be smoother (the standard deviation of the friction coefficient decreased from 0.015 at RT to 0.003 at 100 °C). All curves measured at elevated temperatures were similar to that one measured at 100 °C.

The friction properties of MoSe₂ were unaffected by the temperature up to 200 °C. Typical friction trace of the MoSe₂ at room temperature is shown in Fig. 2 and it remained unchanged at higher temperatures. When comparing Figs. 1 and 2 mind the different scales. The standard deviation of the friction coefficient value was about 0.002 in the case of MoS₂ at elevated temperature and 0.005 in the case of MoSe₂ at RT.

The temperature dependence of the mean values of the friction coefficient measured at 50% relative humidity after 2000 cycles is presented in Fig. 3 for both coatings. The value of MoS₂ friction coefficient at RT in humid air was 0.14, at 100 °C it decreased to values typical for dry air (0.05). The reason was the decrease in relative humidity of the atmosphere surrounding the heated sample (because the humidity was measured at RT). In contrast to MoS₂, the

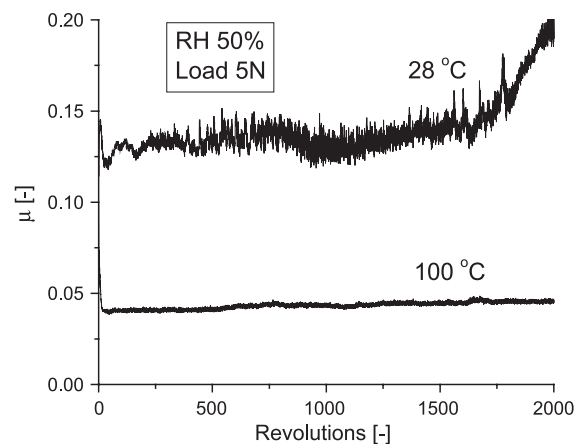


Fig. 1. Typical friction coefficient trace of MoS₂ measured at two different temperatures.

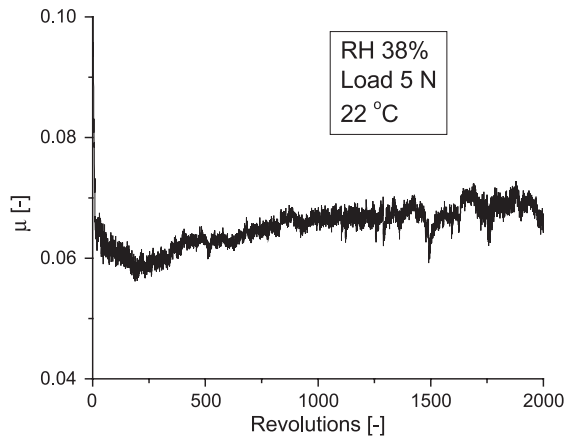


Fig. 2. Typical variation of friction coefficient with number of loading cycles at RT.

MoSe₂ coefficient of friction was stable up to 200 °C at a value of 0.06. At higher temperatures, both friction coefficients increased in similar way. The reason of this increase was the higher degree of oxidation that occurred at elevated temperature. Since the MoS₂ coating failed after 870 cycles at 400 °C, the value given in the Fig. 3 was the mean value measured at this lower number of cycles.

The friction coefficient vs. relative humidity obtained at RT is plotted in Fig. 4. The effect of relative humidity on the coefficient of friction of the MoS₂ corresponds to the results published in [7]. In dry air, the coefficient of friction was very low and rapidly increased with the increase in the relative humidity and the presence of moisture. The values obtained for MoSe₂ were independent of humidity within the range of the measurement uncertainty. Therefore the coating showed very good resistance to humidity in accordance with our expectation.

The MoS₂ layers exhibited considerable decrease in friction coefficient in running-in period proportional to the increase in temperature. At the temperatures above 150 °C, the running-in effect was negligible (less than 2 rev). Along with the changes in running-in period, the value of the

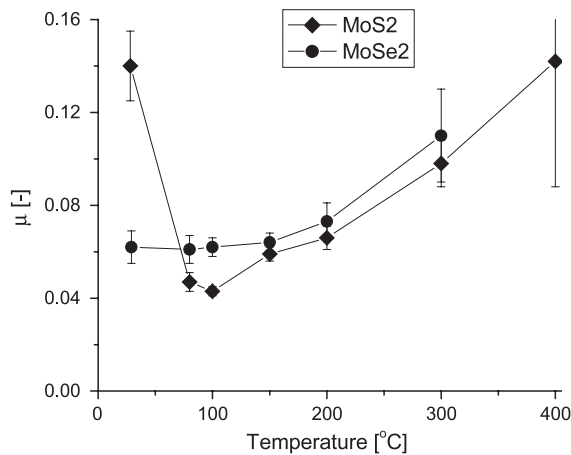


Fig. 3. Evolution of friction coefficient with temperature (relative humidity 50%). The error lines correspond to standard deviation of the mean value.

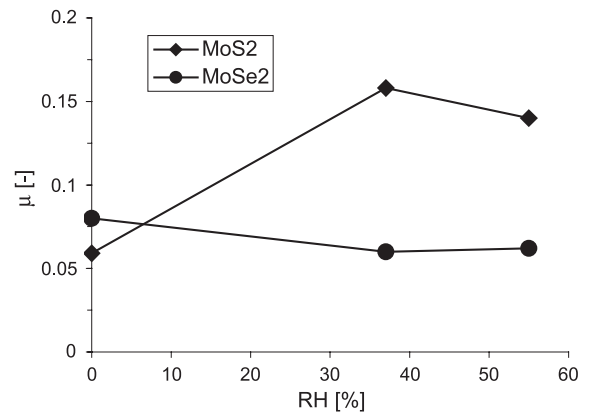


Fig. 4. Coefficient of friction at different values of relative humidity (RH).

friction coefficient in first contact decreased from 0.12 at RT to 0.1 at 100 °C and to 0.07 at 150 °C. It was a consequence of the lower energy necessary to crystal re-orientation at higher temperature [7]. Although the initial value of the friction coefficient at 150 °C was lower than values measured at lower temperature, steady-state value was significantly higher as a result of the oxidation.

Any clear connection between the coefficient of friction in first contact and temperature in the case of MoSe₂ was not found. However, during the running-in period, the friction coefficient decreased proportionally to temperature in the same way as in the case of MoS₂. The running-in effects became negligible above 100 °C. Hence the running-in of MoSe₂ was driven by the same mechanisms mentioned above in studies of MoS₂. The difference values of the friction coefficient at the first contact could be caused by different influence of adsorbed water.

It is assumed that in the case of MoS₂, water diffusion into inter-lamellae gap caused the increase in adhesion between the adjacent lamellae [6]. Thus, the friction coefficient and wear rate increased significantly. We supposed that higher coefficient of friction in the case of MoSe₂ was caused by stronger forces between lamellae. As a consequence, the water diffusion was inhibited. Because

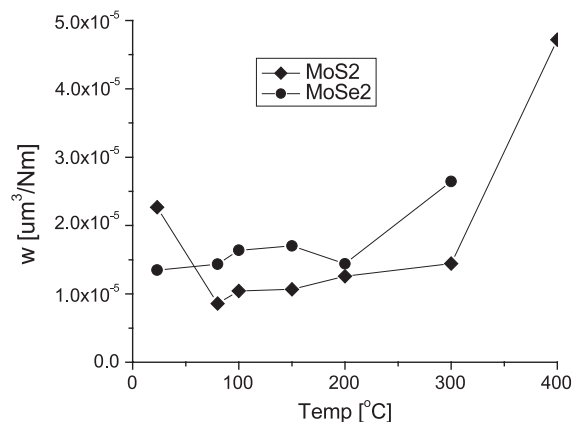


Fig. 5. Dependence of the wear rate on temperature at 50% RH.

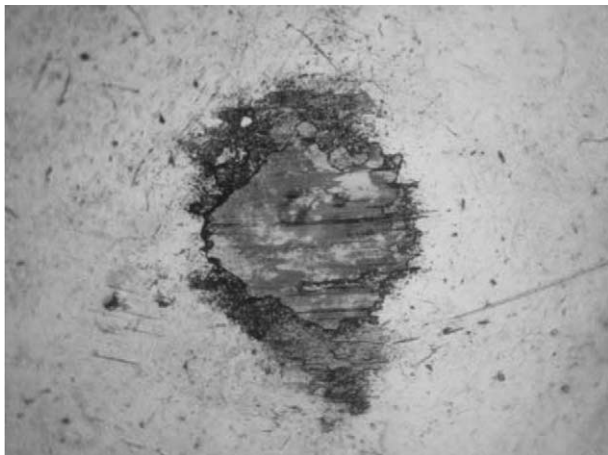


Fig. 6. Film formed on a ball surface after test of MoSe₂ coating at RT, RH 35%.

of the complexity of these processes, more accurate study is necessary.

3.3. Wear measurements

Wear rate was evaluated according to Eq. (1). The results at 50% RH is shown in Fig. 5 as a function of the temperature. At the RT, the MoS₂ wear rate was influenced by the humidity and raised very high value of $4 \times 10^{-5} \text{ mm}^3/\text{Nm}$. At elevated temperature, the wear rate was substantially lower than that of MoSe₂ (0.01 and 0.015). The wear rate of MoSe₂ was more influenced by temperature and increased more rapidly than that of MoS₂. For long-term use, the limiting temperature is about 300 °C.

Another required property of a lubricant is a protection of opposing surface. In the case of both MoS₂ and MoSe₂, the film formation on the counterpart surface was suitable. Fig. 6 shows the ball surface after test of MoSe₂ coating at RT, RH 35%.

4. Conclusion

The results of MoS₂ test were in good agreement with generally accepted expectation. The friction coefficient in

humid air increased rapidly to values three times higher than that in dry air. The increasing in temperature showed the same effect caused by the decrease in relative humidity at sample temperature.

It has been proven that MoSe₂ is a very promising solid lubricant with satisfactory friction properties. The performed test did not show any influence of the moisture on film properties. Both the friction coefficient and the wear rate remained stable in atmosphere with different relative humidity. In dry air, the friction properties were slightly worse compared to MoS₂; however, in terrestrial atmosphere, pure MoS₂ was useless.

Since the friction is driven by the same mechanism in both materials, interesting results could bring co-sputtering of MoSe₂ with any metal. Also, the effect of sputtering parameters on film properties and adhesion should be studied in detail.

Acknowledgements

This work was supported by grant FRV 2413/G1 and GACR 106/02/1321 and research project MSM 212200008.

References

- [1] W.E. Jamison, S.L. Cosgrove, Friction characteristics of transition-metal disulfides and diselenides, *ASLE Trans.* 14 (1971) 62.
- [2] G. Weisse, N. Mattern, H. Hermann, A. Teresiak, I. Bacher, W. Bruckner, H.-D. Bauer, H. Vinzelberg, G. Reiss, U. Kreissig, M. Mader, P. Markschlager, Preparation, structure and properties of MoS_x films, *Thin Solid Films* 298 (1997) 98.
- [3] T. Spalvins, Coatings for wear and lubrication, *Thin Solid Films* 53 (1978) 285.
- [4] D.G. Teer, New solid lubricant coatings, *Wear* 251 (2001) 1068.
- [5] Y.L. Su, W.H. Kao, Tribological behavior and wear mechanism of MoS₂-Cr coatings sliding against various counterbody, *Tribol. Int.* 36 (2003) 11.
- [6] A.R. Lansdown, *Molybdenum Disulphide Lubrication*, Elsevier, 1999.
- [7] C. Pritchard, J.W. Mingley, The effect of humidity on the friction and life of unbonded molybdenum disulphide films, *Wear* 13 (1969) 39.

Tribological behaviour of C-alloyed transition metal dichalcogenides (TMD) coatings in different environments

Manuel Evaristo · Tomas Polcar · Albano Cavaleiro

Received: 20 November 2006 / Accepted: 16 July 2007 / Published online: 28 July 2007
© Springer Science+Business Media B.V. 2007

Abstract W-S-C films were deposited by non-reactive sputtering from a carbon target incrustated with WS₂ pellets in the eroded zone. This process allows depositing coatings with a wide range of compositions, with a precise control of their carbon content. Before the deposition, a Ti interlayer was interposed between the film and the substrate to improve the final adhesion. The carbon content in W-S-C system was varied from 29 at.% to 70 at.%, which led to an hardness enhancement from 4 GPa up to 10 GPa where the maximum hardness was reached in films with a carbon content between 40 at.% and 50 at.%. The tribological behaviour of the coatings was evaluated by pin-on-disk testing, in environments with different humidity levels. Generally, the tribological performance of W-S-C coatings in environments with moderate to high humidity is better for coatings with high carbon content. Friction coefficients, as 0.05 or lower could be reached at low humidity ranges (<7%) to all compositions. However, for higher humidity values, friction coefficient

increased up to 0.30 in the W-S-C film with low carbon content whereas it was kept approximately constant for the others compositions.

Keywords C-TMD · Low friction · Self-lubricant · Wear behaviour · WS₂

1 Introduction

Transition metal dichalcogenides (TMD) have excellent self-lubricant properties in dry air or vacuum; however, these films are easily rusted in the presence of moist environments and their reduced mechanical resistance makes them inappropriate for applications requiring high loading bearing capacity. On the other hand, hard coatings are often employed to protect from abrasive and erosive wear; however, they do not have low friction and they are frequently brittle. Therefore, there is a need to design coatings combining low friction with high load bearing capacity; moreover, a good adhesion to the substrates is required. Recently (Voevodin et al. 1999) made use of the concept of nanocomposite structured coatings to reach very low friction coefficients in a large range of environments. Based on their previous experience with diamond like carbon (DLC) coatings, they co-deposited DLC with WS₂ using pulsed laser deposition. DLC is a very hard material (hardness from 10 GPa to 60 GPa) presenting very low friction coefficient in humid air. However, inversely to WS₂

M. Evaristo · T. Polcar · A. Cavaleiro (✉)
ICEMS – Departamento Engenharia Mecânica, Faculdade de Ciências e Tecnologia da Universidade de Coimbra, Rua Luís Reis Santos, Coimbra, 3030-078, Portugal
e-mail: albano.cavaleiro@dem.uc.pt

T. Polcar
Faculty of Transportation Sciences, Department of Applied Mathematics, CTU in Prague, Na Florenci 25, Prague 1, Czech Republic

coatings, the friction coefficient increases significantly when tested in moisture free environments. Thus, with a nanostructure consisting of nanocrystals of WS₂ and WC enclosed in an amorphous carbon matrix, values lower than 0.1 could be envisaged whatever the testing environment was. Our recent works (Nossa and Cavaleiro 2001, 2003) showed that the synergetic effect of doping W-S films with carbon or nitrogen together with the deposition of a Ti interlayer could give rise to significant improvements of the mechanical properties and the tribological behaviour, particularly in the case of films alloyed with carbon.

There are several ways to produce multi-element thin films by a non-reactive process; one of the most common is by co-sputtering from individual targets (Fox et al. 1999). However, among the drawbacks of this process is either the non-homogeneity in the coatings composition when stationary large substrates are used, or the formation of a multilayer structure if the substrates are rotated (Noshiro et al. 2006). Thus, it was decided to deposit W-S-C coatings by non-reactive magnetron sputtering from carbon target with pellets of WS₂ placed in the target erosion zone, in order to assure the homogeneity in the coatings composition. Furthermore, the chemical composition can also be easily controlled by changing the number of WS₂ pellets.

The objective of this work was the development of coatings capable of being used in a wide range of applications, with different applied loads, temperatures and environments. In this study, the structural and mechanical properties of W-S-C coatings are presented, as well as their tribological behaviour is evaluated when sliding in a pin-on-disc tribometer in different environments.

2 Experimental details

All W-S-C coatings were deposited on 100Cr6 discs with a diameter of 36 mm and M2 polished steel samples with hardness close to 5 GPa and 9 GPa, respectively.

The depositions were carried out in a radio-frequency magnetron sputtering Edwards ESM 100 unit, equipped with two cathodes ($\varnothing = 100$ mm). Prior to the depositions the substrates were sputter cleaned during 20 min by establishing the plasma

close to the substrates electrode. Immediately after, a Ti interlayer was deposited with an approximate thickness of 300 nm. The main sputtering target was pure carbon, partly covered by WS₂ pellets placed in the preferentially eroded zone. The dimensions of the pellets were $4.1 \times 3.5 \times 1.5$ mm. The degree of target coverage determined the overall chemical composition of the sputtered film. The depositions were carried out with constant power density of 7.6 W/cm^2 in the carbon target.

To evaluate the chemical composition of the films, a Cameca SX 50 electron probe microanalysis (EPMA, Cameca, France) apparatus was used. The hardness was determined by depth-sensing indentation technique using a Fisherscope H100; the coatings deposited on M2 steel were used for these measurements. The load was increased in steps (60) until a nominal load of 20 mN was reached, following the procedure indicated somewhere (Antunes et al. 2002).

The tribological tests were carried out with a pin-on-disk tribometer (CSM Instrument) on 100Cr6 samples. The linear speed was kept constant (20 mm s^{-1}), while the diameter varied from 12 mm to 16 mm. The 100Cr6 steel balls were used as sliding partners. The diameter of the ball was 6 mm, which together with the applied 5 N load gives the maximum Hertz contact pressure of ~ 0.7 GPa. The coatings tribological behaviour was evaluated in air with different humidity rate (5–70%). The friction coefficient reported in this study is the average value of the whole sliding test, unless stated otherwise. Each test was repeated three times; standard deviation of the average friction coefficient and the wear rate was lower than 10%. Standard number of laps during pin-on-disc measurement was 1500.

3 Results

Different carbon contents were achieved in the coatings by varying the number of WS₂ pellets in the C target. As it was expected, the carbon content of the films decreases with the increase of the total area of pellets, see Fig. 1; the decrease is almost linear. A closer analysis of the arrangement of the experimental points allows estimating the reproducibility of chemical composition. We deposited coatings with the area of pellets 260 and 1070 mm² (corresponding

to composition of low and high carbon content) three times (always with new re-distribution of pellets), which allows estimating the reproducibility of the coating chemical composition. Considering the variation in the pellet distribution over the target erosion zone and the errors of measurements, it can be concluded that the used deposition process is quite reproducible.

The deposition rate rises up with increasing number of pellets, as may be expected due to the higher deposition rate of WS_2 compared to carbon (Fig. 1). However, after reaching a maximum for an area of pellets of 400–600 mm^2 , the deposition rate started to decrease. This behaviour is difficult to explain, since the difference of the sputtering yield for the target and the pellets is usually considered as the main factor contributing to the increase/decrease of the deposition rate as a function of the pellets area (Yokomichi et al. 2002). Moreover, the densification of the coatings with increasing carbon content, as it will be shown later on, is as well in favour to the increase of the deposition rate with the pellets area. This matter requires further study, particularly with respect to the possible mutual interference of the pellets during the deposition process.

Figure 2 shows the decreasing content of oxygen in the coatings with their carbon content. It is not surprising, since WS_2 pellets exhibit a high porosity and affect the residual atmosphere in the deposition chamber. The variation of S/W ratio is negligible in the range 1.2–1.45; however, a slight increase can be observed, as demonstrated in Fig. 2. The sulphur

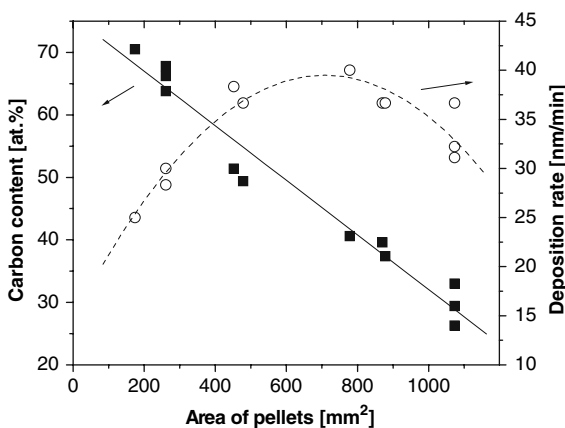


Fig. 1 Carbon content and deposition rate as a function of the total area of WS_2 pellets. The lines are guides to the eye

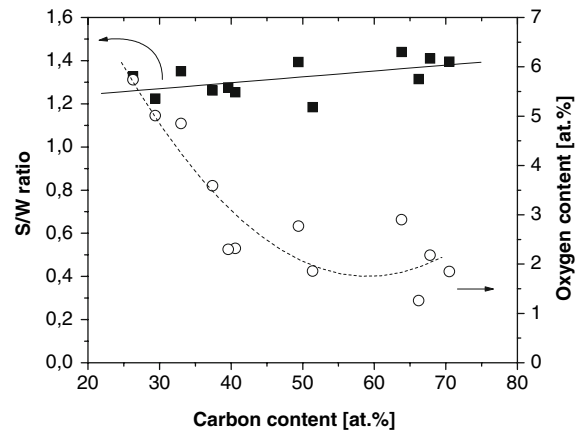
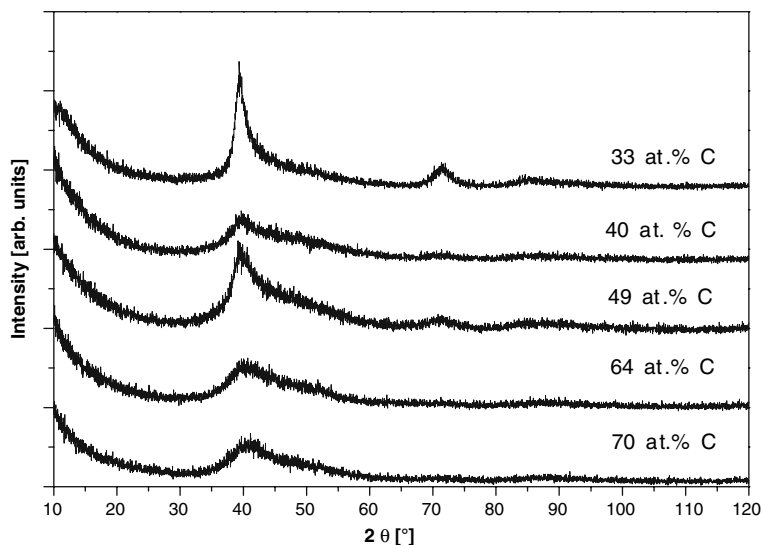


Fig. 2 S/W ratio and oxygen content as a function of carbon content in the coatings. The lines are guides to the eye

deficiency is probably caused by the re-sputtering of the sulphur atoms from the substrate and by the chemical reactions of sulphur with the residual atmosphere. It should be pointed out that the S/W ratio is lower than that of co-sputtering from two targets under similar conditions (~ 1.7) (Evaristo et al. 2005).

Figure 3 presents the X-ray diffraction patterns of W-S-C films with different chemical composition. With the increase of carbon in the coatings, a gradual loss of crystallinity is observed. The films with low carbon content presents the typical XRD patterns of Me-S (Me-transition metal) sputtered films with prominent peaks at $2\theta \approx 40^\circ$ with an extended shoulder corresponding to a turbostrating stacking of (10L) planes ($L = 0, 1, 2, 3$), and $2\theta \approx 70^\circ$ indexed as (110) plans. Weise et al. (1997) demonstrated that these XRD pattern could be explained by a 2D organization of the basal plans which could have several tenths of unit cells dimension. With the progressive decrease of the lateral dimensions of the basal plans, either broadening or drop in the intensity of the (10L) plan occurred until a unique low intensity and broad peak typical of an amorphous structure was detected. This situation would arise when the lateral order of the basal plans did not exceed a couple of lattice parameters. In previous work (Nossa et al. 2005), it was shown by HRTEM that W-S-C films with high C contents were formed by a nanocomposite structure with WS_2 grains with only some nanometers size, in agreement with Weise et al. interpretation.

Fig. 3 XRD patterns of W-S-C as a function of carbon content



Typical cross section morphology of the films deposited on Si wafers obtained by Scanning Electron Microscopy (SEM) can be observed in Fig. 4. As it would be expected, based on previous results with W-S-C films deposited by other procedures (Evaristo et al. 2005), more compact morphologies are reached with increasing C contents.

The hardness of W-S-C films increases with increasing carbon content, reaching a maximum at ~ 40 at.% of carbon. This trend can be related to the increase of the compactness of the films associated with the possible formation of nano-sized carbide phases, intrinsically harder than tungsten disulphide. With the addition of more carbon to the films, there is no more W available to establish W-C bonds and the formation of carbon phases leads to a decrease of the hardness (see Fig. 5). However, the hardness of W-S-C coatings is generally about one order of magnitude higher than that of pure tungsten disulphide (Watanabe et al. 2004).

The evolution of the friction coefficient is almost identical for all coatings up to humidity level of 30%. The average friction coefficient in dry air ($RH < 5\%$) is very low reaching values in the range 0.03–0.06. The tests in humid air exhibited similar increase of the friction value up to about 0.2 for a humidity rate of 40%. Above this value, difference in the coefficient can then be observed (Fig. 6). In general, the coatings with higher carbon content are much less sensitive to high level of humidity, showing even benefits from these conditions as it is demonstrated

by the small decrease in the friction. On the other hand, the coatings with high content of WS_2 behave similarly to pure transition metal dichalcogenide, showing the typical monotonous increase of the friction coefficient with increasing humidity rates.

In contrast to the friction coefficient, the wear rate of the coating with the highest carbon content (66 at.% C) significantly differs from the others when sliding in dry air (see Fig. 7). Moreover, the coatings with 33 and 37 at.% C exhibited the best wear resistance, even in humid air, with wear rates slightly increasing with humidity. The hardest coating (41 at.% C) showed the highest wear in humid air.

To explain the friction and wear behaviour, detailed analysis of either the friction curves or the wear tracks was performed. As documented in Fig. 8, the initial friction coefficient of the coating with 66 at.% C is very high during the first 25 turns and falls down abruptly to a steady-state regime at the lowest stabilised value. The coating with low carbon content reaches the steady-state more slowly, only after approximately 250 laps; nevertheless, its maximum initial friction coefficient is only 0.15 compared to the 0.65 obtained for 66 at.% C coating. The comparison of the wear tracks of both coatings shows fundamental differences. In the case of the coating with high carbon content it is full of large cracks and delaminations (Fig. 9b), while that of low carbon shows only shallow scratches parallel to the relative movement of the ball over the coating surface.

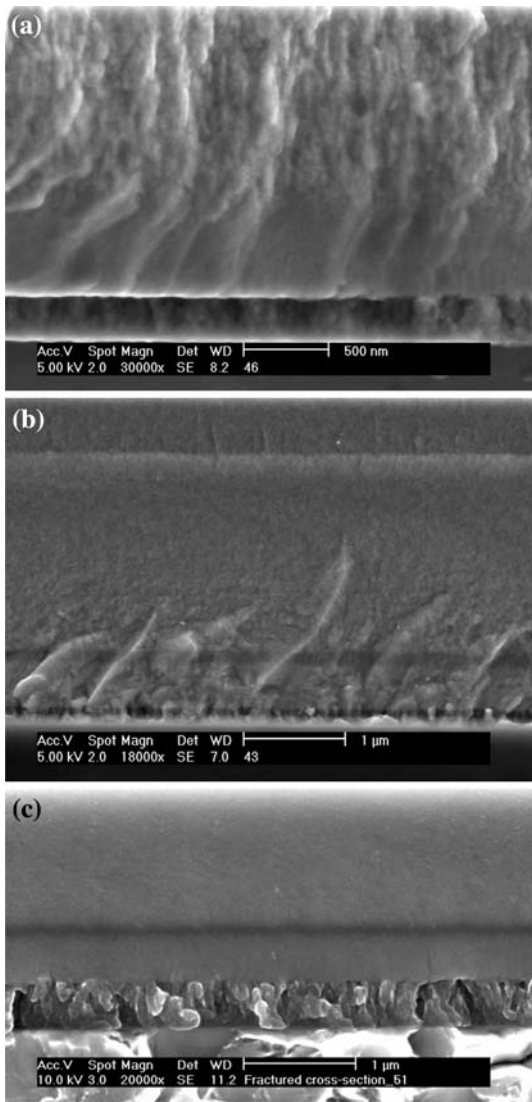


Fig. 4 SEM images of the cross-section of W-S-C films with different carbon contents. (a) 33 at.%; (b) 41 at.%; (c) 66 at.%

The question now is: does the wear rate of the high carbon coating arise from the very high initial friction? To shed some light on this subject, a short sliding test (number of laps was set to 50) in dry air was carried out with this coating. The worn volume of the coating after this short test was almost identical to that of the 1,500 laps test with the wear track exhibiting similar features. It seems that the tribological behaviour in dry air is particularly driven by the formation of a third-body between the surfaces in the contact by the transfer of the self-lubricant

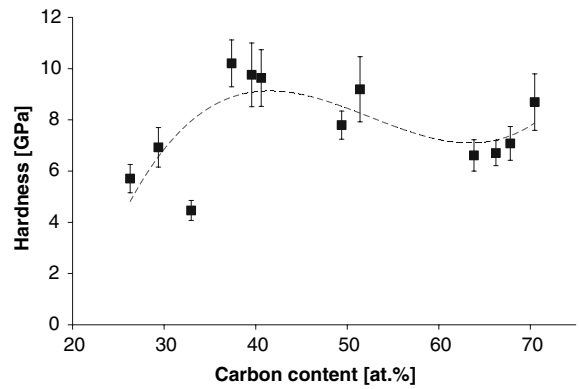


Fig. 5 Evolution of the hardness with the carbon content in the films. The line is a guide to the eye

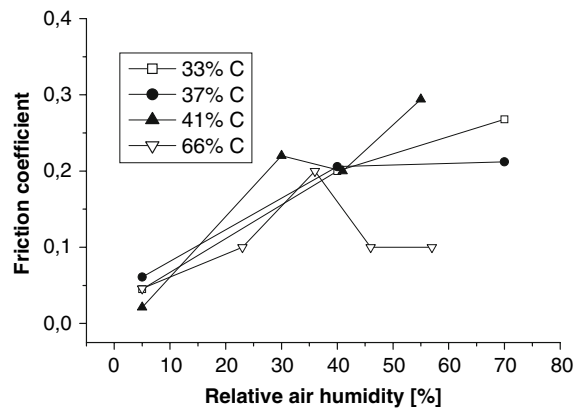


Fig. 6 Evolution of average friction coefficient with humidity

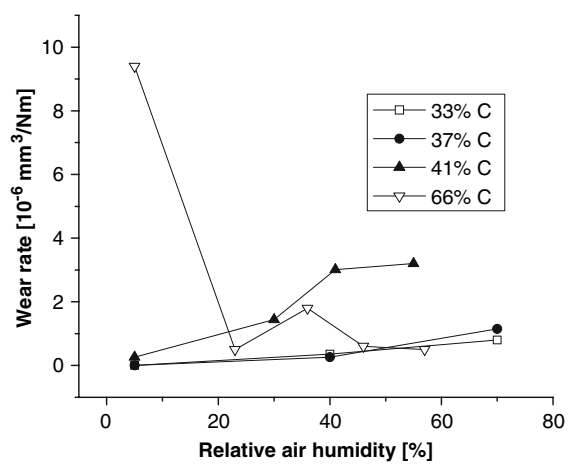


Fig. 7 Wear rate of coatings with different carbon content as a function of relative humidity of air

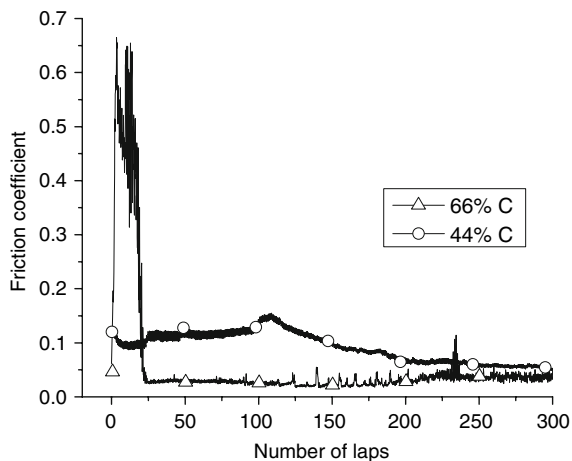


Fig. 8 Friction curves of W-S-C coatings sliding in dry air, first 300 cycles

material to the steel ball. When the third-body and transferred layer are formed, the steady-state wear regime takes place. With the high-carbon coating, in the beginning of the sliding test there is a limited self-lubricant WS_2 material available to form the third body. As a consequence, the initial friction force is very high causing severe damage to the coating

Fig. 9 SEM micrographs of the wear track, sliding in dry air, (a) coating with 33 and (b) coating with 66% of carbon content

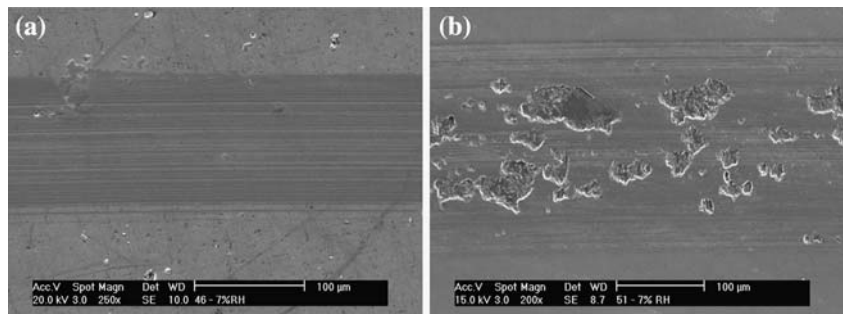
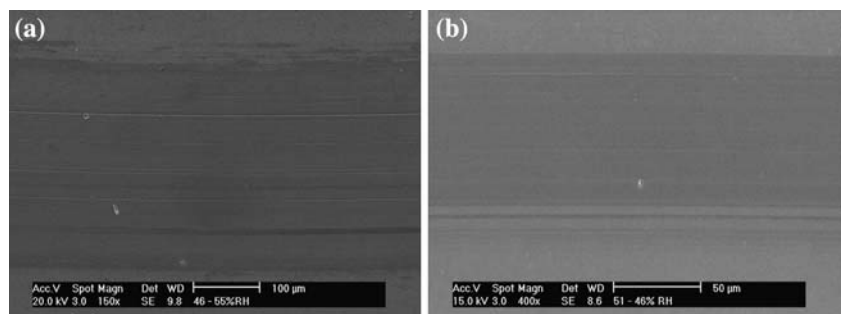


Fig. 10 SEM micrographs of the wear tracks after sliding in humid air, (a) coating with 33 at.% of carbon (RH 40%), (b) coating with carbon content 66 at.% (RH 43%)



surface. During this period a rapid release of a large quantity of material between the ball and the coating occurs, which facilitates the quick forming of the transfer layer of self-lubricant material on the ball surface. From that moment on, the friction rapidly falls down from the highest to the lowest value.

In the coating with low carbon content the high initial wear is much less. Since the worn volume is very limited, it takes more time to reach the steady-state regime. Immediately from the first contact moment, the WS_2 phase starts to influence the friction behaviour with a progressive and moderate decrease of the friction coefficient. We assume that the wear rate of low-carbon coating is as well higher during initial part of sliding tests, though the difference should be much lower compared to high-carbon coating. However, it is difficult to prove this hypothesis, since the wear rate of low-carbon content coating is very low for precise wear track profile measurements.

The values of wear rates of coatings with low and high carbon content sliding in humid air are almost equal. However, the wear tracks of low carbon content coatings exhibit scratches (Fig. 10), thus, the formation of hard large particles is possible.

Moreover, the friction coefficient showed large variation during the test with low carbon content compared to very stable one of high carbon.

4 Conclusions

The W-S-C coatings were deposited by non-reactive magnetron sputtering from the carbon target with WS₂ pellets placed in the erosion zone. The carbon content linearly decreased with increasing area covered with the pellets, from 27 at.% to 70 at.%, while S/W ratio remained almost constant. The coatings exhibited hardness in the range 4–10 GPa; the maximum hardness was obtained in case of coating with 37 at.% of carbon content. The coatings with carbon content 37 and 41 at.% showed the best sliding properties in the dry and humid air.

Acknowledgements This work was supported by the Czech Science Foundation through the project 106/07/P014.

References

- Antunes, J. M., Cavaleiro, A., Menezes, L. F., Simões, M. I., Fernandes, J. V.: Ultra-microhardness testing procedure with Vickers indenter. *Surf. Coat. Technol.* **149**, 27–35 (2002)
- Evaristo, M., Nossa, A., Cavaleiro, A.: W-S-C sputtered films: influence of the carbon alloying method on the mechanical properties. *Surf. Coat. Technol.* **200**, 1076–1079 (2005)
- Fox, V. C., Renevier, N., Teer, D. G., Hampshire, J., Rigato, V.: The structure of tribologically improved MoS₂-metal composite coatings and their industrial applications. *Surf. Coat. Technol.* **116–119**, 492–497 (1999)
- Noshiro, J., Watanabe, S., Sakurai, T., Miyake, S.: Friction properties of co-sputtered sulfide/DLC solid lubricant films. *Surf. Coat. Technol.* **200**, 5849–5854 (2006)
- Nossa, A., Cavaleiro, A.: The influence of the addition of C and N on the wear behaviour of W-S-C/N coatings. *Surf. Coat. Technol.* **142–144**, 984–991 (2001)
- Nossa, A., Cavaleiro A.: Mechanical behaviour of W-S-N and W-S-C sputtered coatings deposited with a Ti interlayer. *Surf. Coat. Technol.* **163–164**, 552–560 (2003)
- Nossa, A., Cavaleiro, A., Carvalho, N. J.M., Kooi, B. J., De Hosson, J.Th.M.: On the microstructure of tungsten disulfide films alloyed with carbon and nitrogen. *Thin Solid Films* **484**, 389–395 (2005)
- Voevodin, A.A., O'Neill, J.P., Zabinski, J.S.: Nanocomposite tribological coatings for aerospace applications. *Surf. Coat. Technol.* **116–119**, 36–45 (1999)
- Watanabe, S., Noshiro, J., Miyake, S.: Tribological characteristics of WS₂/MoS₂ solid lubricating multilayer films. *Surf. Coat. Technol.* **183**, 347–351 (2004)
- Weise, G., Mattern, N., Herman, H., Teresiak, A., Bascher, I., Bruckner, W., Bauer, H.-D., Vinzelberg, H., Reiss, G., Kreissig, U., Mader, M., Markschlager, P.: Preparation, structure and properties of MoS_x films. *Thin Solid Films* **298**, 98–106 (1997)
- Yokomichi, H., Funakawa, T., Masuda, A.: Preparation of boron-carbon-nitrogen thin films by magnetron sputtering. *Vacuum* **66**, 245–249 (2002)

The tribological behavior of W–S–C films in pin-on-disk testing at elevated temperature

T. Polcar^{a,b}, M. Evaristo^a, A. Cavaleiro^{a,*}

^aDep. Eng. Mecânica, ICEMS Faculdade de Ciências e Tecnologia da Universidade de Coimbra, Rua Luís Reis Santos, 3030-788 Coimbra, Portugal

^bDepartment of Applied Mathematics, Faculty of Transportation Sciences, CTU in Prague, Na Florenci 25, Prague 1, Czech Republic

Abstract

W–S–C films were deposited by magnetron sputtering in an Ar atmosphere with a Ti interlayer. A carbon target with several pellets of WS₂ incrustated in the zone of the preferential erosion was used. The number of pellets was changed to modify the carbon content in the films, which varied from 29 up to 70 at%. Doping W–S films with carbon led to a substantial increase of the hardness in the range 4–10 GPa; the maximum of hardness was obtained for coatings with the carbon content of 40 at%. X-ray diffraction (XRD) patterns showed that there was a loss of crystallinity with the increase of the carbon content in the film.

The coatings were tested by pin-on-disk from room temperature (RT) up to 400 °C. At RT, the friction coefficient was in the range 0.2–0.30. At temperatures higher than 100 °C, the friction is below 0.05 for all compositions. The tribological behavior of the coatings with increasing temperatures depended on the films carbon content. For low-carbon content up to 40%, the wear rate was almost independent of the temperature up to 300 °C, while it increased dramatically in the case of the coatings with high-carbon content. In general, the limiting temperature for W–S–C coatings is 400 °C.

© 2007 Elsevier Ltd. All rights reserved.

Keywords: W–S–C coating; Self-lubrication; Tribology; High temperature

1. Introduction

Transition metal dichalcogenides (TMD) have excellent self-lubricant properties in dry air or vacuum; however, these films are easily rusted in the presence of moist environments and their reduced mechanical resistance makes them inappropriate for applications requiring high-load bearing capacity. On the other hand, hard coatings are often employed to protect from abrasive and erosive wear; however, they do not have low friction and they are frequently brittle. Therefore, there is a need to design coatings combining low friction with high-load bearing capacity; moreover, a good adhesion to the substrates is required. Our recent works showed that the synergetic effect of doping W–S films with carbon or nitrogen together with the deposition of a Ti interlayer could give rise to significant improvements of the mechan-

ical properties and the tribological behavior, particularly in the case of films alloyed with carbon [1,2].

The objective of this work was the development of coatings capable of being used in a wide range of applications, with different applied loads, temperatures and environments. In this study, the structural and mechanical properties of W–S–C coatings are presented together with their tribological behavior at elevated temperature.

2. Experimental details

All W–S–C coatings were deposited on 100Cr6 and M2 polished steel samples with hardness close to 5 and 9 GPa, respectively. The depositions were carried out in a radio-frequency (RF) magnetron sputtering Edwards ESM 100 unit, equipped with two cathodes ($\varnothing = 100$ mm). Prior to the depositions the substrates were sputter cleaned during 20 min by establishing the plasma close to the substrates electrode. Immediately after, a Ti interlayer was deposited with an approximate thickness of 300 nm. The

*Corresponding author. Tel.: +351 239 790 700; fax: +351 239 790 70.
E-mail address: albano.cavaleiro@dem.uc.pt (A. Cavaleiro).

main sputtering target was pure carbon, partly covered by WS₂ pellets placed in the preferentially eroded zone. The dimensions of the pellets were 4.1 × 3.5 × 1.5 mm. The degree of target coverage determined the overall chemical composition of the sputtered film. The depositions were carried out with constant power density of 7.6 W cm⁻² in the carbon target.

To evaluate the chemical composition of the films, a Cameca SX 50 electron probe microanalysis was used. The hardness was determined by depth-sensing indentation technique using a Fisherscope H100; the coatings deposited on M2 steel were used for these measurements.

The tribological tests were carried out with a pin-on-disk tribometer (CSM Instrument). 100Cr6 steel balls were used as sliding partners. The diameter of the ball was 6 mm which, together with an applied 5 N load, gives a maximum Hertz contact pressure of ~0.7 GPa. The coatings tribological behavior was evaluated in air with a relative humidity of 30% and in dry nitrogen. The friction coefficient reported in this study is the average value of the whole sliding test, unless stated otherwise. The standard number of laps during the pin-on-disk measurements was 1500.

3. Results and discussion

3.1. Chemical composition, structure and mechanical properties

Different carbon contents were achieved in the coatings by varying the number of WS₂ pellets in the C target. As it was expected, the carbon content of the films decreases almost linearly with the increase of the total area of pellets. The chemical composition of the deposited coatings varied from 29 to 70 at% C (hereinafter, denomination at% C represents carbon content in the coating); the coatings with carbon contents of 29, 40, 51 and 64 at% were tribologically tested. The S/W ratio varied in the range 1.2–1.45; being the slight increase observed with increasing carbon content. The sulfur deficiency is probably caused by the re-sputtering of sulfur atoms from the substrate and by the chemical reactions of sulfur with the residual atmosphere.

X-ray diffraction (XRD) patterns of W–S–C films showed a gradual loss of crystallinity with the increase of carbon in the coatings. The films with a low-carbon content presents the typical XRD patterns of Me–S (Me—transition metal) sputtered films with prominent peaks at $2\theta \approx 40^\circ$ with an extended shoulder corresponding to a turbostrating stacking of (10L) planes ($L = 0, 1, 2, 3$), and $2\theta \approx 70^\circ$ indexed as (1 1 0) planes. Weise et al. [3] demonstrated that referred XRD patterns could be explained by a two-dimensional (2D) organization of the basal plans which could have several tenths of unit cells dimension. With the progressive decrease of the lateral dimensions of the basal plans, either broadening or drop in the intensity of the (10L) plan occurred until a unique low intensity and broad peak typical of an amorphous structure was detected. This situation would arise when the lateral order

of the basal plans did not exceed a couple of lattice parameters [3]. In previous work, it was shown by high-resolution transmission electron microscopy (HRTEM) that W–S–C films with high C contents were formed by a nanocomposite structure which included WS₂ grains with only some nanometers size, in agreement with Weise et al. interpretation [4].

The hardness of W–S–C films increases with increasing carbon content, reaching a maximum at ~40 at% C. This trend can be related to the increase of the compactness of the films associated with the possible formation of nano-sized carbide phases, intrinsically harder than tungsten disulfide. With the addition of more carbon to the films, there is no more W available to establish W–C bonds and the formation of carbon phases leads to a decrease of the hardness (see Fig. 1). However, the hardness of W–S–C coatings is generally about one order of magnitude higher than that of pure tungsten disulfide [5].

3.2. Sliding properties

The easy intra and intercrystalline slip in the friction contact due to weak van der Waal's forces between the lamellae of S–M–S hexagonal basal planes of pure tungsten disulfide facilitates the friction by diminishing the tangential force necessary for the sliding. During a pin-on-disk test, the transfer of the coating material to the ball surface and the reorientation induced by the friction of the randomly oriented WS₂ grains, in the contact area, to the basal plane orientation, transforms the materials in contact. Consequently, the friction force originated in this case is due, predominantly, from the type of slipping referred to above. Zabinski et al. [6] showed for W–S–C system with 20 at% of sulfur content that the friction mechanism intervening in a sliding contact was very similar to that of pure tungsten disulfide and that the contribution of the carbon to the friction was negligible. In the present

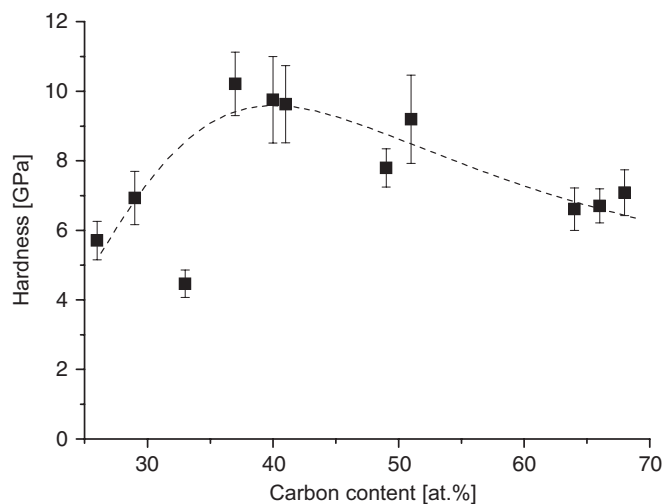


Fig. 1. Evolution of the hardness with the carbon content in the films. The line is a guide to the eye.

study, a thick transferred layer to the ball was observed which exhibits a higher W–S/C ratio than the original one of the coating. It may be assumed that the sliding partner after a couple of turns is represented by that thin layer, mainly tungsten disulfide, with basal planes parallel to the sliding direction.

The evolution of the friction coefficient with temperature is depicted in Fig. 2. The value of the friction coefficient at room temperature (RT) is close to 0.2, with the exception of the coating with 29 at% C, which exhibited a rather higher value of 0.3. However, the friction rapidly falls down with the temperature increase. It is well known that TMD exhibit excellent friction properties in vacuum or in dry atmosphere, while a humidity-containing atmosphere has a detrimental effect leading to the increase of the friction and the wear. Thus, the low-friction coefficient at a test temperature of 100 °C, which can be as low as 0.03–0.04, could be explained by the drying of the air. However, a pertinent remark could be raised: would it be the drying of the air the only factor contributing to the sliding process?

To answer this question, first, the influence of possible structural and chemical changes after heating was taken into account. Neither XRD nor EPMA analyses allowed detecting any change on the structure and chemical composition of the coating tested at 100 °C in relation to the as-deposited condition. Second, sliding tests were carried out in dry nitrogen, with the scope of separating the role of the drying from any other factor contributing to the sliding process. The friction coefficient in dry nitrogen was about 0.02 higher than that measured in 100 °C tests whichever the coating was. Hence, from these results, it seems that besides drying another factor should contribute for the low-friction value measured. The increase of temperature can further facilitate the crystalline slipping of the weakly bonded basal planes and, therefore, contributes for diminishing the friction. Qualitative iden-

tical results were obtained for pure MoS₂ and MoSe₂ coatings also belonging to the TMD family, which showed higher friction in dry nitrogen than at a temperature of 80 or 100 °C [7].

The friction coefficient started to increase with the temperature reaching a maximum at a temperature of 300 °C in both coatings with extreme carbon content (the highest and the lowest studied), while it remained stable for the 40 and 51 at% C films. This increase is influenced by the change in the wear mechanism, as described later on. Up to 300 °C, the wear rate was very low not exceeding $2.5 \times 10^{-6} \text{ mm}^3 \text{ N}^{-1} \text{ m}^{-1}$, see Fig. 3. The only exception was the coating with the highest carbon content which exhibits a steady increase of the wear rate in this temperature range. To understand such a behavior, a detailed analysis of the friction curves and the wear tracks was carried out. For the tests performed with the samples heated, the coating with 64 at% C presented high friction (~0.35) during running-in period taking about 25 revolutions on the pin-on-disc test to reach the steady-state. On the contrary, a rapid decrease in the friction from a value of 0.1 down to the steady state value was observed for the coatings with lower carbon. The wear tracks look polished-like for almost all coatings (Fig. 4(a)), while large delaminated areas are visualized for the one with 64 at% C (Fig. 4(b)). A similar behavior was found for tests in dry nitrogen at RT.

A further set of sliding tests were performed with a short number of cycles (250). The specimen with the highest carbon content showed a very large worn volume of coating material, comparable to the one after 1000 cycles. As referred to above, the tribological behavior in dry air is particularly driven by the formation of a third body between the surfaces in the contact and by the transfer of the self-lubricant material to the steel ball. When the third body and the transferred layer are formed, the steady-state wear regime takes place. Considering the high-carbon

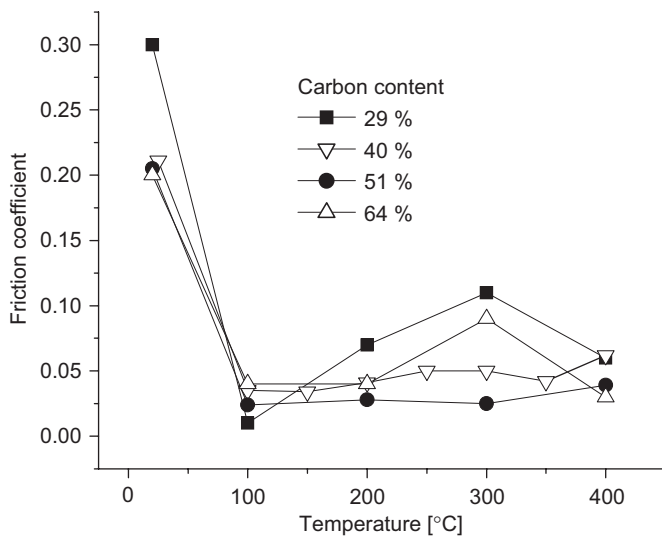


Fig. 2. Friction coefficient of W–S–C coatings as a function of temperature.

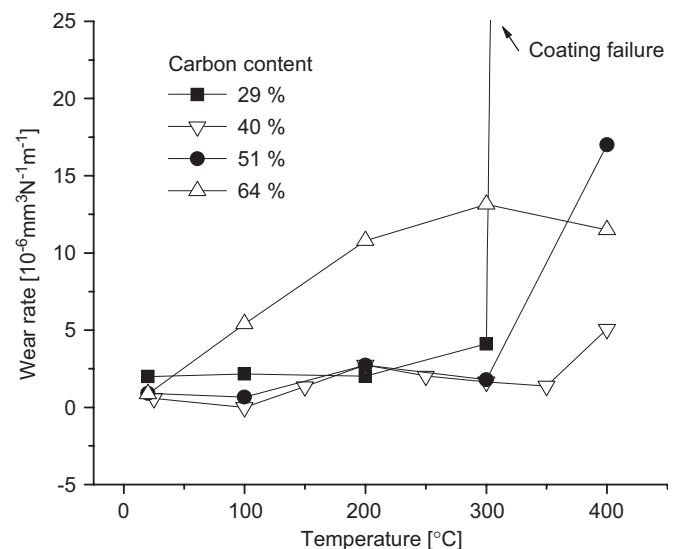


Fig. 3. Evolution of the wear rate of W–S–C coatings with temperature.

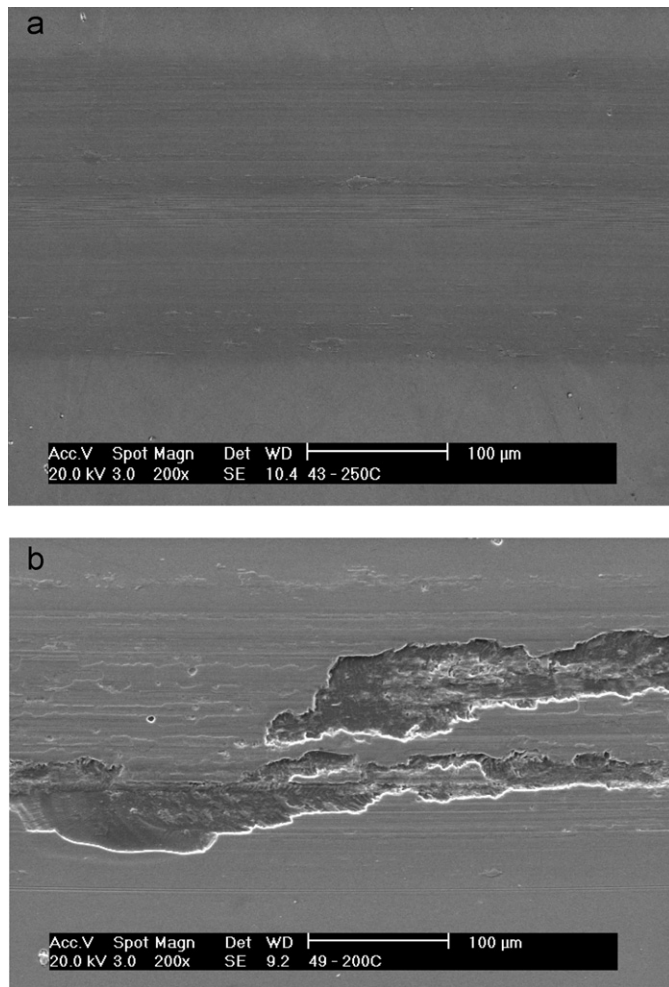


Fig. 4. SEM micrographs of the wear tracks after the tests at a temperature of 200 °C, (a) 40 at% C, (b) 64 at% C.

coating, there is a limited self-lubricant WS_2 material available to form the third body in the beginning of the sliding test. As a consequence, the initial friction force is very high causing severe damage to the coating surface. The scanning electron microscopy (SEM) analysis of the wear debris showed that, generally for all the coatings, they consisted of fine small wear particles (~ 300 nm in diameter). However in the case of 64 at% C film, large particles with sharp edges (up to $5\ \mu\text{m}$) can be observed. Therefore, the delamination of the coating produces large particles causing further abrasive damage, which explain the higher wear of this coating.

The testing at 500 °C leads to rapid coating destruction; therefore, a temperature of 400 °C can be considered as the

functional limit for the W–S–C coatings presented in this study. The coating with 29 at% C was partially peeled off from the substrate whereas the wear track was very deep (close to the titanium interlayer) for the 51 and 64 at% C samples; only the coating with 40 at% C can be an appropriate candidate for potential industrial applications, since the wear rate only increased slightly at this temperature. The friction coefficient remained very low, even decreased in some cases, which supports the hypothesis that the sliding process is still driven by the self-lubricant mechanism typical of TMD, despite the partial oxidation of the coatings revealed by energy dispersive X-ray (EDX) measurements.

4. Conclusions

W–S–C coatings deposited by RF magnetron sputtering from a carbon target embedded with a different number of WS_2 pellets were tribologically tested at elevated temperature. The friction mechanism of the coatings is similar to that of pure transition metal dichalcogenides. The friction coefficient dramatically decreased to very low level when temperature was increased, reaching values even lower than the ones measured during the tests in dry nitrogen at RT. It was suggested that the increased temperature facilitates the intercrystalline slipping of the transferred layer with the hexagonal WS_2 structure being formed in the contact area. The limiting temperature for sliding applications with W–S–C coatings is 400 °C.

Acknowledgements

This work was supported by the Czech Science Foundation through the project 106/07/P014.

References

- [1] Nossa A, Cavaleiro A. Surf Coat Technol 2001;142–144:984.
- [2] Nossa A, Cavaleiro A. Surf Coat Technol 2003;163–164:552.
- [3] Wise G, Mattern N, Herman H, Teresiak A, Bascher I, Bruckner W, et al. Thin Solid Films 1997;298:98.
- [4] Nossa A, Cavaleiro A, Carvalho NJM, Kooi BJ, De Hosson JThM. Thin Solid Films 2005;484:389.
- [5] Watanabe S, Noshiro J, Miyake S. Surf Coat Technol 2004;183:347.
- [6] Voevodin AA, O'Neill JP, Zabinski JS. Surf Coat Technol 1999;116–119:36.
- [7] Kubart T, Polcar T, Kopecky L, Novak R, Novakova D. Surf Coat Technol 2005;193:230.

NANOCOMPOSITE COATINGS OF CARBON-BASED AND TRANSITION METAL DICHALCOGENIDES PHASES: A REVIEW

T. Polcar, A. Nossa, M. Evaristo and A. Cavaleiro

ICEMS -Faculdade de Ciências e Tecnologia da Universidade de Coimbra, Dep. Eng. Mecânica, Rua Luís Reis Santos, 3030-788 Coimbra, Portugal

Received: January 22, 2007

Abstract. The results obtained at Instituto de Ciências e Engenharia de Materiais e Superfícies-ICEMS on the development of W-S-C coatings are reviewed and compared with literature data on the same system. The coatings have been deposited by r.f. magnetron sputtering using several approaches including reactive and co-sputtering processes. The chemical composition, structure and morphology of the coatings were analyzed and correlated with the mechanical properties. A complete detailed tribological characterization was performed by pin-on-disk tests varying the applied load, the humidity ratio and the temperature.

The most important result achieved was the significant increase in the hardness with C addition that allows expecting a higher loading bearing capacity. From the tribological point of view, the coatings with C content close to 40 at.% showed a remarkable thermal stability up to 400 °C, with friction coefficients lower than 0.05 and 0.1 in dry and room environments, respectively.

1. INTRODUCTION

The great advantage of solid lubricants is the possibility to be used in environments where oil lubrication is prohibited as the vacuum applications or the sliding contacts where the presence of contaminants must be avoided, such as in food industry. Furthermore in last years European Union has emanated restrict directives for the use of environment harmful products which is the case of most of the liquid lubricants. Thus, the development of self lubricating materials has increased exponentially in last decades with the main scope of reducing or even eliminating the use of synthetic oil lubrication.

As wear and friction are surface phenomena, it is not surprising that a great part of the research

work on self lubricating materials was dedicated to thin coatings. Among the different alternatives which have being suggested, transition metal dichalcogenides (TMD) have been adopted by several research groups for studying. Therefore, several TMDs were analysed although the main focus had been pointed on MoS₂. However, it was shown that for some particular applications WS₂ could be advantageous since its thermal resistance in oxidant atmospheres outstands that of MoS₂ in more 100 °C and its oxide, WO₃, has lower friction coefficient and is more protective than MoO₃ [1,2]. In comparison to their competitors, such as C-based coatings, particularly those known as diamond like carbon (DLC), TMDs have the advantages of presenting extremely low friction coefficients in vacuum or dry environments and a better tribological per-

Corresponding author: A. Cavaleiro, e-mail: albano.cavaleiro@dem.uc.pt

formance at high temperatures (<400 °C). The main drawbacks of TMDs, which has been the most important reason for their limited application in many situations where low friction is required, is their low tribological performance in H₂O containing atmospheres as well as their low hardness values [3-6]. Thus, their use is prohibited in most of terrestrial applications requiring high loading bearing capacity. Besides the existence of weak Van der Waals forces between basal planes, the very low mechanical strength is also been attributed to typical columnar morphology with high levels of porosity when they are deposited in the form of thin coatings [6-9].

In order to overcome the drawbacks of TMDs, many different approaches have been tried almost always involving an improvement of the density with the double aim of impeding the coating oxidation and increasing the mechanical strength. The alloying of the coatings with metals or compounds are good examples of these solutions [10-13].

Still in the 90's, at Air Force Research Laboratory in the USA, a research work was started concerning the deposition of coatings integrating simultaneously carbon and TMDs. The objective of the study was the use of the well known concept of composite materials, i.e. trying to deposit coatings which could take advantage of the good properties of both materials and avoid their drawbacks. This study was prolonged during several years [14-17] and, already in this century, ICEMS, Portugal, enlarged the range of chemical compositions studied by those authors from 0 to 100% of TMDs [18-24]. Finally, very recently another group in Japan presented their first results of the deposition of C-TMDs by co-sputtering [25].

The aim of this paper is to present a review of the results obtained up to now at ICEMS on the alloying of TMDs coatings with C. Whenever important, the results of the other authors on W-S-C system will be presented and discussed for comparison means.

2. EXPERIMENTAL DETAILS

All W-S-C coatings have been deposited on 100Cr6 and M2 polished steel samples, with hardness close to 5 GPa and 9 GPa, respectively, and mirror-like polished Si wafers. Three different approaches were tried for co-deposition of coatings using a radio-frequency magnetron sputtering Edwards ESM 100 unit, equipped with two cathodes or targets ($\varnothing=100$ mm): (1) reactive sputtering, with one Ti target for an adhesion interlayer,

one WS₂ target and deposition in a CH₄-containing atmosphere; (2) co-sputtering from individual C and WS₂ targets, and (3) co-sputtering from a C target embedded with WS₂ pellets (composite target) and one Ti target. Prior to deposition the substrates were sputter cleaned during 20 min by establishing the plasma close to the substrates electrode. Immediately after, in the cases where it was possible, a Ti interlayer was deposited with an approximate thickness of 300 nm for improving the coating adhesion. The chemical composition of coatings was varied by playing in each approach with the flow rate of the reactive gas, the power applied to the C target (the power of the WS₂ target was kept constant at 160 W) and the number of WS₂ pellets on the C target, respectively.

To evaluate the chemical composition of coatings, a Cameca SX 50 electron probe microanalysis (EPMA, Cameca, France) apparatus was used. The chemical composition is an arithmetic average of four values measured in different parts of samples. The standard deviation was in the range ± 0.02 to ± 0.3 . The hardness was determined by depth-sensing indentation technique using a Fisherscope H100 with a nominal load of 20 mN, following the procedure indicated elsewhere [26]. The hardness value was obtained by averaging eight different indentation results. The adhesion of coatings was evaluated with a commercially available scratch testing equipment (CSEM Revetest), under standard conditions. The critical load, for each coating, was obtained by averaging four different scratch results. The structure of coatings was analysed by X-ray diffraction (XRD) in glancing mode using a Phillips diffractometer (Co K _{α} radiation).

Most of tribological tests were carried out in a pin-on-disk tribometer (CSM Instrument). 100Cr6 steel balls were used as sliding partners. The diameter of balls was 6 mm and the load was varied in the range (5-48) N. Different testing environments were used by varying either the humidity degree (from 5 to 90%) or the testing temperature (from room to 400 °C). The sliding speed was 0.05 m·s⁻¹. The friction coefficient reported is the average value of the whole sliding test, unless stated otherwise.

The wear coefficient for the coated disk (K) was calculated using the equation:

$$K = v / (s \cdot l), \quad (1)$$

where v is the worn volume, s the total distance of sliding of the ball over the disk and l the normal load. The worn volume of the coated disk was de-

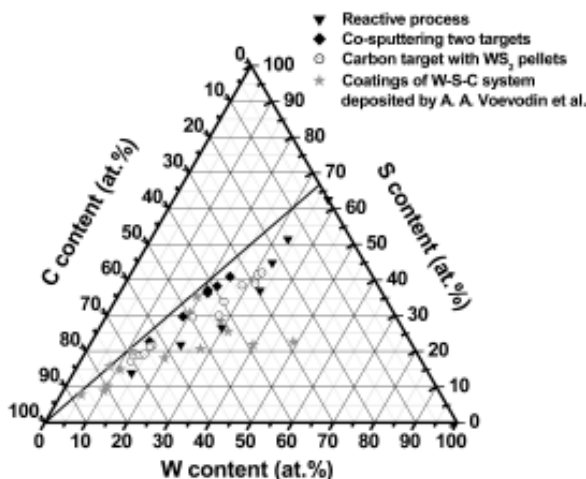


Fig. 1. Chemical composition of the W-S-C coatings. Literature data on the same system are also shown for comparison [14].

terminated by integrating the mean area of 6 profiles, taken across the sliding track, over its entire perimeter. The measure of the tangential force allowed the calculation of the friction coefficient.

The microstructure and the changes in the bonding structure were investigated using a Renishaw micro-Raman spectroscopy system 1000 at a wavelength of 514.5 nm. Raman spectroscopy was carried out in different places in the wear tracks and outside. Two groups of peaks could be observed, one corresponding to carbon (i.e. D and G peaks) and another consisting of two peaks (325 and 416 cm^{-1}) identified as WS_2 . The ratio I_c/I_{WS_2} was calculated as the sum of the carbon peaks areas divided by the sum of the WS_2 peaks areas.

3. RESULTS

3.1. Chemical composition and structure of coatings

Coatings with various C contents have been deposited as summarized in the ternary diagram shown in Fig. 1. From now coatings with C contents higher than 50 at.% will be considered as high C-content coatings. In relation to the samples studied by Zabinski *et al.* [14], there is an extension of the domain of analysis for lower C contents. It should be noted that almost all the coatings are shifted in relation to the tie line representative of the stoichiometry $S/W=2$, meaning that the coatings are sulphur deficient compared to WS_2 pel-

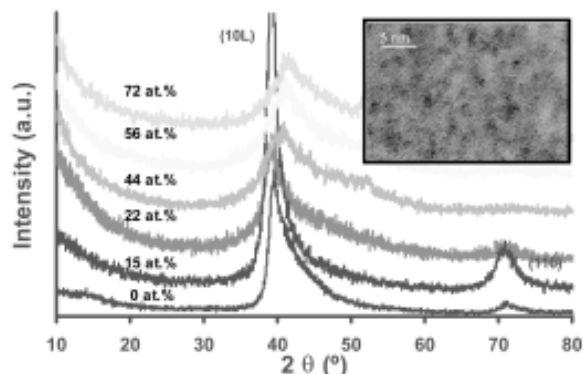


Fig. 2. XRD patterns of reactively deposited W-S-C coatings with increasing C content. A TEM micrograph of the cross section of a high C content coating is shown inset [22].

lets. The shift reaches high values particularly for coatings with low C contents studied in [14]. The coating procedure which seems more favourable for keeping the stoichiometry close to $S/W=2$ is co-sputtering, particularly when performed from individual targets (see \blacklozenge and \circ in Fig. 1). The deposition with reactive gas (\blacktriangledown) is very detrimental for S/W ratio. This trend can be attributed to the presence of energetic H species in the discharge due to the decomposition of CH_4 . These species combine with sputtered S atoms forming H_2S which is evacuated from the deposition chamber leading to a lower S incorporation in the growing coating.

Coatings of the W-S-C system deposited by co-sputtering from individual targets (WS_2 and carbon) were also deposited by other authors [25]. They showed that, depending on the power applied to the WS_2 target, the coatings could have different arrangements (nanocomposite or nanolaminate) depending on the possibility of forming a continuous TMD layer during the short time as the substrate is passing over each target. With ICEMS conditions, the formation of a laminate structure does not seem to be possible since a period lower than 0.2 nm is expected, which does not permit the formation of a layered structure. Since Noshiro *et al.* [25] presented a power ratio between WS_2 and C targets, $P(\text{WS}_2)/P(\text{C})$, much lower than the ICEMS case (range [0.04-0.4] against [0.29-1.07], respectively) their coatings should exhibit higher C contents.

The coatings deposited by co-sputtering from the two individual targets (WS_2 and C) presented XRD patterns typical of an amorphous structure,

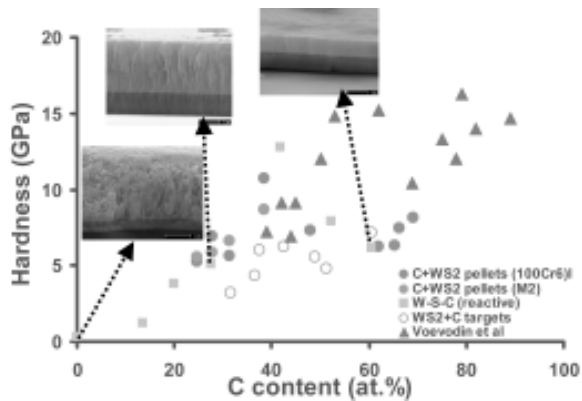


Fig. 3. Hardness of W-S-C sputtered coatings as a function of the C content. SEM micrographs of the cross section of selected coatings are shown inset. W-S-C system deposited by A. A. Voevodin *et al.* are also shown for comparison [14].

whatever the C content. For the others process (reactive sputtering and co-sputtering form a C target with WS_2 pellets) crystallinity could be observed, which was progressively lost with increasing C content (see e.g. the evolution of XRD patterns in Fig. 2 for reactively sputtered coatings). Very similar results were also achieved by Voevodin *et al.* [14]. Pure W-S, (or with a low C content) coatings present a dark surface which, if wiped with a soft cotton, changed to a metallic aspect, fact accompanied with the appearing of a peak that corresponds to the (002) plans of the 2H- WS_2 phase due to the re-orientation of the basal planes parallel to the coating surface. The main XRD peak placed at $2\theta \sim 40^\circ$ with a long tail corresponds to the turbostratic stacking of (10L) planes ($L=1, 2, 3, \dots$) which can be interpreted as a 2D organization of the basal planes [27]. With increasing C content, the lateral dimension of the basal planes decreases leading to broader and less intense peaks until only one typical peak of an amorphous structure is observed. For C contents higher than 40 at.% small features in the XRD pattern suggest the presence of other phases such as tungsten carbides. Such a fact was confirmed by X-ray photon-electron spectroscopy (XPS) [21] which clearly showed the presence of different types of bonds such as, W-S, W-C and C-C suggesting the formation of a nanocomposite structure where nanocrystals of WS_2 and W-C phases were dispersed in a C-rich amorphous matrix. The differently contrasted zones in the TEM micrograph of

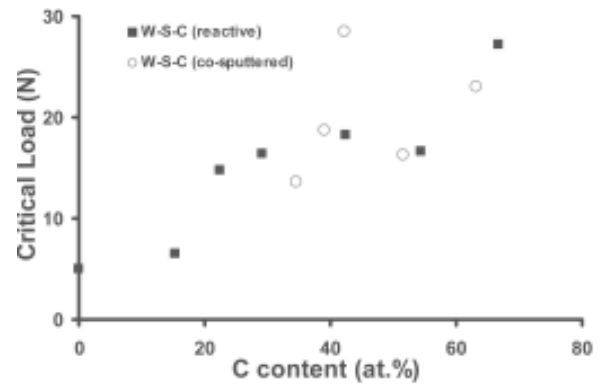


Fig. 4. Scratch test critical load of W-S-C sputtered coatings as a function of the C content.

one of these coatings (inset in Fig. 2) and the direct observation of crystalline planes in darker areas support this assessment.

3.2. Mechanical properties and morphology of coatings

Fig. 3 presents the evolution of the hardness (H) of coatings with increasing carbon content for all the approaches adopted for deposition. The general trend was: the hardness rises with increasing C content, up to ~ 45 at.%, and decreases thereafter. The first increase should be closely correlated to either the great improvement in the density of coatings (see typical cross section morphologies inset Fig. 3) or the formation of other harder phases such as W-C or C-based. With the addition of carbon in the coating, there is no more W available to establish W-C bonds and the domination of carbon phases takes place. As the deposition conditions used in this work leads to only 7 GPa for the hardness of pure C coatings, the growing influence of C in the W-S-C coatings justify the observed decrease in hardness values.

The hardness values reported by other authors [14,25] were found to be overlapped with those presented above but only up to C contents close to 50 at.%. For higher contents, those authors stated the continuation of the monotonous growing of hardness with increasing C content. This difference can be attributed to the much higher hardness value of their single C coating (close to 18 GPa) which,

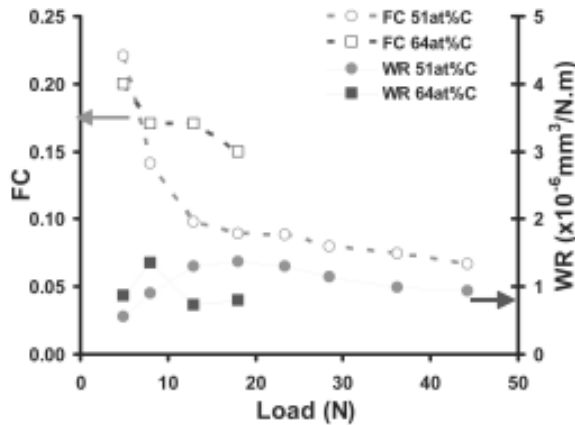


Fig. 5. Friction and wear coefficients of W-S-C coatings as functions of the testing applied load.

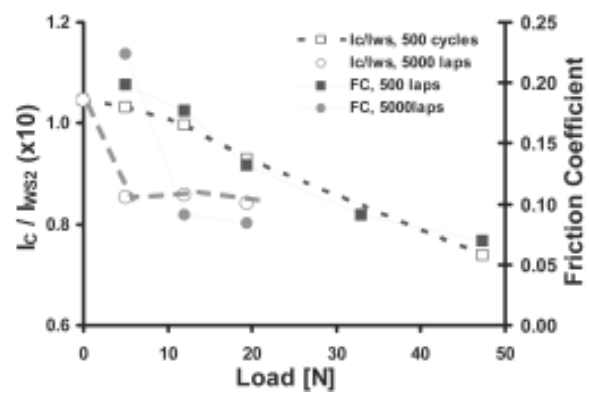


Fig. 6. Friction coefficient and I_C/I_{WS2} ratio, determined by Raman spectroscopy, of a W-S-C coating, containing approximately 41 at.% of C, as functions of the testing applied load.

again, determines the hardness of W-S-C coatings when its importance progressively grows. Also Noshiro *et al.* [25] found a higher value for single C content (17 GPa) and the consequent monotonous decrease down to 10 GPa with increasing TMD content. It should be remarked, as referred to above, that these authors only deposited C-rich coatings which can explain that the hardness did not decrease under 10 GPa. Both these research groups worked with lower deposition pressures (in the range from 0.2 to 0.3 Pa) than in ICEMS work (~0.8 Pa) which can explain the higher hardness values reached for pure C coatings.

Whatever are the results considered, what is really remarkable is the huge increase in hardness resulting from C alloying, more than one order of magnitude, in relation to the single W-S coating (<0.5 GPa).

As for the hardness, a great improvement in the adhesion of W-S-C coatings could be found by scratch testing. Fig. 4 presents the evolution of the critical load with increasing C content. Although the highest values were not still high enough for guarantee a perfect success in real service applications, no problems were found for the tribological tests even when the highest testing loads were applied.

3.3. Friction and wear properties of coatings

The tribological characterization was accessed by studying the influence of different testing parameters during the pin-on-disk measurements as fol-

lows: applied load, temperature and humidity of the environment. Coatings with various C contents were studied and only the main trends are presented here.

3.4. Testing load

Fig. 5 shows the evolution of the friction (μ) and wear (K) coefficient as a function of testing load for two coatings, representative of coatings with high and low C contents. The same trend can be observed in both cases which is often found for self-lubricated coatings, particularly those based on TMDs coatings [28-30]. This is the first indication that the presence of TMD phases should determine the friction behaviour of these nanocomposite coatings. However, the coatings with C contents lower than ~50 at.%, have high μ values for low applied loads decreasing progressively with increasing load up to a steady state is achieved. On the other hand, in coatings with high C contents a small decrease in μ is detected being the values kept at a much higher level (>0.15) although it could be expected that, if the coatings were tested with a high number of cycles and higher loads, lower friction coefficient could be achieved as for the coatings with low C content.

The analysis of the wear track of the coatings allowed identifying some differences which can explain the different behaviour. SEM observations showed, on the one hand, that a transferred layer consisting of W, S, C, and O was formed on the pin, whatever the testing conditions protecting the

coating surface since no wear was there possible to be measured. On the other hand, a very smooth surface was found for coatings with low C contents whereas grooves were detected in the other coatings. Furthermore, Raman spectroscopy carried out on the worn tracks allowed to conclude that the low friction coefficients could be associated to an increase in the TMD concentration on its near surface by the action of the sliding process. Such enrichment was found neither with C-rich coatings nor under low loads [31].

Finally, as can be observed in Fig. 6, the changes in the surface layer of the wear track are also determined by the number of cycles. This figure presents the evolution of the I_C/I_{WS_2} ratio, i.e., the ratio between the area of carbon peaks (D and G band) and area of WS_2 peaks (325 and 416 cm^{-1}) calculated from Raman spectra, as well as the friction coefficient, as functions of the testing load for the same coating ($\sim 41\text{ at.}\%C$) tested with 500 or 5000 laps. Firstly, it confirms what was referred to above, i.e., for reaching a low friction coefficient it is necessary to apply a threshold load which is able to promote the enrichment of W-S phases in the surface of the sliding contact. Secondly, these changes can be achieved at lower applied loads but after much higher number of cycles. It seems that the surface transformation requires a threshold amount of work to occur, which can arise either from increasing load or number of cycles.

The decrease in friction coefficient with load of TMD coatings was explained by several authors as consequence of the frictional heating of the surfaces in the contact causing drying of the air humidity [32]. However, by applying the frictional heating analysis [33] for the tribological behaviour of TMD materials, it was possible to demonstrate that the low friction behaviour of nanocomposite W-S-C coatings cannot be interpreted by this way [31]. Thus, the decrease in friction coefficient with increasing load should not be attributed to the frictional heating, since the rate of the frictional heating per unit sliding area remained almost constant regardless on contact pressure. A different friction mechanism should exist for these materials in spite of the similar friction behaviour that they present in relation to pure TMDs.

The profiles of the wear tracks were very difficult to be evaluated with depths of only some hundreds of nanometers. As can be seen in Fig. 5, it does not seem there being significant influence of the applied load on the wear rate of coatings. The values are similar to those found by Voevodin *et*

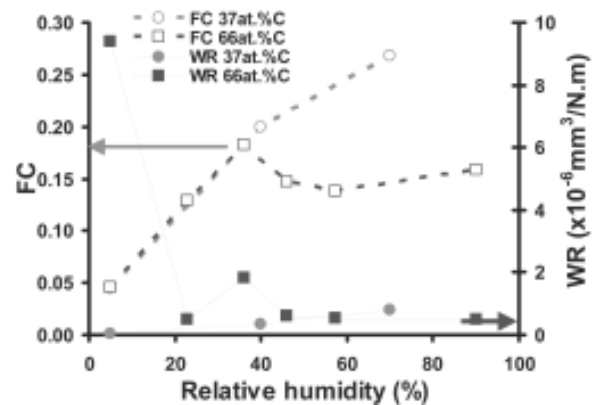


Fig. 7. Friction and wear coefficients of W-S-C coatings as functions of the humidity content in the testing environment.

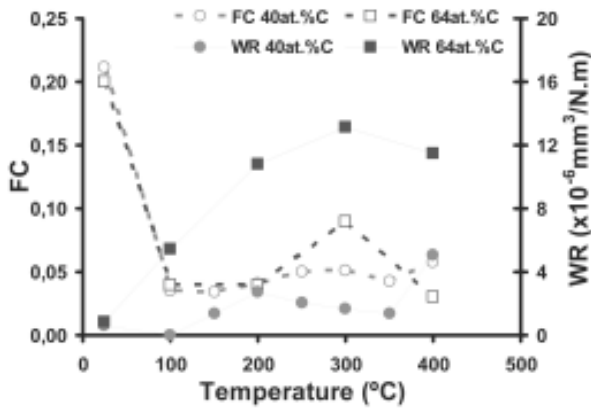
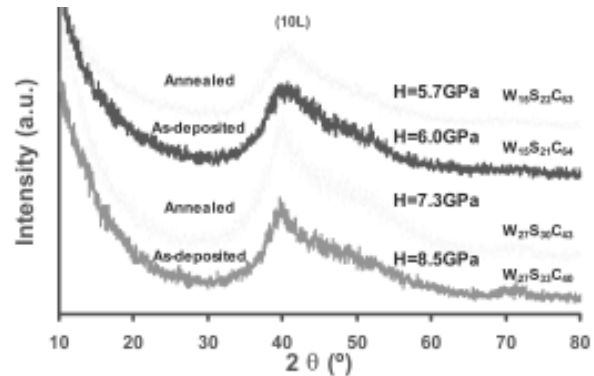
al. [14] for tests in dry environments and clearly inferior to those achieved in humid atmospheres.

3.5. Relative Humidity (RH)

One of the main objectives of the present research was to extend the application of TMD coatings to humidity containing environments. Thus, their tribological behaviour was studied as a function of the relative humidity. Fig. 7 shows the friction and wear coefficients achieved for two selected coatings exemplifying the tribological behaviour of the tested coatings, one with high and the other with low C contents, as a function of the relative humidity in the testing environment. As it would be expected, in dry nitrogen the coatings present very low friction coefficients (<0.05) including the one with high C content, in spite of the presence of C-based phases. Such behaviour suggests that the tribological behaviour should be exclusively determined by the presence of TMD phases in the sliding contact. With increasing relative humidity, a steadily degradation of the friction properties could be observed, with an increase in friction coefficient up to values close to 0.15 for 40 % of RH. However, for higher RH values an opposite trend is detected for both coatings: μ continue to increase for coatings with low C contents whereas a decrease has occurred for coatings with high C-contents. In this coating, the presence of C-based phases should permit improving the frictional properties as suggested by Wu *et al.* [15]. The μ values measured in these conditions are close to those found by these authors: (1) coatings with S con-

Table 1. Wear data for a high C containing W-S-C coating tested in dry nitrogen as a function of the duration of the test.

	Width of the wear track (μm)	Depth of the wear track (μm)	Friction coefficient
After 60 cycles	190	0.55	0.12
After 1500 cycles	250	0.52	0.05

**Fig. 8.** Friction and wear coefficients of W-S-C coatings as functions of the testing temperature.**Fig. 9.** XRD patterns of W-S-C coatings of various compositions, structures and hardness before and after annealing at 300 °C.

tents higher than 20 at.% (roughly C content lower than 70 at.%, which is typically the range of samples studied at ICEMS) exhibit friction coefficients in dry conditions lower than 0.05 whereas, in humid air, μ was in the range from 0.2 to 0.3; (2) for the coatings with lower S contents, down to 15 at.%, μ was in the range [0.18-0.3] and [0.25-0.4] when tested in dry or humid environment, respectively.

The wear rate of the coating with 37 at.% of C, representative of the W-S-C coatings with low C contents, is almost nil in dry tests. With increasing RH values the wear rate starts to increase which is characteristic of TMD materials in humid atmospheres. However, it should be remarked that it stays quite low and no destruction of the coating was detected. The C-rich coatings show a very high wear rate when tested in dry environment. However, such a high value should be attributed to an abnormal consumption of coating material in the initials cycles necessary to create the conditions for establishing lubricious surfaces. In fact, very short tests performed on these coatings in dry conditions (only 60 laps) showed that the dimensions of the wear track after the test are similar to those achieved in longer duration tests (Table 1). Thus, even with a low TMD content it is possible to cre-

ate conditions for a C-rich coating to reach low friction coefficients when tested in dry atmosphere. With increasing RH in the testing environment, there is an increased influence of the C-based phases leading to a significant decrease in wear rate which is kept approximately constant up to the highest RH studied.

3.6. Testing temperature

As it would be expected, when W-S-C coatings were tested at 100 °C, an abrupt decrease in friction coefficient was observed (Fig. 8). In fact, at this temperature the atmosphere will dry establishing the low friction conditions analysed above for the influence of RH. Excepting some punctual oscillation, the μ values are kept approximately constant up to 400 °C. For higher temperatures the destruction of the coating occurred.

The decrease in friction coefficient is not accompanied by a similar trend in the wear rate. For the coating with a C content of ~40 at.% the wear rate is kept approximately constant for all testing temperatures whereas an increase of almost one order of magnitude was observed for those with high C contents. Any changes observed in the tribological behaviour should not be attributed to

changes in the structural and mechanical properties, at least from what XRD and nanoindentation results make think. In fact, as it is shown in Fig. 9, no significant changes in the chemical composition, the XRD patterns and in the hardness values of the coatings could be detected, which could justify, for example, the increase in wear rate with testing temperature for the coatings with high C contents.

4. CONCLUSIONS

W-S-C films have been deposited by reactive and non-reactive magnetron sputtering with increasing C contents. The most suitable method for coating deposition was by co-sputtering from a C target embedded with pellets of WS₂. The C content was varied from 0 to 100 at.%. All coatings were sub-stoichiometric in relation to the ratio S/W=2. Significant improvements in the morphology of the coatings were achieved with increasing C content, whereas the crystallinity was progressively lost with a decrease in intensity and a broadening of the diffraction peaks. High resolution transmission electron microscopy allowed concluding that the coatings with high carbon contents were formed by a nanocomposite structure consisting of nanocrystals of W-S and W-C phases embedded in a C-rich amorphous matrix.

As a result of these variations a huge increase in hardness was reached with a difference of more than one order of magnitude between single W-S coating and those containing carbon (from 0.5 to more than 10 GPa). In the same way an increase in critical load determined by scratch testing was achieved from 5 N up to more than 30 N.

The coatings were tribologically tested in pin-on-disk equipment by varying the applied normal load, the humidity content and the testing temperature. The evolution of the mean friction coefficient as a function of the applied load was typical of TMD materials (i.e. decrease in friction coefficient with increasing load) which allowed suggesting that an enrichment of this phase in the sliding contact surfaces would be needed for achieving low friction coefficient. It should be noted that with loads higher than 40 N, μ values as low as 0.07 could be reached which is remarkable for a TMD rich material sliding in humid air. As it would be expected the coatings showed an excellent tribological behaviour in dry conditions which degraded when the RH value increased, again a typical behaviour for a TMD material. Finally, testing at temperatures higher than 100 °C led to very low friction coefficients due to

the drying of the atmosphere. The coatings with C content close to 40 at.% showed the best thermal stability keeping very low friction and wear coefficients when tested at temperatures up to 400 °C.

As a final remark, TMD-C coatings are very promising for industrial applications even when different environments could be present during the component lifetime. In-service testing is now required to test the validity of this assumption.

REFERENCES

- [1] J.S. Zabinski, M.S. Donley, S.V. Prasad and N.T. McDevitt // *J. Mater. Sci.* **29** (1994) 4834.
- [2] B. Bhushan and B.K. Gupta, *Handbook of Tribology—Materials, Coatings, and Surface Treatments* (McGraw-Hill Inc., USA, 1991), p. 51.
- [3] R. Bichsel, P. Buffat and F. Lévy // *J. Phys., D. Appl. Phys.* **19** (1986) 1575.
- [4] P.A. Bertrand // *J. Mater. Res.* **4** (1989) 180.
- [5] S.V. Prasad, J.S. Zabinski and N.T. McDevitt // *Tribol. Trans.* **38** (1995) 57.
- [6] Da-Yung Wang, Chi-Lung Chang and Wei-Yu Ho // *Surf. Coat. Technol.* **111** (1999) 123.
- [7] V. Buck // *Vacuum* **36** (1986) 89.
- [8] M.R. Hilton, R. Bauer and P.D. Fleischauer // *Thin Solid Films* **188** (1990) 219.
- [9] M. R. Hilton // *Surf. Coat. Technol.* **68-69** (1994) 407.
- [10] M. R. Hilton, G. Jayaram and L. D. Marks // *J. Mater. Res.* **13** (1998) 1022.
- [11] N. M. Renevier, V. C. Fox, D. G. Teer and J. Hampshire // *Surf. Coat. Technol.* **127** (2000) 24.
- [12] Y. L. Su and W. H. Kao // *Tribol. Int.* **36** (2003) 11.
- [13] S. Watanabe, J. Noshiro and S. Miyake // *Surf. Coat. Technol.* **183** (2004) 347.
- [14] A. A. Voevodin, J. P. O'Neill and J. S. Zabinski // *Surf. Coat. Technol.* **116-119** (1999) 36.
- [15] J. -H. Wu, M. Sanghavi, J. H. Sanders, A. A. Voevodin, J. S. Zabinski and D. A. Rigney // *Wear* **255** (2003) 859.
- [16] J.-H. Wu, D. A. Rigney, M. L. Falk, J. H. Sanders, A. A. Voevodin and J. S. Zabinski // *Surf. Coat. Technol.* **188-189** (2004) 605.
- [17] A. A. Voevodin and J. S. Zabinski // *Comp. Sci. and Technol.* **65** (2005) 741.
- [18] A. Nossa and A. Cavaleiro // *Surf. Coat. Technol.* **142-144** (2001) 948.
- [19] A. Nossa and A. Cavaleiro // *Surf. Coat. Technol.* **163-164** (2003) 552.

- [20] A. Nossa and A. Cavaleiro, In: *Advanced Materials Forum II*, ed. by R. Martins, E. Fotunato, I. Ferreira and C. Dias Vol.455, 456 (Trans Tech Pub. Switzerland 2004), p.515.
- [21] A. Nossa and A. Cavaleiro // *J. Mater. Res.* **19** (2004) 2356.
- [22] A. Nossa, A. Cavaleiro, N. J. M. Carvalho, B. J. Kooi and J. Th. M. De Hosson // *Thin Solid Films* **484** (2005) 389.
- [23] M. Evaristo, A. Nossa and A. Cavaleiro // *Surf. Coat. Technol.* **200** (2005) 1076.
- [24] M. Evaristo, A. Nossa and A. Cavaleiro // *Ciência & Tecnologia dos Materiais* **18** (2006) 21.
- [25] Junichi Noshiro, Shuichi Watanabe, Takahiko Sakurai and Shojiro Miyake // *Surf. Coat. Technol.* **200** (2006) 5849.
- [26] J. M. Antunes, A. Cavaleiro, L. F. Menezes, M. I. Simões and J. V. Fernandes // *Surf. Coat. Technol.* **149** (2002) 27.
- [27] G. Wise, N. Mattern, H. Herman, A. Teresiak, I. Bascher, W. Bruckner, H.-D. Bauer, H. Vinzelberg, G. Reiss, U. Kreissig, M. Mader and P. Markschlager // *Thin Solid Films* **298** (1997) 98.
- [28] B. J. Briscoe and A. C. Smith // *ASLE Trans.* **25** (1982) 349.
- [29] I. L. Singer, R. N. Bolster, J. Wegand, S. Fayeulle and B. C. Stupp // *Appl. Phys. Lett.* **57** (1990) 995.
- [30] A.K. Kohli and B. Prakash // *Tribol. Trans.* **44** (2001) 147.
- [31] T. Polcar, M. Evaristo, A. Cavaleiro, *Friction of self-lubricating W-S-C sputtered coatings sliding under increasing load*, submitted to *Plasma Processes and Polymers*.
- [32] J. Gansheimer // *ASLE trans.* **10** (1967) 390.
- [33] A. K. Kohli and B. Prakash // *Tribol. Trans.* **44** (2001) 147.

Friction of Self-Lubricating W-S-C Sputtered Coatings Sliding Under Increasing Load

Tomas Polcar, Manuel Evaristo, Albano Cavaleiro*

W-S-C films were deposited by non-reactive magnetron sputtering from a carbon target with several pellets of WS₂ incrusted in the zone of the preferential erosion. The number of the pellets was changed to modify the carbon content in the films, which varied from 26 up to 70 at.-%. Alloying W-S films with carbon led to a substantial increase in the hardness in the range of 4–10 GPa; the maximum hardness was obtained for the coatings with carbon contents close to 40 at.-%. XRD diffraction patterns showed that there was a loss of crystallinity with the increase of the carbon content in the film. C-contents in the range (37–66 at.-%) were selected for sliding tests (pin-on-disk, 100Cr6 steel ball as a counterpart) carried out in humid air under increasing contact load. The friction coefficient was observed to decrease continuously with increasing load. The wear tracks and wear debris were also analyzed by Raman spectroscopy to understand the structural transformations induced by the increasing load. The friction results were compared with existing models for pure transition metal dichalcogenides (TMD), and it could be concluded that the friction mechanisms of W-S-C coatings fundamentally differ from those of pure TMD.

Introduction

Transition metal dichalcogenides (TMD) have excellent self-lubricant properties in dry air or vacuum; however, these films are easily rusted in the presence of moist environments and their reduced mechanical resistance makes them inappropriate for applications requiring high load bearing capacity. On the other hand, hard coatings are often employed to protect parts from abrasive and erosive wear; however, they do not have low friction and they are frequently brittle. Therefore, there is a need to design coatings combining low friction with high load-bearing capacity; moreover, a good adhesion to the substrates is required. Our recent works showed that the synergetic effect of doping W-S films with carbon or nitrogen together with the deposition of a Ti interlayer could give rise to significant improvements in the mechanical properties

and the tribological behavior, particularly in the case of films alloyed with carbon.^[1,2]

The objective of this work was to develop coatings capable of being used in a wide range of applications, with different applied loads, temperatures and environments. In this study, the structural and mechanical properties of W-S-C coatings are presented together with their sliding properties under different load conditions.

Experimental Part

All W-S-C coatings were deposited on 100Cr6 and M2 polished steel samples with hardness close to 5 and 9 GPa, respectively. The depositions were carried out in a radio-frequency magnetron sputtering Edwards ESM 100 unit, equipped with two cathodes ($\varnothing = 100$ mm). Prior to the depositions, the substrates were sputter cleaned for 20 min by establishing the plasma close to the substrates electrode. Immediately after, a Ti interlayer was deposited with an approximate thickness of 300 nm. The main sputtering target was pure carbon, partly covered by WS₂ pellets placed preferentially in the eroded zone. The dimensions of the pellets were $4.1 \times 3.5 \times 1.5$ mm. The degree of target coverage

T. Polcar, M. Evaristo, A. Cavaleiro
ICEMS - Faculdade de Ciências e Tecnologia da, Departamento de Engenharia Mecânica, Universidade de Coimbra, Rua Luís Reis Santos, Coimbra 3030-788, Portugal
Fax: (+351) 239 790 701; E-mail: albano.cavaleiro@dem.uc.pt

determined the overall chemical composition of the sputtered film. The depositions were carried out with constant power density of $7.6 \text{ W} \cdot \text{cm}^{-2}$ in the carbon target.

To evaluate the chemical composition of the films, a Cameca SX 50 electron probe microanalysis was used. The hardness was determined by a depth-sensing indentation technique using a Fisherscope H100; the coatings deposited on M2 steel were used for these measurements.

Tribological tests were carried out with a pin-on-disk tribometer (CSM Instrument). 100Cr6 steel balls were used as sliding partners. The diameter of the ball was 6 mm, load was in the range of 5–47 N. The tribological behavior of the coatings was evaluated in air with a relative humidity of 30%, the sliding speed was $0.05 \text{ m} \cdot \text{s}^{-1}$. The friction coefficient reported in this study is the average value of the whole sliding test, unless stated otherwise.

Results and Discussion

Chemical Composition, Structure, and Mechanical Properties

Different carbon contents were achieved in the coatings by varying the number of WS_2 pellets in the C target. As it was expected, the carbon content of the films decreased almost linearly with the increase in the total area of pellets. The chemical composition of the deposited coatings varied from 29 to 70 at.-% C (hereinafter, the denomination “at.-% C” represents the carbon content in the coating). The S/W ratio varied in the range of 1.2–1.5, a slight increase was observed with increasing carbon content. The sulfur deficiency is probably caused by either the resputtering of sulfur atoms from the growing film by energetic neutrals or by the chemical reactions of sulfur with the residual atmosphere.

X-ray diffraction patterns of W-S-C films showed a gradual loss of crystallinity with the increase of the carbon in the coatings. The films with a low carbon content present typical XRD patterns of Me-S (Me, transition metal) sputtered films with prominent peaks at $2\theta \approx 40^\circ$ with an extended shoulder corresponding to a turbostrating stacking of (10L) planes ($L = 0, 1, 2, 3$), and $2\theta \approx 70^\circ$ indexed as (110) planes. Wiese et al.^[3] demonstrated that these XRD patterns could be explained by a 2D organization of the basal planes which could have a dimension of several tens of unit cells. With the progressive decrease of the lateral dimensions of the basal planes, either broadening or drop in the intensity of the (10L) plan occurred until a unique low intensity and broad peak typical of an amorphous structure was detected. This situation would arise when the lateral order of the basal planes did not exceed a couple of lattice parameters.^[3] In previous work,^[4] it was shown by HRTEM that W-S-C films with high C contents were formed by a nanocomposite structure which included WS_2 grains of a few nanometers size, in agreement with Wiese et al.'s interpretation.

The hardness of W-S-C films increased with increasing carbon content to reach a maximum at ~ 40 at.-% C (10 GPa). Further increase of the carbon content led to smaller values of the hardness. This trend can be related to the synergetic actions of the compactness increase of the films associated with the possible formation of nano-sized carbide phases, intrinsically harder than tungsten disulfide. With the addition of more carbon to the films, there is no more W available to establish W–C bonds and the formation of carbon phases leads to a decrease of the hardness (see Figure 1). It should be remarked that with the deposition conditions used in this work, a pure C film exhibited only about 8 GPa hardness. However, the hardness of W-S-C coatings is generally about one order of magnitude higher than that of pure tungsten disulfide.^[5]

Friction and Wear Properties

The first set of sliding tests was carried out with 500 laps. The depth of the wear track was very low to calculate the wear rate and, thus, selected coatings were tested with 5 000 laps. The average friction coefficient of the coatings as a function of the load is shown in Figure 2. As a general trend, the friction coefficient decreases with increasing load. Nevertheless, there is significant difference between the values corresponding to 500 and 5 000 laps. A detailed analysis of the friction curves revealed two different typical trends: (i) the coatings up to 51 at.-% C exhibited high friction in the first hundred laps (running-in), which was followed by a drop in the friction to a lower level corresponding to the steady state wear; (ii) the coatings with the highest carbon contents showed a higher friction coefficient, which remained almost constant during the entire test. As a consequence, the average friction for the

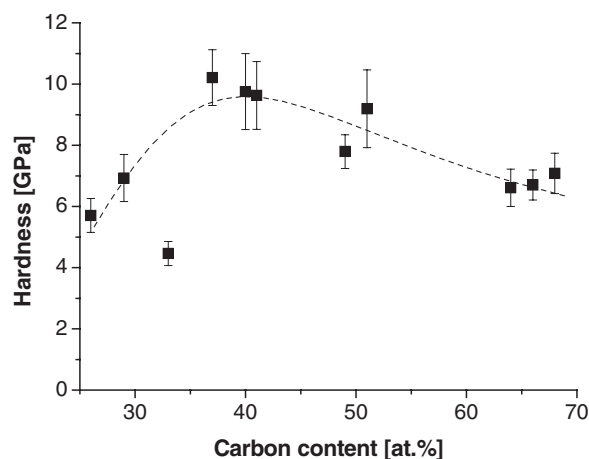


Figure 1. Evolution of the hardness with the carbon content in the films. The dashed line is a guide to the eye.

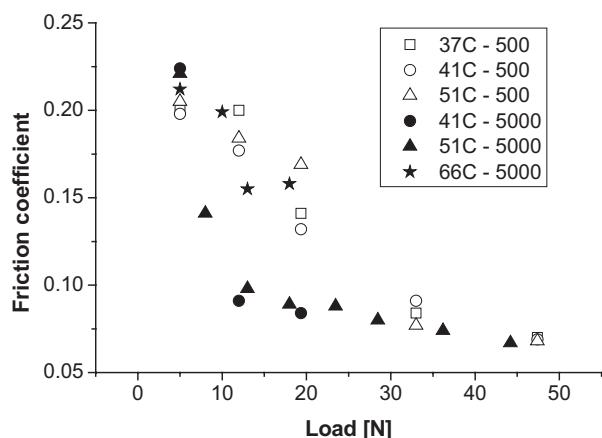


Figure 2. Friction coefficient of W-S-C coatings as a function of the load (note the different number of laps).

low and medium carbon content coatings decreases with the number of laps, while it remains the same in the case of high carbon content.

The wear tracks produced by the sliding were very shallow for 500 laps tests (typically less than 200 nm), which gives rise to very small worn volumes and, consequently, wear rate calculations are very difficult. Therefore, we can report only on the wear rate of the coatings which underwent tests with 5000 laps. The wear rate of the 51 at.% C coating initially increased from 0.55 (5 N) to 1.36×10^{-6} (18 N) and then slowly decreased to 0.93×10^{-6} , while the 41 at.% C coating (tested up to 19 N load) showed rather constant low wear rates, i.e., a small increase from 0.60 (5 N) to 1.06×10^{-6} (19 N)

Analysis of the Worn Surfaces

The balls after the tests were covered by an adhered layer of the material transferred from the coating. When the adhered layer was removed, the optical observation revealed no wear scar on the ball. Chemical maps of this layer showed an almost homogeneous distribution of W, S, C, and O. No vestiges of Fe originating from steel were observed, which confirms that the ball wear rate was negligible.

The wear tracks of the coatings with carbon content up to 51 at.% observed by SEM were very smooth with no significant scratches even when the highest load was applied. The EDX analysis of the center of the wear tracks showed the same chemical composition as the unworn surface. However, at higher loads exceeding 20 N, the sides of the wear tracks were covered by adhered wear debris rich in tungsten and oxygen. The wear tracks produced by sliding on the high carbon content coatings were covered

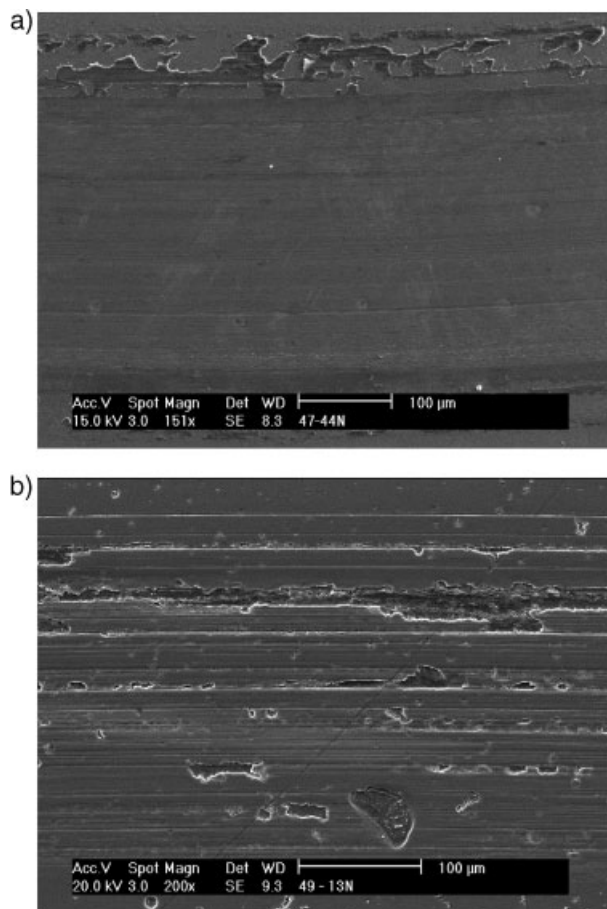


Figure 3. SEM micrographs of the wear tracks: (a) coating with 51 at.% C, load 44 N and (b) 66 at.% C, 13 N.

by scratches parallel to the relative movement of the ball. The wear debris layer formed isles adhered on the worn surface of the coating (Figure 3).

Raman spectroscopy was carried out in different places in the wear tracks and outside. Two groups of peaks could be observed, one corresponding to carbon (i.e. D and G peaks) and another consisting of two peaks (325 and 416 cm^{-1}). The later group was identified as WS_2 , since both peaks match well to the Raman spectrum taken from a WS_2 pellet. Unfortunately, the laser power had to be lowered to very low values in order to avoid the coating damage, predominantly graphitization, which could be observed for higher power values. Consequently, the obtained spectra were very noisy and their deconvolution difficult. However, an interesting feature was observed, the ratio I_c/I_{WS_2} , calculated as the sum of the carbon peaks areas divided by the sum of the WS_2 peaks areas, decreased from the unworn surface to the center of the wear track. This behavior is typical for all coating compositions; an example is shown in Figure 4.

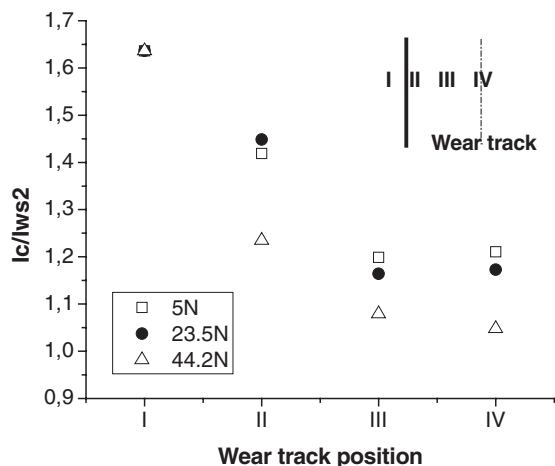


Figure 4. I_c/I_{WS2} ratio for different loads as a function of the position in the wear track, coating with 51 at.-% C.

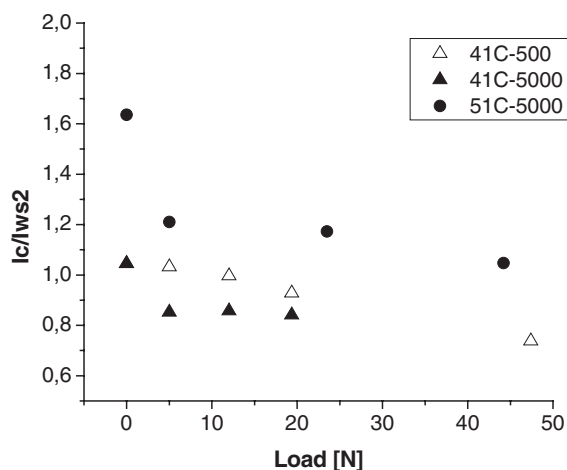


Figure 5. I_c/I_{WS2} ratio as a function of load for coatings with 41 and 51 at.-% C. Note the different number of laps, 500 and 5000.

Frictional Mechanism

The results of the frictional analysis complemented by the observation of the worn surfaces show that the third body formed between the two surfaces in the contact plays a dominant role in the friction process. Only coatings with a carbon content up to 51 at.-% C were selected for further analysis of the frictional mechanisms, since the third body was not homogeneous in the case of the wear tracks produced on the coating with the highest carbon content. Wu et al. tested W-S-C coatings with similar chemical composition sliding in air and they concluded that the development of a uniform well-bonded layer on the pin was associated to the low friction.^[6] They observed no surface layer on the coating after the test and their Raman spectrum obtained in the wear track was identical with that of the unworn surface. However, as referred to above, significant changes in the Raman spectra taken from different parts of the wear tracks were observed in this work.

The decrease in the I_c/I_{WS2} ratio towards the center of the wear track presented in Figure 4 indicates that an increasing contact pressure induces the formation of a thin tungsten sulfide film on the coating surface, or a structural change in the bulk of the coating, or a combination of both. The I_c/I_{WS2} ratio obtained from the Raman spectra taken from the center of the wear tracks of a selected coating is lower in the case of tests with higher number of laps, see Figure 5. Therefore, whatever the change in the coating induced by sliding is, it is enhanced by the increasing number of laps.

The decrease of the friction with increasing load of W-S-C coatings is very similar to the frictional behavior of pure TMD coatings.^[7–9] The easy intra- and intercrystalline

slip in the friction contact due to weak Van der Waal's forces between the lamellae of S-W-S hexagonal basal planes of pure tungsten disulfide facilitates the friction by diminishing the tangential force necessary for the sliding. During a pin-on-disk test, the transfer of the coating material to the ball surface and the reorientation induced by the friction of the randomly oriented WS_2 grains, in the contact area, to the basal plane orientation, transforms the materials in contact. Consequently, the friction force that originated in this case is due, predominantly, to the slipping referred to above. Zabinski et al.^[10] showed, for the W-S-C system with 20 at.-% of sulfur content that the friction mechanism intervening in the sliding contact was very similar to that of pure tungsten disulfide and that the contribution of the carbon to the friction was negligible.

Therefore, the methodology used for the analysis of the frictional properties of pure TMD coatings, particularly for MoS_2 coatings, has been used for W-S-C coatings as a function of the load.

Frictional Heating

The friction coefficient is significantly higher when TMD materials are sliding in humid air than in dry air. The heating of the TMD surface during sliding causes the drying of the air and, consequently, the decrease in the friction.^[11] Therefore, if the increase in the contact pressure causes an increase in the temperature of the coating surface, the friction should diminish. The rate of the frictional heating (R_{FH}) per unit sliding area can be derived as

$$R_{FH} = \frac{P_{FC}}{2al} \quad (1)$$

where a is the Hertzian radius^[12], l the sliding distance, and P_{FC} the rate of the frictional heating calculated as

$$P_{FC} = \mu Ls \quad (2)$$

where μ is the friction coefficient, L the normal load, and s the sliding speed. The calculations show that there is no significant increase in R_{FH} with increasing normal load. Therefore, the drying of the air due to the frictional heating does not contribute to the observed decrease in the friction with load.

Shear Stress Contribution

For MoS₂ coatings, the Hertzian contact model was used to explain the frictional behavior for a pin-on-disk configuration. The model was derived from the formula approximating the shear stress of solids at high pressures as

$$\tau = \tau_0 + \alpha P \quad (3)$$

where τ is the shear strength and P is the contact pressure.^[13] The constants τ_0 and α are material properties. Dividing Equation 3 by the contact pressure calculated as the mean Hertzian pressure^[14] gives

$$\mu = \tau_0 \pi \left(\frac{3R}{4E} \right)^{\frac{2}{3}} L^{-\frac{1}{3}} + \alpha \quad (4)$$

where R is the radius of the ball, L the normal load, and E the composite modulus of the couple given by

$$\frac{1}{E} = \frac{1 - \nu_1^2}{E_1} + \frac{1 - \nu_2^2}{E_2} \quad (5)$$

where $E_{1,2}$ and $\nu_{1,2}$ are the Young's moduli and the Poisson ratios of the coating and the ball. The experiments showed that the described model can be used as a good approximation to explain the decrease in the friction of MoS₂ with the contact pressure. Singer et al. used the power analysis applied to Equation 4 satisfying $L^{-1/3}$ behavior, which allowed to calculate α as 0.001 ± 0.001 .^[8] Grosseau-Poussard et al. used a linear analysis considering α being close to zero and they too confirmed $L^{-1/3}$ behavior.^[14]

However, the calculations of the present research show that the referred approach is not applicable for W-S-C coatings. The power analyses applied to Equation 4, where power over L and α were variables, give as the best fit values -0.54 and a negative α . Therefore, Equation 4 is not applicable to this case. This result was also confirmed by the examination of the $\log(\mu)$ against $\log(L)$ plots.

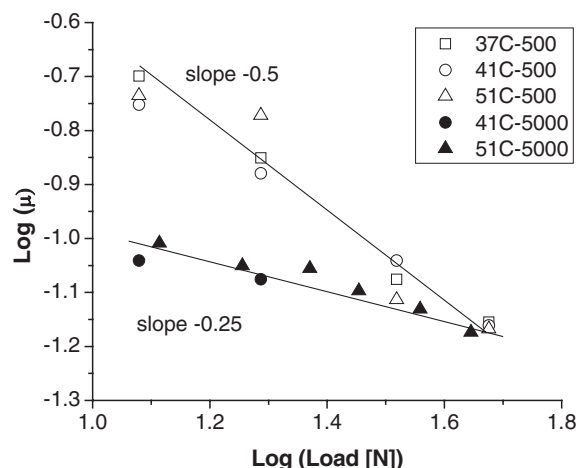


Figure 6. $\log(\text{friction})$ versus $\log(\text{load})$. Straight lines are the least square fits of all points corresponding to 500 and 5000 laps, respectively.

Mechanisms of Friction of W-S-C Coatings

The formation of a thin surface layer on both surfaces in the contact significantly decreases the friction coefficient. This formation corresponding to the running-in process is connected with a high friction coefficient and the polishing of asperities in the contact. However, a minimal W-S content in W-S-C coatings is required to decrease the friction. The coatings with high carbon content, i.e. with 66 at.-%, exhibit no running-in period and their friction remained high during the entire test. The evolution of the friction coefficient with the load of W-S-C coatings up to 51 at.-% C is very similar to that of pure TMD and no significant differences among various chemical compositions have been found. Since Raman spectroscopy has shown an increase of W-S to carbon ratio in the wear track, the formation of a thin WS₂ layer, supposedly with (002) orientation, should be expected. However, the shear stress analysis has shown that the frictional process of W-S-C coatings is not fully comparable to that of TMD. Therefore, the intra- and intercrystalline slip between S-W-S lamellae is not the exclusive frictional mechanism.

Nevertheless, the evolution of the friction coefficient with load shows other interesting features, since a linear dependence of $\log(\mu)$ with $\log(L)$ has been obtained (Figure 6). It seems that the friction coefficient can be calculated as a function of the load by a simple empirical equation

$$\mu = AL^B \quad (6)$$

where A is a constant corresponding to the material and the contact conditions, and the constant B represents the influence of the number of laps, i.e. the formation of a third

body and/or the structural changes of the coating in the contact area. This behavior is independent of the carbon content of the coating in the range 37–51 at.-%.

Conclusion

W-S-C coatings deposited by rf magnetron sputtering from a carbon target embedded with a different number of WS₂ pellets were tribologically tested under different loads in humid air. The average friction coefficient generally decreased with the increase of the load reaching values as low as 0.05. Raman spectroscopy analysis revealed a structural change of the coating in the contact area. The decrease of the friction with increasing load is not connected with the frictional heating, since the rate of the frictional heating per unit sliding area remained almost constant regardless of the contact pressure. Despite the similarity in the frictional behavior of W-S-C coatings and pure TMD, the friction mechanism is different.

Acknowledgements: The authors would like to acknowledge the financial support by FCT (Project POCTIEME 46548/2002).

Received: September 11, 2006; Revised: November 21, 2006;
Accepted: December 4, 2006; DOI: 10.1002/ppap.200731402

Keywords: hardness; magnetron sputtering; self-lubricant; thin films; tribology; WSC

- [1] A. Nossa, A. Cavaleiro, *Surf. Coat. Technol.* **2001**, 142–144, 984.
- [2] A. Nossa, A. Cavaleiro, *Surf. Coat. Technol.* **2003**, 163–164, 552.
- [3] G. Wiese, N. Mattern, H. Herman, A. Teresiak, I. Bascher, W. Bruckner, H.-D. Bauer, H. Vinzelberg, G. Reiss, U. Kreissig, M. Mader, P. Markschlager, *Thin Solid Films* **1997**, 298, 98.
- [4] A. Nossa, A. Cavaleiro, N. J. M. Carvalho, B. J. Kooi, J. Th. M. De Hosson, *Thin Solid Films* **2005**, 484, 389.
- [5] S. Watanabe, J. Noshiro, S. Miyake, *Surf. Coat. Technol.* **2004**, 183, 347.
- [6] J.-H. Wu, M. Sanghavi, J. H. Sanders, A. A. Voevodin, J. S. Zabinski, D. A. Rigney, *Wear* **2003**, 255, 859.
- [7] B. J. Briscoe, A. C. Smith, *ASLE Trans.*, 25, 349.
- [8] I. L. Singer, R. N. Bolster, J. Wegand, S. Fayeulle, B. C. Stupp, *Appl. Phys. Lett.* **1990**, 57, 995.
- [9] A. K. Kohli, B. Prakash, *Tribol. Trans.* **2001**, 44, 147.
- [10] A. A. Voevodin, J. P. O'Neill, J. S. Zabinski, *Surf. Coat. Technol.* **1999**, 116–119, 36.
- [11] T. Kubart, T. Polcar, L. Kopecky, R. Novak, D. Novakova, *Surf. Coat. Technol.* **2005**, 193, 230.
- [12] W. C. Young, *Roark's Formulas for Stress and Strain*, McGraw Hill, New York 1989.
- [13] L. D. Towle, *J. Appl. Phys.* **1971**, 42, 2368.
- [14] J. L. Grosseau-Poussard, P. Moine, M. Brendle, *Thin Solid Films* **1997**, 307, 163.

Synthesis and structural properties of Mo–Se–C sputtered coatings

T. Polcar^{a,b}, M. Evaristo^a, M. Stueber^c, A. Cavaleiro^{a,*}

^a SEG-CEMUC - Department of Mechanical Engineering, University of Coimbra, Rua Luís Reis Santos, P-3030 788 Coimbra, Portugal

^b Department of Applied Mathematics, Faculty of Transportation Sciences, Czech Technical University in Prague, Na Florenci 25, Prague 1, Czech Republic

^c Forschungszentrum Karlsruhe, Institute of Materials Research I, Hermann-von-Helmholtz-Platz 1, 76344 Eggenstein-Leopoldshafen, Germany

Available online 23 August 2007

Abstract

Transition metal dichalcogenides have attracted considerable attention due to their self-lubricant properties. Their drawbacks, such as low load-bearing capacity or environmental sensitivity, have been partially overcome by alloying or doping with metals, carbon, or nitrides. Nevertheless, there is still a considerable potential for further improvement, since the majority of studies has been aimed at MoS₂ and WS₂ based coatings and the properties of diselenides remain almost unknown.

Mo–Se–C coatings were prepared by non-reactive r.f. magnetron sputtering from carbon target with embedded MoSe₂ pellets. The carbon content and Se/Mo ratio determined by electron probe microanalysis increased from 29 to 68 at.% and from 1.7 to 2.0, respectively, as a function of the decreasing number of pellets. The coating structure analyzed by X-ray diffraction, Raman spectroscopy and X-ray photoelectron spectroscopy showed that Mo–Se–C was a mixture of amorphous carbon and Mo–Se phases, since no traces of molybdenum carbides were observed. Linear increase of the hardness from 0.7 (29 at.% C) to 4.1 GPa (68 at.% C) showed a significant improvement compared to values typical for pure MoSe₂ coating.

© 2007 Elsevier B.V. All rights reserved.

Keywords: MoSe₂; Self-lubrication; Carbon based coating

1. Introduction

Transition metal dichalcogenides (TMD—sulfides, selenides or tellurides of tungsten, molybdenum and niobium) are well-known for their lubricating property [1]. MoS₂ is the most popular member of the above-mentioned family and it is widely used as a solid lubricant in vacuum and inert atmospheres. Most of the research efforts developed on these materials have been carried out in the form of coatings and thin films. Magnetron sputtering has been one of the most used techniques for their deposition due to its ability to provide the modification of the chemical composition and crystal structure which can lead to improvements on their tribological properties [2]. The detrimental influence of humidity on the coating properties is the main problem of MoS₂ and other TMD when used as a lubri-

cant. Moreover, other drawbacks of TMD are their low load-bearing capacity, poor adhesion on substrates and low hardness.

There are a lot of different possibilities to improve the tribological behavior of these coatings at humid atmosphere. One of the most successful ways is to deposit a composite material associating high strength with self-lubricants materials, i.e. doping TMD films with other metals, such as Ti [3], Pb [4], Cr [5,6], or Au [6].

Carbon was considered as a promising doping candidate with expected “chameleon” effect, i.e. low friction coefficient either in vacuum and dry air due to the presence of TMD, or in humid air where the carbon will be dominant for the sliding process. Voevodin et al. [7] have introduced the W–C–S system for self lubrication applications concluding that it exhibits excellent tribological properties in space simulation tests. Later on, the structure [8], mechanical properties [9] and tribological performance [10,11] of W–S–C coatings prepared by magnetron sputtering were intensively studied by the present authors. It could be concluded that doping with carbon leads to the

* Corresponding author. Tel.: +351 239 790 700; fax: +351 239 790 701.
E-mail address: albano.cavaleiro@dem.uc.pt (A. Cavaleiro).

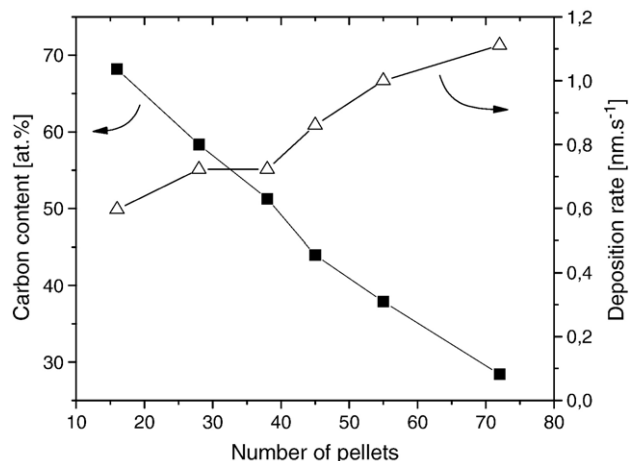


Fig. 1. Carbon content and deposition rate as a function of number of MoSe₂ pellets embedded into carbon target.

improvement of the mechanical (hardness, adhesion) and tribological (friction and wear resistance when sliding at humid air) properties.

This study deals with the synthesis and structural properties of Mo–Se–C coatings prepared by non-reactive magnetron sputtering from a carbon target with MoSe₂ pellets.

2. Experimental details

The coatings were deposited on both silica wafers and M2 (AISI) steel substrates (hardness close to 9 GPa). A thin titanium interlayer (~300 nm) was deposited in order to improve the adhesion of the coatings to the substrate. The coatings were deposited by magnetron sputtering in argon atmosphere from a carbon target with pellets of MoSe₂ (100 mm diameter). The pellets (99.8% pure) with dimensions of 1.5 × 3 × 4 mm were distributed uniformly in the circular erosion zone of the carbon target; their number varied between 16 and 72. The discharge pressure and the power density were 0.75 Pa and 8 W cm⁻², respectively. The deposition time was 1 h giving rise to a final thickness of the coatings in the range [2.5–4 μm]. The coating microstructure was studied by X-ray diffraction (XRD) in glancing mode (Co Kα radiation) and the chemical composition was obtained by electron probe microanalysis (EPMA), while Raman (Ar⁺ laser, 514.5 nm wavelength) and X-ray photoelectron spectroscopies (XPS) were applied to analyze the chemical bonding. Mg Kα radiation ($E=1253.6$ eV) was used and the spectra were taken before and after ion etching with Ar⁺ ions (3 KeV and 5 μA/cm²) during 3 min. The pure sputtered MoSe₂ coating deposited from MoSe₂ target described in our previous study has been used as a reference for Raman analysis [12].

The coating morphology was studied by scanning electron microscopy (SEM). The hardness of the coatings was evaluated by depth-sensing indentation technique using a Fischer Instruments-Fischerscope H100. The indentation load was increased in 60 steps up to a maximum load of 20 mN; the same number of steps was used during unloading.

3. Results and discussion

3.1. Deposition of Mo–Se–C coatings and their chemical composition

The coatings were deposited with different number of MoSe₂ pellets implanted in carbon target in order to achieve different chemical composition. The carbon content in the coatings decreased linearly with the increasing number of pellets, see Fig. 1. The deposition rate increased with the number of pellets due to the higher sputtering rate of MoSe₂ compared to carbon (Fig. 1). The Se/Mo and (Se+C)/Mo ratios are depicted in Fig. 2. Despite relatively high cumulated error of the chemical composition measurements, it could be summarized that both Se/Mo and (Se+C)/Mo ratios increased with carbon content.

The chemical composition measurement revealed as well relatively low oxygen contents in the coatings, which decreased monotonically from 5 to 2 at.% with increasing carbon content. This evolution was expected, since the porous MoSe₂ pellets acted as a source of the atmospheric contamination.

3.2. Morphology and structure

SEM micrograph of the cross-section of the coating with the lowest carbon content showed a columnar structure perpendicular to substrate, which is typical for pure transition metal dichalcogenides [2,8]. However, this structure exhibited a very small number of pores compared to pure TMD deposited by magnetron sputtering [2,12]. The columns length decreased with increasing carbon content and columns started to grow in a dendritic way. The coatings with 58 and particularly 68 at.% C were amorphous-like with no clear columns visible (Fig. 3). Higher density and compactness of the coating compared to pure MoSe₂ should significantly increase the hardness and positively increase the coating resistance to environmental attack; therefore, improved tribological properties in humid atmosphere are expected, as was demonstrated in the case of W–S–C system [10].

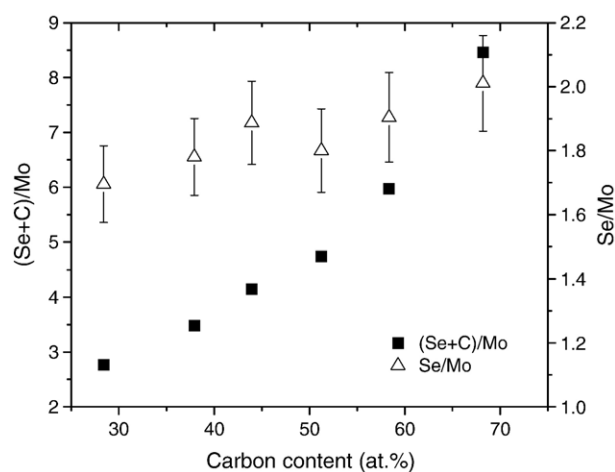


Fig. 2. (Se+C)/Mo and Se/Mo ratio as a function of carbon content in the coatings.

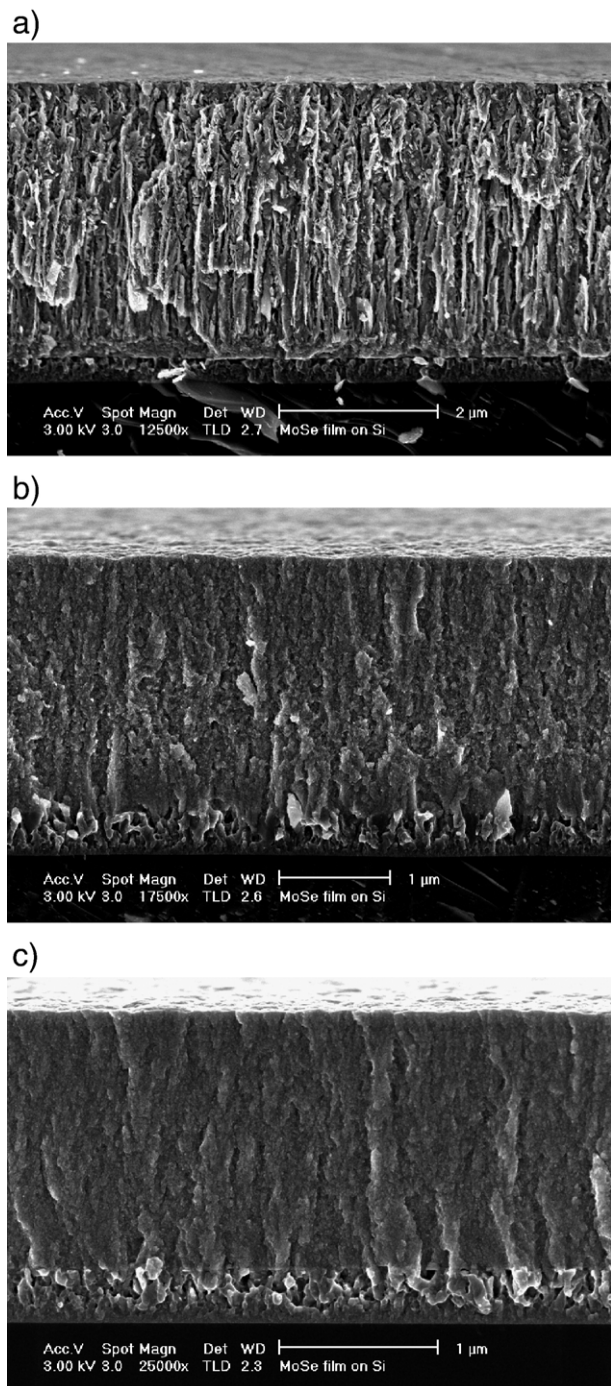


Fig. 3. SEM micrographs of Mo–Se–C coatings cross-sections, a) 29 at.% C, b) 51 at.% C, c) 68 at.% C.

The XRD diffractograms of Mo–Se–C coatings showed a peak close to $2\theta \approx 37.5^\circ$ (MoSe₂ phase with (100) orientation) followed by a second one at $2\theta \approx 44.5^\circ$ (Fig. 4). The later is highly asymmetric with a long tail towards higher 2θ . Finally a last peak positioned at $2\theta \approx 70^\circ$ has been indexed as (110). Weise et al. [13] demonstrated that the extended shoulder of the sputtered MoSe₂ peak positioned close to $2\theta \approx 40^\circ$ corresponded to a turbostrating stacking of (10L) planes ($L=0, 1, 2, 3$). XRD patterns then could be explained by a 2D organization of the basal plans which could have several tenths of

unit cells dimension. With the progressive decrease of the lateral dimensions of the basal plans, either broadening or drop in the intensity of the (10L) plan occurred until a unique low intensity and broad peak typical of an amorphous structure was detected. This situation would arise when the lateral order of the basal plans did not exceed a couple of lattice parameters [13]. It has been shown that similar extended peak shoulder was present in XRD of W–S–C films, where the existence of WS₂ nanograins in a carbon matrix was confirmed by HRTEM observation [8]. As demonstrated in Fig. 4, the presence of molybdenum carbide phases could not be detected by XRD.

Therefore, we may suggest that Mo–Se–C coatings consist of small MoSe₂ grains (grains size lower than 5 nm) embedded in an amorphous carbon matrix. Moreover, the X-ray diffraction patterns showed a gradual loss of crystallinity with the increase of the carbon in the coatings.

3.3. Chemical bonding and Raman spectroscopy

The detection of any possible molybdenum carbide peaks in Mo3d XPS spectra, which is shown in Fig. 5a, is very difficult, since the electronegativity of either selenium or carbon is 2.55. Therefore, no significant shift of the peak is expected if besides the Mo–Se bond a Mo–C bond (presence of molybdenum carbide phases) can also exist. Fig. 5b shows the C1s spectra of Mo–Se–C together with the standard positions of C–C and Mo–C (i.e. Mo₂C and Mo₃C₂) binding energies. The C1s peak

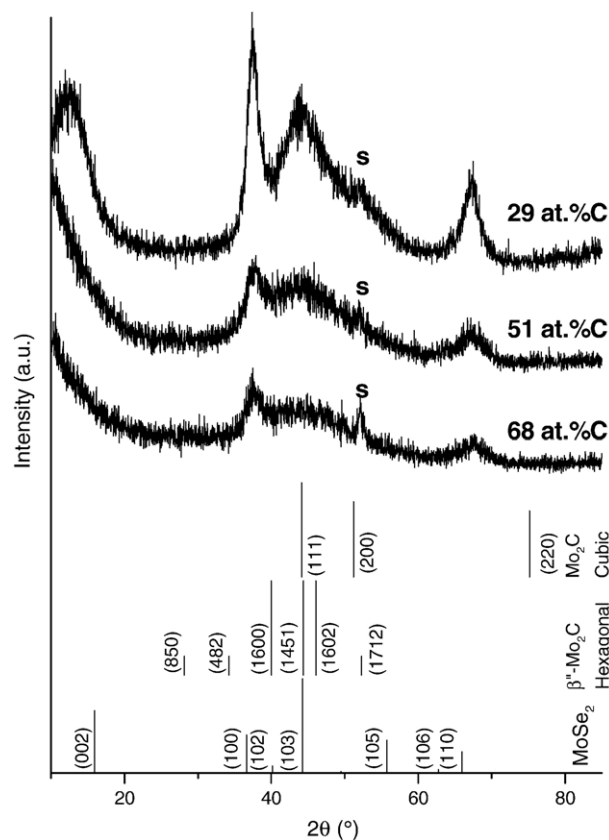


Fig. 4. XRD spectra of Mo–Se–C coatings and standard diffraction lines from ICDD cards of MoSe₂ and selected Mo–C compounds (s — substrate).

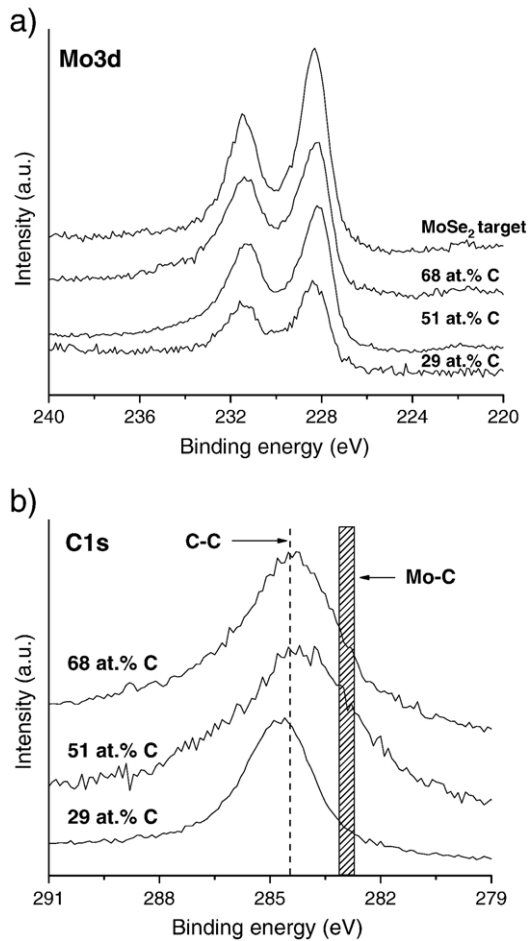


Fig. 5. Mo3d (a) and C1s (b) spectra of sputtered Mo–Se–C coatings.

exhibited no shift towards lower binding energy values compared to C–C bonding position, which suggests the absence of Mo–C bonds in the coatings.

The Raman spectra of Mo–Se–C coatings are presented in Fig. 6 together with the referential spectra of MoSe₂ pellet and pure sputtered MoSe₂. MoSe₂ pellet exhibited a strong peak placed at $\sim 240\text{ cm}^{-1}$, and small and not well defined peaks positioned at higher values of the Raman shift. The sputtered MoSe₂ exhibited only one very broad and asymmetric peak. The broadening of the Raman modes is related to the presence of structural defects and/or stress gradients in the scattering volume [14]. Therefore, the significant broadening of the peak at $\sim 240\text{ cm}^{-1}$ indicates a degradation of the structural quality of the MoSe₂ lattice when MoSe₂ is sputtered.

Typical spectrum of Mo–Se–C coatings could be divided into three parts: (i) a group of peaks belonging to molybdenum diselenide phases in the range of $200\text{--}700\text{ cm}^{-1}$, (ii) a region at $700\text{--}900\text{ cm}^{-1}$ corresponding to molybdenum oxide peaks, and (iii) the peaks representing D and G bands of carbon in the range $[1100\text{--}1800\text{ cm}^{-1}]$. Since the MoSe₂ peak is even broader in the case of Mo–Se–C compared to pure sputtered MoSe₂, a further decrease of the structural quality can be expected. It confirms the result obtained by XRD and supports Wiese' interpretation, i.e. the presence of Mo–Se grains with dimen-

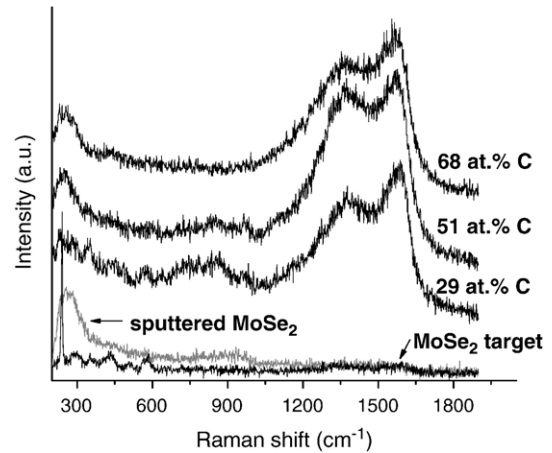


Fig. 6. The Raman spectra of selected Mo–Se–C coatings. The spectra of MoSe₂ pellet and sputtered MoSe₂ are shown as reference.

sions significantly lower than 10 nm. The molybdenum oxide peak was identified as MoO₃ [15]; its intensity decreased with increasing carbon content being proportional to the oxygen content referred above.

The analysis of the carbon-based peaks required considering not only the major D and G bands, but as well as one minor modulation. The deconvolution was initially done by applying either Gaussian or Lorentzian curves or Breit–Wigner–Fano line for the G peak and a Lorentzian line for the D peak; however, the results did not fit to the experimental data. Finally, a reasonable fit was achieved by adding a new peak in the position close to 1150 cm^{-1} . This fitting procedure is sometimes used in the case of DLC coatings, see Ref. [16]; the existence of referred peak could be connected with the existence of a very poorly organized carbonaceous material [17].

When the carbon content in the coating increased, the G peak shifted from 1585 to 1575 cm^{-1} and $I(D)/I(G)$ ratio remained almost constant (i.e. in the range $0.9\text{--}1.1$ with no clear dependency on carbon content). According to the widely adopted three-stage model presented by Ferrari and Robertson in Ref.

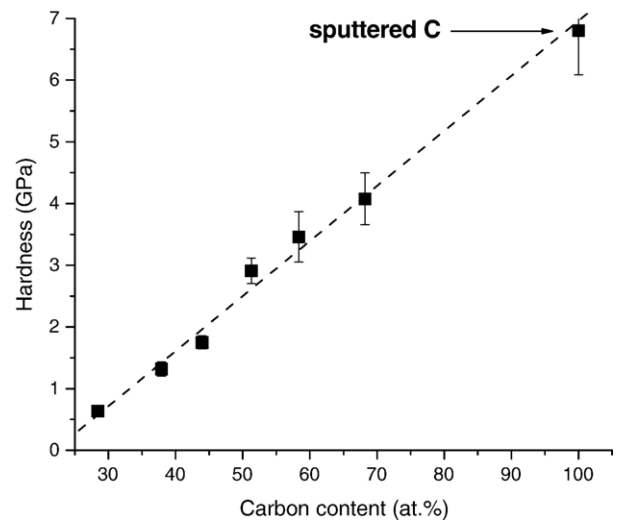


Fig. 7. Evolution of the Mo–Se–C coatings hardness with carbon content.

[16], it could be suggested that defects are progressively introduced into the graphite layer as the carbon content increased. Considering the high value of the I(D)/I(G) ratio, no significant amount of sp^3 bonds in Mo–Se–C coatings is expected. It should be pointed out that the Raman spectra of Mo–Se–C coatings with the highest carbon content are almost identical (obviously only in the range 1100–1900 cm^{-1}) to that of a pure carbon film sputtered from carbon target without pellets.

3.4. Hardness

The low hardness of sputtered $MoSe_2$ (~ 0.5 GPa) could be significantly improved by co-sputtering with carbon, as shown in Fig. 7. The hardness of the coating with 29 at.% C was only slightly higher than that of pure $MoSe_2$ but, then, it increased linearly with carbon content up to the level of the sputtered carbon coating. This behavior is closely related to the morphology of Mo–Se–C films, particularly its densification, as referred from above. The hardness evolution confirmed as well as the absence of molybdenum carbides in the coatings, since the existence of these hard phases would lead to a significant hardness increase above the level of pure carbon, as shown in the previous work with similar W–S–C system [18].

4. Conclusions

The Mo–Se–C coatings were prepared by r.f. magnetron sputtering from a carbon target with $MoSe_2$ pellets with carbon contents in the range [29–68 at.%]. The Se/Mo ratio increased with carbon content from 1.7 to 2.0; this high values could be favorable for tribological applications. Co-sputtering with carbon led to a significant improvement in the hardness compared to the pure sputtered $MoSe_2$. Based on XRD, XPS and Raman spectroscopy analyses, it could be stated that the Mo–Se–C coatings consisted of small $MoSe_2$ grains with size lower than 5 nm embedded into a carbon matrix; no vestiges of molybdenum carbides were observed.

Acknowledgements

This work was supported by the Czech Science Foundation through the project 106/07/P014 and by the Fundação para a Ciência e a Tecnologia through the project POCTI/EME/46548/2002.

References

- [1] W.E. Jamison, S.L. Cosgrove, ASLE Trans. 14 (1971) 62.
- [2] A.R. Lansdown, Molybdenum Disulphide Lubrication, Elsevier, 1999.
- [3] D.G. Teer, Wear 251 (2001) 1068.
- [4] K.J. Wahl, L.E. Seitzman, R.N. Bolster, I.L. Singer, Surf. Coat. Technol. 73 (1995) 152.
- [5] Y.L. Su, W.H. Kao, Tribol. Int. 36 (2003) 11.
- [6] M.C. Simmonds, A. Savan, E. Pfluger, H. Van Swygenhoven, Surf. Coat. Technol. 126 (2000) 15.
- [7] A.A. Voevodin, J.S. Zabinski, Compos. Sci. Technol. 65 (2005) 741.
- [8] A. Nossa, A. Cavaleiro, J. Mater. Res. 19 (2004) 2356.
- [9] M. Evaristo, A. Nossa, A. Cavaleiro, Surf. Coat. Technol. 200 (2005) 1076.
- [10] A. Nossa, A. Cavaleiro, Surf. Coat. Technol. 142–144 (2001) 984.
- [11] A. Nossa, A. Cavaleiro, Surf. Coat. Technol. 163–164 (2003) 552.
- [12] T. Kubart, T. Polcar, L. Kopecký, R. Novák, D. Nováková, Surf. Coat. Technol. 193 (2005) 230.
- [13] G. Weisse, N. Mattern, H. Hermann, A. Teresiak, I. Bacher, W. Bruckner, H.-D. Bauer, H. Vinzelberg, G. Reiss, U. Kreissig, M. Mader, P. Markschlager, Thin Solid Films 298 (1997) 98.
- [14] J. Álvarez-Garsía, J. Marcos-Ruzafa, A. Pérez-Rodríguez, A. Romano-Rodríguez, J.R. Morante, R. Scheer, Thin Solid Films 361–362 (2000) 208.
- [15] A.A. Voevodin, J.S. Zabinski, Wear 261 (2006) 1285.
- [16] A.C. Ferrari, J. Robertson, Phys. Rev., B 61 (2000) 14095.
- [17] O. Beyssac, J.N. Rouzaud, B. Goffé, F. Brunet, C. Chopin, Contrib. Mineral. Petrol. 143 (2002) 19.
- [18] M. Evaristo, A. Nossa, A. Cavaleiro, Surf. Coat. Technol. 200 (2005) 1076.

TEM investigation of MoSeC films

C.Silviu Sandu^{a,b}, Tomas Polcar^{a,c} and Albano Cavaleiro^{a,*}

^a ICEMS - Mechanical Engineering Department, University of Coimbra, Polo 2, 3030-788 Coimbra, Portugal

^b EPFL – Ecole Polytechnique Federale de Lausanne, CH-1015 Lausanne, Switzerland

^c Department of Control Engineering, Faculty of Electrical Engineering, Czech Technical University in Prague, Technická 2, Prague 6, Czech Republic

*albano.cavaleiro@dem.uc.pt

Transition metal dichalcogenides (TMD) are widely used as self-lubricating material either as oil additive or directly as thin films. Magnetron sputtering is a deposition method allowing depositing such films with high density and adhesion. However, their spread use in practical applications is still hindered since their excellent sliding properties are deteriorated in the presence of humidity and under high contact pressures. MoSe₂, one of the members of TMD family recently studied [1], has been co-sputtered with carbon in order to improve the mechanical and tribological properties when compared to pure MoSe₂ films.

The films have been deposited by co-sputtering from a C target embedded with a different number of MoSe₂ pellets. Prior to the deposition of Mo-Se-C films a 300 nm Ti layer was deposited on the steel and Si substrates in order to improve the adhesion. The chemical composition was measured by electron probe microanalysis (EPMA). Cross-sectioned specimens were prepared from samples containing 38, 51 and 68 at.% of carbon (Se/Mo ratio 1.8, 1.8 and 2.0, respectively) by mechanical polishing and ion milling. The morphology and the chemical composition of the coatings were investigated by HRTEM and EDS in a Philips-CM300 microscope. To support TEM analysis, the coatings were tested by Raman spectroscopy (Ar⁺ laser, 514.5 nm wavelength), X-Ray Photoelectron spectroscopy (XPS - Mg K α radiation) and X-ray diffraction (XRD - Bragg-Brentano configuration in glancing mode, Co K α radiation) and their hardness was evaluated by depth sensing indentation (Fisherscope H100, maximum load 50 mN). The XPS spectra were taken after ion etching with Ar⁺ ions (3 KeV and 5 μ A/cm²) during 3 min.

TEM micrographs show that film morphology strongly depends on the C content (Fig. 1). By increasing the C content of the films, the MoSe₂ nanocrystallites became smaller as indicated by the increase of the width of the diffraction rings in SAED patterns. At the same time the film morphology became more homogeneous. The contrast observed in the Mo-Se-C layers, after about 200 nm thickness, can be attributed to the material porosity, probably related to the typical columnar morphology usually developed in TMD films. The lower part of the films looks more dense and homogeneous (low porosity). The films porosity clearly decreases with increasing C content (Fig. 1 and 2); simultaneously, the columnar structure almost vanishes. This result complements the information obtained by previous SEM analysis of Mo-Se-C coatings published in Ref [1], (see the right part of the pictures in figure 1) where the aspect of low density is kept even for high C content films. Based on TEM analysis, it seems that the columnar growth is typical only for low carbon coatings and the dendritic growth described in Ref [2] and observed in figure 1 is probably only an artifact originated during sample breaking. The increase of the material density could promote the improvement of the hardness from 1.4 to 4.0 GPa with increasing C content in the range 38-68 at.%.

The alignment of the basal planes of the MoSe₂ phase leads to the formation of platelets which, in contrast images, have the appearance of wires (Figs. 2 and 3). The increase of C

amount in the layer stops the development of the ordering of the basal MoSe_2 planes leading to decreasing platelets dimensions, as can be concluded by the shortening of these apparent wires. Fig. 2a shows long curved chains consisting of tens of parallel MoSe_2 basal planes, in contrast to Fig. 2c, where the platelets thickness is shorter (about 5 nm) and clearly separated. The most interesting feature in XRD diffractograms of Mo-Se-C coatings is the presence of a highly asymmetric peak, with a long tail towards higher 2θ , positioned at $2\theta \approx 44.5^\circ$ (Fig. 2d). It has been shown [1] that the extended shoulder of the sputtered MoS_2 peak positioned close to $2\theta \approx 40^\circ$ corresponds to a turbostrating stacking of (10L) planes ($L = 0, 1, 2, 3$). XRD patterns then could be explained by a 2D organization of the basal planes which could have several tenths of unit cells dimension. The broadening or drop in the intensity of the (10L) plan is observed with the progressive decrease of the lateral dimensions of the basal planes and the platelets. This situation would arise when the lateral order of the basal planes did not exceed a couple of lattice parameters [3]. It should be pointed out that similar results have been obtained in case of W-S-C films, where the existence of WS_2 nanograins in a carbon matrix was confirmed by HRTEM observation [4].

TEM results are confirmed as well by Raman analysis, as documented in Ref [2]. The peak representing MoSe_2 phase, positioned at $\sim 240 \text{ cm}^{-1}$, is very broad compared to the one of MoSe_2 bulk material indicating a strong degradation of its structural quality. At the same time, almost no change of the carbon peaks (i.e. intensity ratio between G and D peaks and G peak position) is observed, see inset of Fig. 4. It should be pointed out that EDS investigation reveals a lateral and transverse chemical homogeneity of all the analyzed Mo-Se-C films at a 10 nm scale.

The MoSe_2 platelets with diameters of approximately 0.4 nm appear to be embedded in an amorphous matrix. In spite of the difficulty in proving the assumed nanocomposite structure and to model the chemical bonding of the Mo-Se-C films by TEM analysis, Raman results proved the existence of independent MoSe_2 and C-based mixed phases. Furthermore, with high resolution TEM, no traces of molybdenum carbides nanograins could be detected confirming the results of XPS analysis [2]. XPS C1s peak was almost identical, whatever the C content was, with only a symmetrical peak positioned at C-C binding energy and not requiring deconvolution considering any other peak. Also, the presence of molybdenum carbide phases could not be detected by XRD spectra.

In this work, Mo-Se-C coatings deposited by magnetron sputtering from carbon target with different number of MoSe_2 pellets were analyzed by TEM. The addition of the C played a decisive role in the modification of the chemical bonding, morphology and structure of the coating. The formation of a nanocomposite material (nanocrystals of MoSe_2 embedded in an amorphous matrix) was possible over a wide range of deposition conditions. The dimension of the crystalline zones seemed to decrease with increasing C content as could be concluded by the progressive broadening of XRD peaks. The appearance of features like wires in the TEM observations suggested that MoSe_2 platelets were embedded in an amorphous carbon matrix.

Acknowledgements

This work was supported by the Czech Science Foundation through the project 106/07/P014, by the Ministry of Education of the Czech Republic (project MSM 6840770038) and by the Fundação para a Ciência e a Tecnologia through the project SFRH/BPD/34515/2006. CIME-EPFL team is acknowledged for the technical support.

References

- [1] T. Kubart, T. Polcar, L. Kopecký, R. Novák and D. Nováková, Surf. Coat. Technol. 193 (2005) 230.
- [2] T. Polcar et al., Surf. Coat. Technol. (2007), doi:10.1016/j.surfcoat.2007.08.019.
- [3] G. Weisse, N. Mattern, H. Hermann, A. Teresiak, I. Bacher, W. Bruckner, H.-D. Bauer, H. Vinzelberg, G. Reiss, U. Kreissig, M. Mader, P. Markschlager, Thin Solid Films 298 (1997) 98.
- [4] A. Nossa, A. Cavaleiro, J. Mater. Res. 19 (2004) 2356.

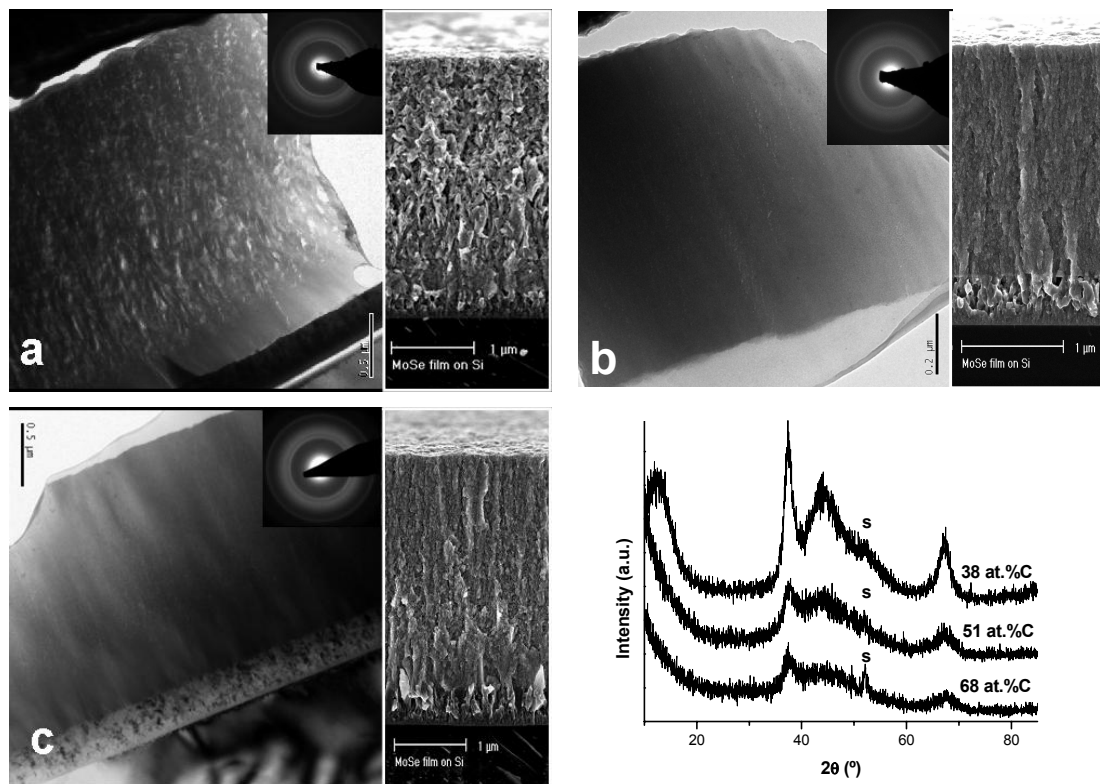


Fig.1 TEM images of MoSeC films cross-sections with corresponding SEM micrographs: a - 38% C, b - 51% C, c - 68% C, and d) XRD diffraction patterns.

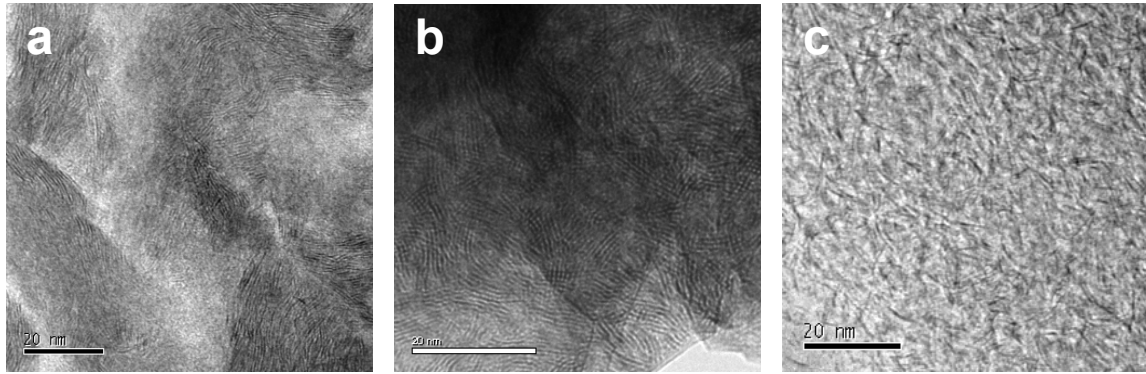


Fig.2 TEM images of Mo-Se-C films: a - 38% C, b - 51% C, c - 68% C.

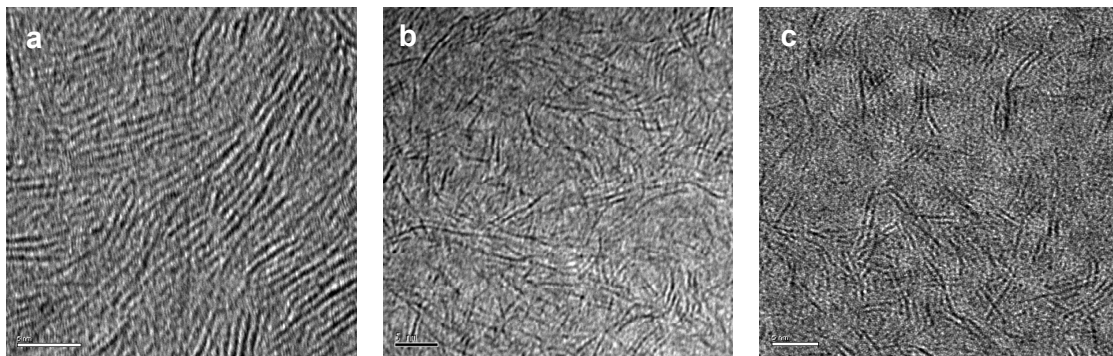
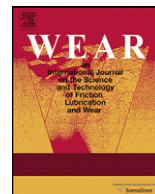


Fig. 3 HRTEM images of Mo-Se-C films: a - 38% C, b - 51% C, c - 68% C.



Mechanical and tribological properties of sputtered Mo–Se–C coatings

T. Polcar^{a,b}, M. Evaristo^a, M. Stueber^c, A. Cavaleiro^{a,*}

^a ICEMS, Mechanical Engineering Department, University of Coimbra, Coimbra, Portugal

^b Department of Control Engineering, Faculty of Electrical Engineering, Czech Technical University in Prague, Technická 2, Prague 6, Czech Republic

^c Forschungszentrum Karlsruhe, Institute of Materials Research I, Hermann-von-Helmholtz-Platz 1, 76344 Eggenstein-Leopoldshafen, Germany

ARTICLE INFO

Article history:

Received 1 October 2007

Received in revised form 29 February 2008

Accepted 7 April 2008

Available online 6 June 2008

Keywords:

Molybdenum diselenide

Self-lubrication

Dry sliding

Elevated temperature

ABSTRACT

Transition metal dichalcogenides belong to the more developed class of materials for solid lubrication. However, the main limitation of these materials is the detrimental effect of air humidity causing an increase in the friction. In previous works, molybdenum diselenide has been shown to be a promising coating retaining low friction even in very humid environment. In this study, Mo–Se–C films were deposited by sputtering from a C target with pellets of MoSe₂. Besides the evaluation of the chemical composition, the structure, the morphology, the hardness and the cohesion/adhesion, special attention was paid to the tribological characterization.

The C content varied from 29 to 68 at.% which led to a progressive increase of the Se/Mo ratio. As a typical trend, the hardness increases with increasing C content. The coatings were tested at room temperature with different air humidity levels and at temperatures up to 500 °C on a pin-on-disc tribometer. The friction coefficient of Mo–Se–C coatings increased with air humidity from ~0.04 to ~0.12, while it was as low as 0.02 at temperature range 100–250 °C. The coatings were very sensitive to the elevated temperature being worn out at 300 °C due to adhesion problems at coating–titanium interface.

© 2008 Elsevier B.V. All rights reserved.

1. Introduction

In late 1990s, a new concept of coatings based on the alloying of transition metal dichalcogenides (TMDs) with carbon started to attract the attention of various scientific groups. The original idea was to join the excellent frictional behavior of TMD in vacuum and dry air with the tribological properties of DLC coatings. Moreover, an increase in the coatings compactness in relation to TMD and an improvement of the mechanical properties, particularly the hardness, could be expected.

Voevodin and Zabinski [1] prepared W–S–C coatings either by magnetron-assisted pulsed laser deposition (MSPLD—target WS₂) or by laser ablation of a composite target made of graphite and WS₂ sectors. The friction coefficient in dry air was lower than that measured in humid air (0.02 and 0.15, respectively), and the frictional stability during an environmental cycling was considered as the most interesting feature. The low friction in dry air increased in the presence of humid air and fell down when the atmosphere was dried again.

Cavaleiro et al deposited W–S–C coatings by magnetron sputtering from carbon target with embedded WS₂ pellets [2,3]. The

maximum coating hardness was around 10 GPa, i.e. about one order of magnitude higher than that of pure sputtered WS₂. The tribological behavior of the coatings was tested under different conditions, such as temperature, air humidity or load. The friction decreased significantly with load varying in the range 5–48 N from 0.2 to 0.07 in humid air; the cyclic change of the air humidity showed the same “chameleon” behavior as referred to above.

However, both referred W–S–C systems still show relatively high wear and friction coefficients in humid environment. To remedy this lack, it was decided to select other member of the TMD family, the molybdenum diselenide, which showed low friction almost independently of the air humidity [4], and to study the mechanical and tribological properties of Mo–Se–C coatings prepared by non-reactive magnetron sputtering from a carbon target with MoSe₂ pellets.

2. Experimental details

The coatings were deposited on both silica wafers and steel substrates (chromium steel, quenched and tempered with a final hardness of 62 HRC) polished to final roughness Ra ≤ 30 nm. The thin titanium interlayer (~300 nm) was deposited in order to improve the adhesion of the coatings to the substrate. The coatings were deposited by magnetron sputtering in argon atmosphere from a carbon target with pellets of MoSe₂. The pellets (99.8% pure) were

* Corresponding author.

E-mail address: albano.cavaleiro@dem.uc.pt (A. Cavaleiro).

positioned in the erosion zone of the carbon target with a diameter of 100 mm. The dimensions of pellets were 1.5 mm × 3 mm × 4 mm, the number of pellets varied between 16 and 72. The discharge pressure and the power density were 0.75 Pa and 8 W cm⁻², respectively. The deposition time was 1 h.

The coating microstructure was studied by X-ray diffraction (XRD—Philips diffractometer, Bragg–Brentano configuration, Co K α radiation ($\lambda = 0.178897$ nm)); the chemical composition was determined by electron probe micro-analysis (EPMA—Cameca SX-50). The hardness (H) and Young's modulus (E) of the coatings were evaluated by depth-sensing indentation technique using a Fischer Instruments-Fischerscope.

Wear testing was done using a high temperature pin-on-disc tribometer (CSEM Instruments) adapted to work in controlled atmosphere; sliding partners were steel 100Cr6 balls with a diameter of 6 mm and a 5 N load. The number of laps was 1000, if not stated otherwise. The air humidity (RH) was controlled by a precise hygrometer; the atmosphere with relative air humidity 5% is referred in this study as dry air. The friction tests were carried out as well at elevated temperature up to 500 °C. The morphology of the coating surface, ball scars, wear tracks and wear debris were examined by scanning electron microscopy (SEM—Philips); the chemical analysis of the wear tracks and the wear debris was obtained by energy-dispersive X-ray analysis (EDS). The profiles of the wear tracks were measured by mechanical profilometer. The wear rate of the coating was calculated as the worn material volume per sliding distance and normal load. The average value of three profiles measured on one wear track was used to calculate the coating wear rate.

3. Results

3.1. Main characteristics of Mo–Se–C coatings

The coatings were deposited with different number of MoSe₂ pellets implanted in carbon target in order to achieve different chemical compositions, as presented in Fig. 1. The carbon content in the coatings decreased linearly with increasing number of pellets, while the deposition rate increased due to the higher sputtering

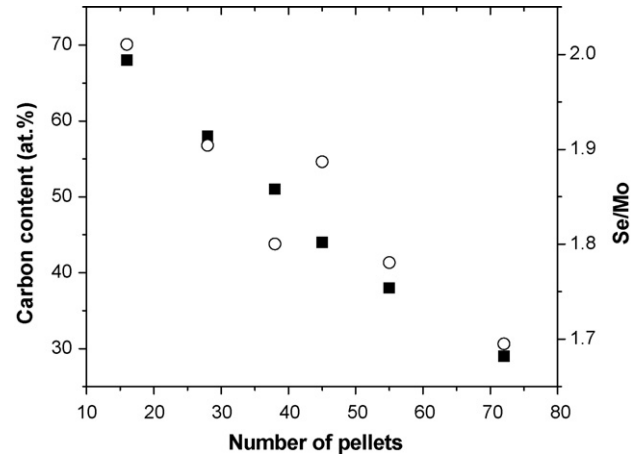


Fig. 1. Carbon content (full symbol) and Se/Mo ratio (open symbol) as a function of number of MoSe₂ pellets embedded into carbon target.

rate of MoSe₂ compared to carbon. Since the deposition time was kept constant (60 min), the coatings thickness increased as well from 2.2 (68 at.% C) to 4.0 μ m (29 at.% C). As it was expected, a monotonic decrease of the C content with increasing number of MoSe₂ pellets was observed with the simultaneous drop of the Se/Mo ratio from 2.0 to 1.7.

The coating with the lowest carbon content showed a columnar structure typical for pure transition metal dichalcogenides [5]. The columns length decreased with increasing carbon content and the morphology started to be amorphous-like for 58 at.% C (see Fig. 2). The XRD diffractograms of Mo–Se–C coatings were almost identical to those of W–S–C system discussed in detail elsewhere [6] (see typical example in Fig. 2); therefore only brief information is given in this paper. The well-defined peak at $\sim 37^\circ$ corresponded to (1 0 0) orientation and it was followed by a peak at $\sim 43^\circ$ with a long tail representing a turbostratic stacking, i.e. the presence of (10L) orientations, where $L = 1, 2, 3, \dots$. The peak at $\sim 67^\circ$ could be attributed to the (1 1 0) orientation.

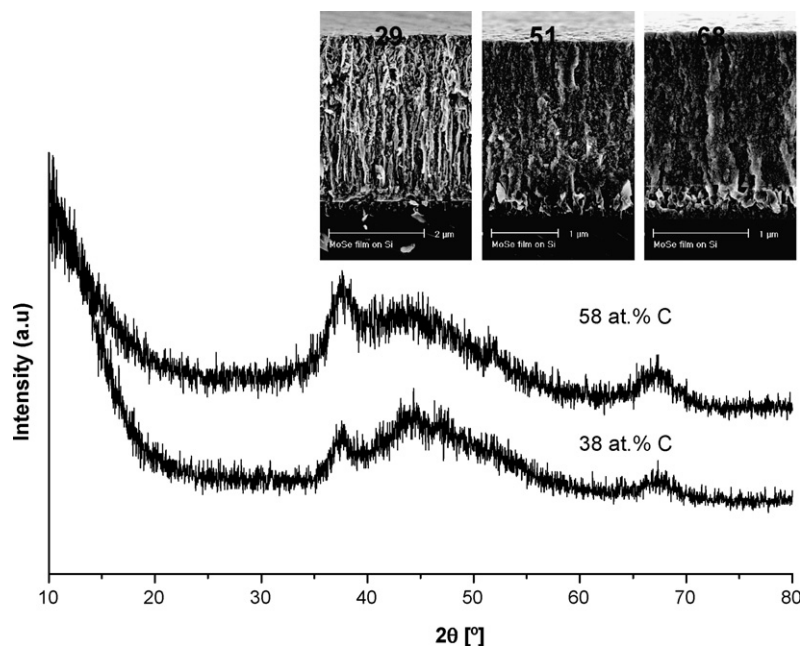


Fig. 2. XRD diffractograms and cross-section morphologies of a Mo–Se–C coatings.

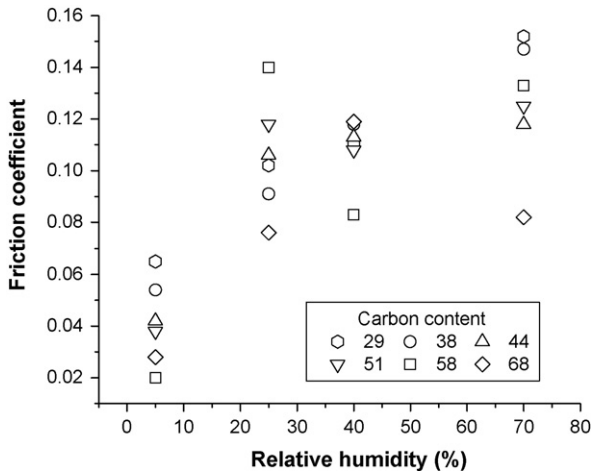


Fig. 3. Friction coefficient of Mo–Se–C coatings as a function of the relative humidity in the testing environment.

The hardness of the coating linearly increased with carbon content from 0.6 to 4.1 GPa.

3.2. Friction and wear behavior

The friction coefficients measured as an average value of the entire test and the wear rates of the MoSeC coating as a function of the air humidity are presented in Figs. 3 and 4, respectively. As expected, the lowest friction was reached in dry air. In general, the friction increased with the humidity level. All the friction curves showed an initial increase of the friction reaching a maximum after 40–70 laps, and, then a subsequent decrease. When tested in dry air, the friction after running-in was very stable with the values about one half of the maximum reached during the initial stages. The friction curves obtained at humid air were very noisy and sometimes it was difficult to separate the running-in from the steady-state regime.

The wear track analysis showed that the coating with the lowest (29 at.%) carbon content was partially peeled off, probably due to adhesion problems. The coating with 38 at.% C was worn out after the test at 70% RH, while the coatings with the highest carbon content (58 and 68 at.%) did not survive to tests in dry air and in low RH. The coatings with 44 and 51 at.% C withstood the sliding tests

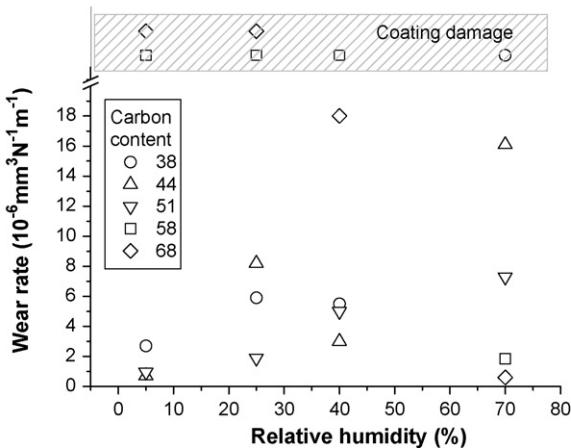


Fig. 4. Wear rate of Mo–Se–C coatings as a function of the relative humidity in the testing environment. The points positioned in the “coating damage” area represent partially worn coatings.

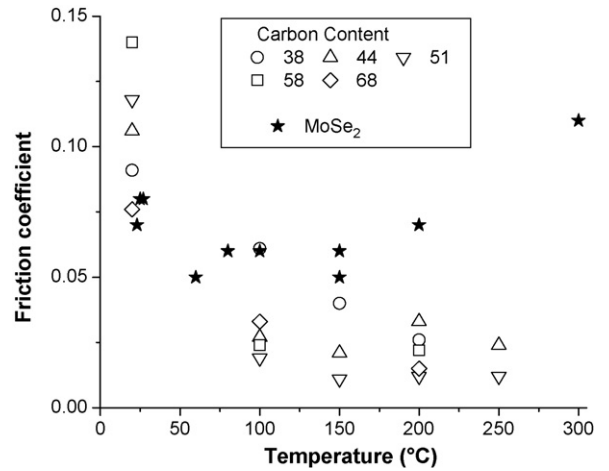


Fig. 5. Friction coefficient of Mo–Se–C coatings vs. testing temperature. The results of MoSe₂ published in [4] are shown for comparison.

without any sign of adhesive damage. It should be pointed out that the wear tracks were usually very shallow (typically 100–500 nm) and determination of the worn area was very difficult. As a consequence, it should be remarked that the error in the values depicted in Fig. 4 is very high and this graph represents mainly the tendencies of the wear behavior.

The coatings were tested as well at elevated temperatures. The tests were planned up to 500 °C; however, only two coatings survived the test duration of 1000 cycles at 250 °C and none at 300 °C. The evolution of the friction and wear rate is shown in Figs. 5 and 6 together with our previous results obtained for pure MoSe₂ coating [4]. The results for the coating with 29 at.% C are not shown in this figure since it was worn out. The coating with 68 at.% C also exhibited partial adhesion failure in the end of the tests; nevertheless, the friction values of this coating are reported, since no increase of the friction was observed, due to the effect of transferring coating material to the counterbody. In general, the wear rate of the Mo–Se–C coatings surviving the tests at elevated temperature is lower than that observed at room temperature. The average friction coefficient measured at elevated temperatures was extremely low varying in the range 0.01–0.04. The friction decreased immediately after the test start to a stable steady-state level; in general, the running-in period decreased with increasing temperature from ~100 laps at 100–150 °C to ~50 laps at 200 °C and only 5–10 laps at 250 °C.

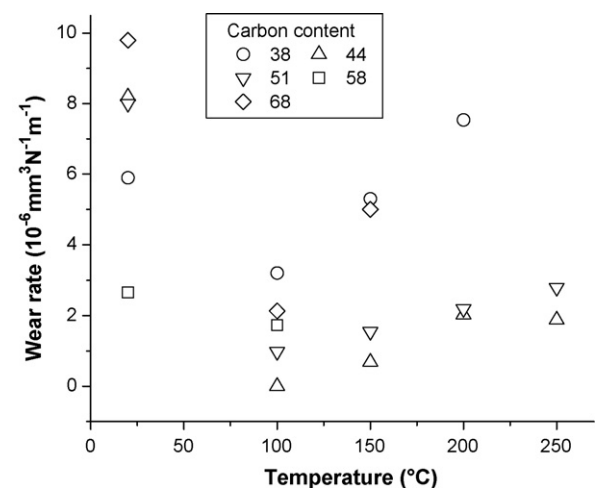


Fig. 6. Wear rate of Mo–Se–C coatings vs. testing temperature.

4. Discussion

4.1. Effect of humidity

The low friction of metal dichalcogenides is attributed to their anisotropic layered structure, where the adjacent lamellae with strong covalent bonding interact through relatively weak Van der Waals forces. The orientation of the basal planes parallel to the surface in contact provides the “easy” inter- and intra-crystalline slipping. Since the sputtered TMD have usually basal planes oriented perpendicularly to the surface, the reorientation through the energy input induced by the mechanical action during sliding is required to achieve the low friction. The thickness of such reoriented tribolayer is estimated to be lower than 5 nm [5]. Therefore, the friction in the initial stage of sliding (running-in) is higher and starts to decrease with the formation of (002) TMD phase on the top of either the coating or the counterbody, which is covered by the adhered TMD material transferred from the coating. The evolution of the friction during the tests with Mo–Se–C exhibits the same trend, i.e. a short running-in with a higher friction and then the stabilization of the friction corresponding to a steady-state stage. The Raman spectroscopy was used to analyze the wear track. Despite the penetration depth of the Raman scattering is difficult to estimate, the formation of a MoSe₂ tribolayer on the surface of the wear track should be visible. The Raman spectra of the MoSe₂ target, MoSe₂ sputtered coating and Mo–Se–C coatings with different carbon content were discussed in detail in the previous study [7]; therefore, only a brief summary is provided in this paper. MoSe₂ target exhibited only one sharp peak in Raman spectra, close to 240 cm⁻¹. This peak became very broad and asymmetric in case of sputtered MoSe₂. Mo–Se–C Raman spectra consisted of referred broad Mo–Se peak, D and G band characteristic of C-based coatings (~1390 and ~1575 cm⁻¹, respectively), and MoO₃ peak at ~860 cm⁻¹.

In general, the wear tracks were very smooth and featureless (Fig. 7a); however, some isles of adhered material with “blue” appearance in the optical microscope could be detected. Fig. 8 shows the typical Raman spectra taken from outside and inside

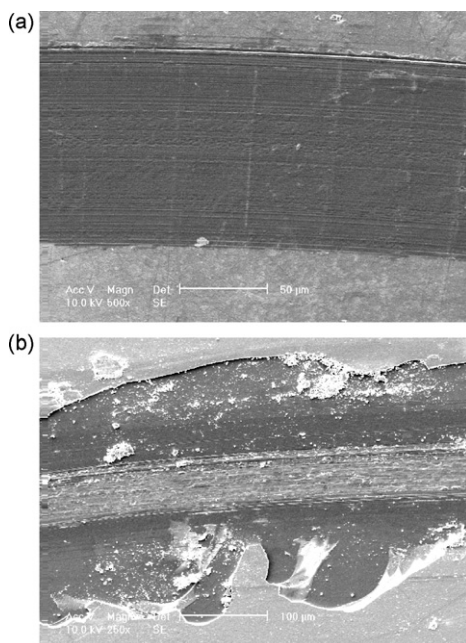


Fig. 7. The SEM micrographs of the 44 at.% C coating wear tracks. (a) Tested at 40% RH and (b) tested at 300 °C.

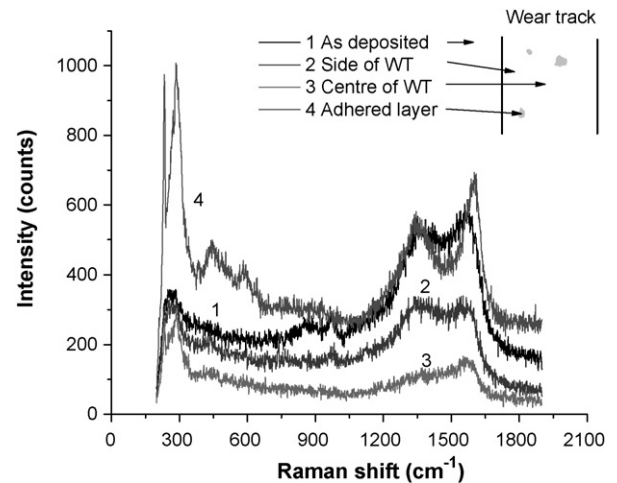


Fig. 8. Raman spectra taken from a tribologically tested Mo–Se–C coating (51 at.%C), (1) free surface, (2) side of the wear track, (3) centre of the wear track, (4) adhered blue layer in the wear track (see text).

of the wear track. The wear track was scanned from the side to the centre and the “blue” isles were analyzed concerning its position in the wear track as well. The decrease of the intensity of the carbon peaks when the laser is pointed into the centre of the wear track is obvious. The ratio between Mo–Se and carbon peaks intensities ($I_{\text{MoSe}}/I_{\text{C}}$) is lowering from the centre to the border of the wear track, which suggests a decrease of the Mo–Se tribolayer thickness. This behavior may be attributed to a distribution of the contact pressure, which reaches a maximum in the centre of the wear track, as it has been shown in a similar study dealing with W–S–C system [2]. The “blue” adhered layer exhibited a sharp MoSe₂ peak and clearly separated D and G peaks (graphitization); no variation in the Raman spectra of this layer was found whatever its position in the wear track is. Thus, it can be concluded that the wear track is covered by a thin MoSe₂ layer, probably thicker in the centre of the wear track, and partially superimposed by a second layer consisting of MoSe₂ and graphitic carbon.

4.2. Effect of temperature

The low friction coefficient at elevated temperature supports the hypothesis of the predominant influence of MoSe₂ tribolayer on the tribological behavior of the Mo–Se–C coatings. There is a lack of information about the frictional behavior of non-hydrogenated DLC coatings at elevated temperatures; nevertheless, it has been observed that the friction coefficient of these coatings rapidly increases with temperature regardless on the counterpart material (aluminum alloy [8,9], high speed steel and 100Cr6 [10]). Since the air humidity vanishes with increasing temperature, the DLC coatings show a tribological behavior similar to that in dry air. In the absence of air humidity (i.e. vacuum or dry atmosphere), the non-hydrogenated DLC exhibits high friction due to the existence of dangling carbon bonds on the worn surfaces, which cannot be rapidly passivated [11]. Therefore, the low friction coefficient of Mo–Se–C coatings at elevated temperature supports the hypothesis that should be the MoSe₂ tribolayer playing the dominant role. Comparing MoSe₂ and Mo–Se–C coatings, the later present lower friction at elevated temperature and smoother friction curves. The Mo–Se–C coatings are harder and, particularly, more dense than MoSe₂. As a consequence, the tribolayer is well supported by the coating itself and it is more stable, i.e. more difficult to be worn out.

Raman spectroscopy did not show significant oxidation in the wear track, even at the highest temperature tested (250 °C), while

the free surface of the coating was clearly oxidized. This surprising result was confirmed by EDS which showed a much lower content of oxygen in the wear track than in the free coating surface. It is possible that the formation of the tribolayer protects the coating from oxidation due to the reorientation of the basal planes parallel to the surface, avoiding the combination of O with the dangling bonds, but this hypothesis has to be further studied. Nevertheless, such a result demonstrates that the coating damage at elevated temperature cannot be attributed to the oxidation of the coating. The observation of the wear tracks of partially worn coatings after testing at elevated temperature suggests that an adhesive failure on the MoSeC/Ti interface occurs that can be responsible for the poor tribological behavior, as demonstrated in Fig. 7b.

Any increase of friction during the running-in period has not been observed in the temperature range 100–250 °C. Moreover, the friction coefficient drops more rapidly to the steady-state level when the temperature is increased. Therefore, the formation of the self-lubricant tribolayer is enhanced not only by drying of air humidity, but as well by the synergetic effect of the temperature.

5. Conclusions

Mo–Se–C coatings were deposited by r.f. magnetron sputtering from a carbon target with MoSe₂ pellets; the carbon content varied from 29 to 68 at.% as a function of the number of pellets. The Se/Mo ratio slightly increased with carbon content being close to MoSe₂ stoichiometry. The coating became denser losing their columnar structure and hardness linearly increased with increasing carbon content. XRD showed that Mo–Se–C coatings could be considered as a nanostructured material.

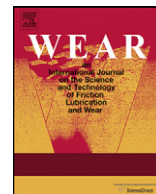
The tribological tests in dry and humid air and the wear tracks analysis showed that the sliding process was mainly driven by the formation of a thin MoSe₂ tribolayer. The influence of the carbon on the frictional behavior was not clear; however, it was expected to be marginal. The coatings exhibited extremely low friction coefficient at elevated temperature and low wear rate. Nevertheless, the adhesive failures on the coating/Ti interlayer limited their functionality to a maximum temperature of 250 °C.

Acknowledgements

This work was supported by the Czech Science Foundation through the project 106/07/P014, by the GAAV through the project KJB201240701, by the Ministry of Education of the Czech Republic (project MSM 6840770038) and by the Fundação para a Ciência e a Tecnologia through the project SFRH/BPD/34515/2006.

References

- [1] A.A. Voevodin, J.S. Zabinski, *Thin Solid Films* 370 (2000) 223.
- [2] T. Polcar, M. Evaristo, A. Cavaleiro, *Plasma Process. Polym.* 4 (2007) S541.
- [3] T. Polcar, M. Evaristo, A. Cavaleiro, *Vacuum* 81 (2007) 1439.
- [4] T. Kubart, T. Polcar, L. Kopecký, R. Novák, D. Nováková, *Surf. Coat. Technol.* 193 (2005) 230.
- [5] A.R. Lansdown, *Molybdenum Disulphide Lubrication*, Elsevier, 1999.
- [6] A. Nossa, A. Cavaleiro, *J. Mater. Res.* 19 (2004) 2356.
- [7] T. Polcar, M. Evaristo, A. Cavaleiro, *Surf. Coat. Technol.* 202 (2008) 2418.
- [8] W. Ni, Y. Cheng, A.M. Weiner, T.A. Perry, *Surf. Coat. Technol.* 201 (2006) 3229.
- [9] E. Konca, Y.-T. Cheng, A.M. Weiner, J.M. Dasch, A.T. Alpas, *Surf. Coat. Technol.* 200 (2006) 3996.
- [10] T. Vítů, R. Novák, D. Nováková, *Plasma Process. Polym.* 4 (2007) S237.
- [11] J. Jiang, S. Zhang, R.D. Arnell, *Surf. Coat. Technol.* 167 (2003) 221.



Comparative study of the tribological behavior of self-lubricating W–S–C and Mo–Se–C sputtered coatings

T. Polcar^{a,b,*}, M. Evaristo^b, A. Cavaleiro^b

^a Department of Control Engineering, Faculty of Electrical Engineering, Czech Technical University in Prague, Technická 2, Prague 6, Czech Republic

^b ICEMS – Faculdade de Ciências e Tecnologia da Universidade de Coimbra, Dep. Eng. Mecânica, Polo II, Coimbra, Portugal

ARTICLE INFO

Article history:

Received 1 October 2007

Received in revised form 29 February 2008

Accepted 7 April 2008

Available online 6 June 2008

Keywords:

WS₂

MoSe₂

Self-lubrication

Coating

Tribology

ABSTRACT

Transition metal dichalcogenides (TMD) have been one of the best alternatives as low friction coatings for tribological applications, particularly in dry and vacuum environments. However, besides their deficient behavior in humid containing atmospheres, their extensive application has also been restricted due to their low load-bearing capacity. In order to overcome these problems, recently the alloying with C has been tried with the expectation of simultaneously improving the coatings hardness and reaching sliding contacting phases more convenient for achieving low friction in humid environments.

The practical application of this concept was extensively studied with the W–S–C system, with the C addition being achieved either by reactive or co-sputtering processes. The best tribological results were obtained by co-sputtering from a C target embedded with an increasing number of WS₂ pellets. Excellent results were reached from the more than one order of magnitude increase in the coatings hardness up to friction coefficients which are close to those of the references of self-lubricating coatings: TMD for dry or vacuum atmospheres or C-based coatings for terrestrial sliding conditions.

Following the good results achieved with W–S–C system, other TMDs systems have been envisaged to be studied. The main focus was placed on the Mo–Se–C system.

In this paper, the general comparison between W–S–C and Mo–Se–C coatings is presented. The main effort is pointed on the tribological behavior of both systems when tested by pin-on-disk against steel counterpart balls under different testing conditions: applied normal loads, temperatures and relative humidity of the atmospheres. Both coatings were deposited by co-sputtering from a C target with a varying number of TMD pellets which could lead to C contents in the films in the range from 30 up to 70 at.%. A Ti interlayer was interposed between the films and the substrates for improving the adhesion.

Typically, W–S–C films are harder than Mo–Se–C films. From the tribological point of view, W–S–C films are more thermally stable than Mo–Se–C films although the friction coefficients of these last ones are lower when tested in humid containing atmospheres.

© 2008 Elsevier B.V. All rights reserved.

1. Introduction

The solid self-lubricating materials based on transition metal dichalcogenides (TMD: sulfides, selenides or tellurides of tungsten, molybdenum and niobium) have been studied for more than 50 years. Their excellent lubricating properties are based on the extreme crystal anisotropy [1] and when sliding under ideal conditions (very dense material deposited and tested in ultra high vacuum) they can be considered as “frictionless”, i.e. with friction coefficient as low as 0.001 [2,3]. However, the presence of oxygen and water vapour in the atmosphere or the intrinsic imperfections of the crystal structure quickly deteriorate their lubrication proper-

ties and significantly decrease their wear resistance. Thus, the pure TMDs are used mainly in space applications or as additives to liquid lubricants. Moreover, a further significant drawback of TMD is the lack of adhesion and low hardness resulting in low load-bearing capacity.

Among many different possibilities to improve the tribological behavior of TMD coatings in humid atmosphere, the co-deposition with other material is one of the most successful ways. Metals, as dominant doping material, were tested, such as Ti [4], Pb [5], Cr [6,7], etc.

Voevodin and Zabinski [8,9] deposited the WS₂/WC/DLC system concluding that it exhibited excellent tribological properties in space simulation tests, but with sliding properties still hindered by the presence of air humidity. W–S–C coatings prepared by magnetron sputtering have been intensively studied by the present authors, concerning: the structure [10], the mechanical properties

* Corresponding author.

E-mail address: tomas.polcar@dem.uc.pt (T. Polcar).

[11] and the tribological performance [12–14]. It could be concluded that doping with carbon led to the improvement of the mechanical (hardness, adhesion) and tribological (friction and wear resistance when sliding in humid air) properties.

There is a lack of information on the behavior of MoSe₂ sputtered coatings. In a previous study, the tribological properties of pure MoS₂ and MoSe₂ coatings deposited by non-reactive dc magnetron sputtering were compared [15] showing that MoSe₂ exhibited lower friction coefficient in humid atmosphere. Recently, the analysis of Mo–Se–C system has also been published [16].

Despite the effort to increase the load-bearing capacity of TMD coatings, almost no corresponding measurements have been done to demonstrate the limits of their capacity. The majority of the tribological tests has been carried out with a steel ball as the counteracting body (rotating or reciprocating tests) and a moderate load giving Hertzian contact pressure below 1 GPa. To the best of our knowledge, there is no evidence in literature that higher contact pressures were used except for Teer and co-workers [17] who studied the MoST system with a maximum load of 80 N and a 5 mm diameter WC–6%Co ball. Therefore, there is still a significant gap between testing the doped TMD coatings and the high-load sliding application demands.

To remedy this lack, we have compared the tribological properties of two systems synthesized by r.f. magnetron sputtering undergoing increasing contact pressures during the sliding contact: W–S–C (deposited either from carbon and WS₂ targets or composite C–WS₂ target) and Mo–Se–C (deposited from composite C–MoSe₂ target).

2. Experimental details

W–S–C and Mo–Se–C coatings have been deposited on 100Cr6 and M2 polished (Ra < 30 nm) steel samples (hardness close to 5 and 9 GPa, respectively) and mirror-like polished Si wafers. Two different approaches were used for co-deposition of the coatings using a radio-frequency magnetron sputtering Edwards ESM 100 unit, equipped with two cathodes (target diameter 100 mm): (1) co-sputtering from individual C and WS₂ targets (hereinafter identified as W–S–C T) and (2) co-sputtering from a C target embedded with WS₂ or MoSe₂ pellets (composite target) being a Ti target placed in the other electrode (hereinafter identified as W–S–C P or Mo–Se–C). Mo–Se–C coatings were only prepared by the last method. Prior to the deposition the substrates were sputter cleaned during 20 min by establishing the plasma close to the substrates electrode. Immediately after, in the cases where it was possible, a Ti interlayer was deposited with an approximate thickness of 300 nm for improving the coating adhesion. To evaluate the chemical composition of the coatings, a Cameca SX 50 electron probe microanalysis (EPMA, Cameca, France) apparatus was used. The chemical composition is an arithmetic average of four values measured in different parts of the samples. The standard deviation was in the range [±0.02 to ±0.3]. The hardness was determined by depth-sensing indentation technique using a Fisherscope H100 with a nominal load of 20 mN, following the procedure indicated elsewhere [18]. The hardness value was obtained by averaging eight different indentation results. The adhesion of the coatings was evaluated with commercially available scratch testing equipment (CSEM Revetest), under standard conditions. The critical load, for each coating, was obtained by averaging four different scratch results. The structure of the coatings was analysed by X-ray diffraction (XRD) in glancing mode using a Phillips diffractometer (Co K α radiation). The tribological tests were carried out in a SRV-OPTIMOL reciprocating testing equipment. 100Cr6 steel balls were used as sliding partners. The

diameter of the balls was 10 mm and the load was varied in the range 20–1000 N. Different testing environments were used, such as humid air (30–40% relative humidity) or dry nitrogen. The reciprocating tests were carried out with a frequency of 20 Hz. The friction coefficient reported is the average value of the whole sliding test, unless stated otherwise. The typical test duration was 10 min (24,000 cycles); the duration of long-term tests is specified in the text.

3. Results and discussion

3.1. Basic characteristics of deposited coatings

Based on the mechanical and tribological properties of TMD–C coatings presented elsewhere [12,13,19,20], the optimum range of the carbon content for high-load tribological tests was determined as 40–50 at.% C. The deposition parameters, i.e. the power applied to the carbon target or the number of TMD pellets, were selected in order to reach the required chemical composition, which is summarized in Table 1 together with the mechanical properties of all the three studied systems. The coatings W–S–C T and Mo–Se–C coatings exhibited S/W or Se/M ratios much closer to the stoichiometry of the target than the W–S–C P ones.

3.2. Coating morphology and structure

Pure sputtered WS₂ and MoSe₂ coatings exhibited very porous columnar morphology [10,15]. It was shown that the addition of carbon led to their significant densification; for carbon contents of about 40 at.%, the columnar structure almost disappeared [10,16]. XRD spectra showed the peaks typical of sputtered TMD coatings, see Fig. 1: (1) the peak representing (1 0 1) TMD phase at 36–38°; (2) the broad peak with long tail revealing a turbostrating stacking of (1 0 L) planes (L = 0, 1, 2, ...) at 40–44°; and, finally, (3) the peak at ~70° corresponding to the (1 1 0) planes. Small features in W–S–C XRD spectra indicated the presence of tungsten carbides [10], while no vestiges of Mo–C phases was found in the Mo–Se–C diffractogram [16]. Such a fact was confirmed by XPS clearly showing the existence of W–C bonds [10]. Again, for Mo–Se–C system, Mo–C bonds were not observed [16].

According to Weisse et al. [21], the aspect of these XRD patterns is typical of WS₂ or MoSe₂ nanograins embedded in a carbon matrix; the size of these nanograins not exceeding a couple of lattice parameters, as confirmed by HR TEM observations [10]. Therefore, it can be concluded that W–S–C coatings exhibited a nanocomposite structure with WC and WS₂ grains in an amorphous carbon matrix,

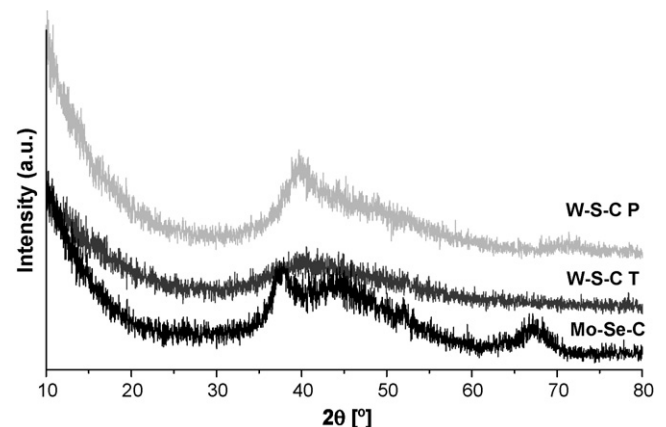


Fig. 1. XRD diffractograms of TMD–C coatings.

Table 1
Chemical composition, hardness and thickness of the TMD–C coatings

Coating	C content (at.%)	O content (at.%)	S/W or Se/Mo [–]	Hardness (GPa)	Thickness (μm)
W–S–C T	42	6	1.7	5.9 ± 1.8	1.0
W–S–C P	42	3	1.2	9.7 ± 1.2	2.1
Mo–Se–C	50	4	1.6	2.9 ± 0.2	2.2

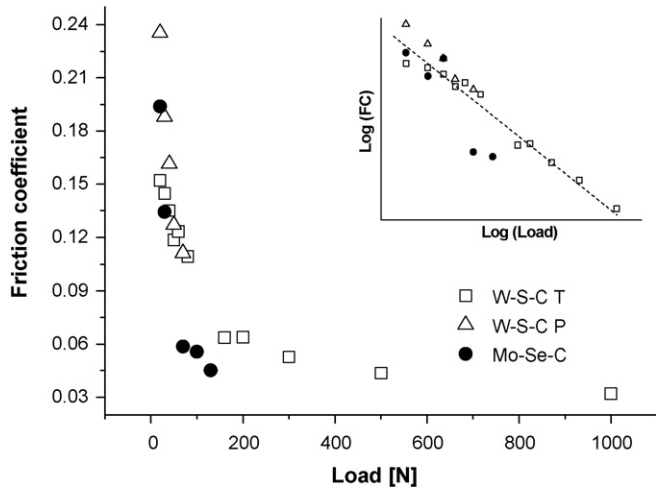


Fig. 2. Friction coefficient vs. load in humid air. The trend line shown in the inset is only a guide for the eyes.

while Mo–Se–C was simply a nanostructured material combining carbon and MoSe₂ phases.

3.3. Friction

Figs. 2 and 3 show the evolution of the average friction coefficient with load in humid air and dry nitrogen, respectively. In general, the friction coefficient decreased with increasing load. This behavior is typical of pure TMD coatings [22,23] being observed as well for W–S–C P coating tested by pin-on-disc [20]. Mo–Se–C exhibited slightly lower friction coefficient for higher loads. Both coatings deposited from composite targets peeled off from the substrate when the load reached ~ 150 N, while the W–S–C T withstood the maximum tested load 1000 N without significant damage. The coatings wear was typically very limited being the depth of the wear tracks in the order of hundreds nanometers. All the coatings

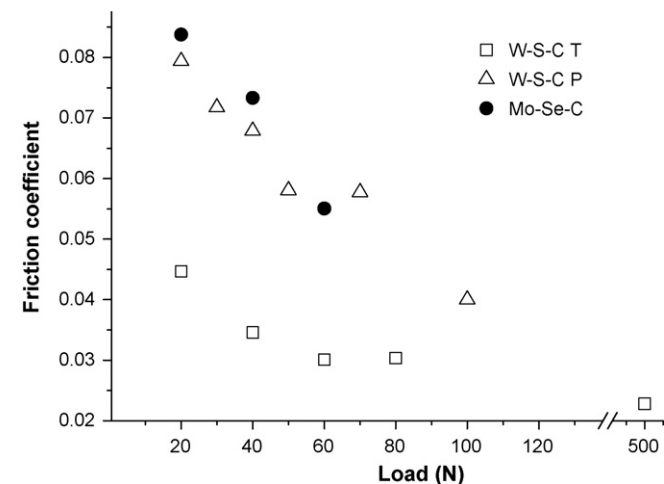


Fig. 3. Evolution of the friction coefficient with load in dry nitrogen.

exhibited excellent cohesion and the peeling off was consequence of adhesion problems as documented in Fig. 4 showing a typical adhesive failure. It should be pointed out that, unexpectedly, in this specific case W–S–C T coatings which were directly sputtered on the steel substrates seem adhering much better than those deposited with a titanium interlayer.

The tests carried out in dry nitrogen showed as well a decrease of the friction with the load. The comparison between Figs. 2 and 3 revealed that the absence of the air humidity resulted in lower friction except for, surprisingly, Mo–Se–C coating tested at higher loads.

To understand the frictional behavior, the wear tracks were thoroughly analysed by SEM/EDS and Raman spectroscopy. The analysis of the wear track will be documented in detail for two wear tracks of the following coatings: W–S–C T (humid air, load 80 N) and Mo–Se–C (humid air, 20 N).

The first referred wear track was smooth without any significant scratches, as shown in Fig. 5 (point 2). The adhered material was accumulated at the end of the wear track making a positive relief (point 3). The free wear debris was concentrated outside of the wear track (point 4). EDS analyses exhibited almost no difference in the chemical composition measured at the free surface (point 1) and at the wear track (points 2 and 3), only free debris contained slightly more oxygen and carbon. Raman spectra taken from points 3 and 4, see Fig. 6, confirmed the presence of oxygen (tungsten trioxide) and the excess of carbon in the free wear debris. The increase of the WS₂ peak intensity (compare spectra from points 1 and 2) in the wear track could be explained by the formation of a WS₂ thin tribolayer, as it was suggested in a previous work [20].

The Mo–Se–C wear tracks analysis showed slightly different behavior. The wear track could be divided into three main zones: A, a dominant zone showing a smooth appearance; B, small scattered isles of the adhered layer with blue appearance when observed in an optical microscope; and C, concentrations of black powder-like materials on the sides of the wear track. Fig. 7 shows the typical

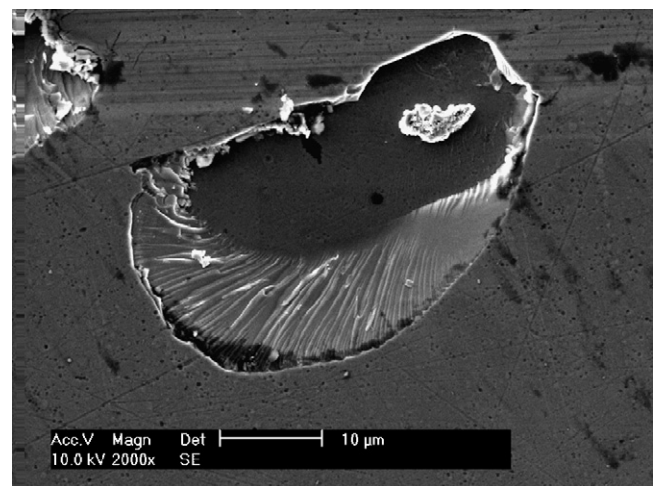


Fig. 4. Adhesive failure of the Mo–Se–C coating tested with load 160 N. The wear track in the upper part of the photo is very shallow, i.e. the wear resistance of the coating is entirely hindered by the adhesion problems.

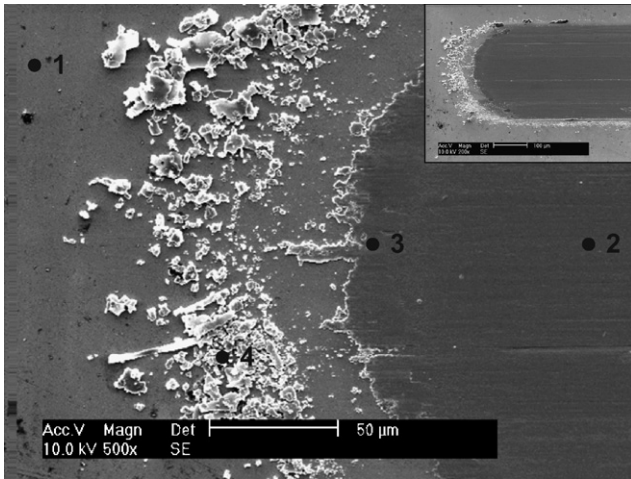


Fig. 5. End of the wear track of W–S–C T coating tested in humid air with a 80 N load observed by SEM. The numbers correspond to the positions of EDS and Raman measurements (see text). The inset shows the overview of the wear track.

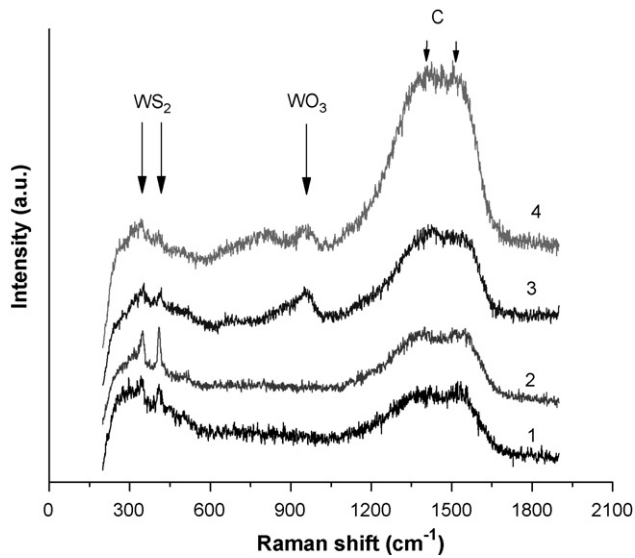


Fig. 6. Raman spectra taken in different positions of the wear track of the W–S–C T coating tested with a load 80 N in humid air (see text).

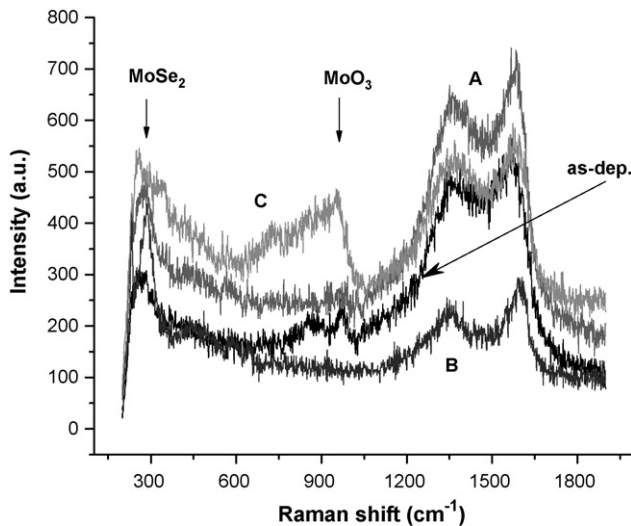


Fig. 7. Raman spectra taken in different positions of the wear track of the Mo–Se–C coating tested with a load 40 N in humid air (see text).

Raman spectra taken from the three zones referred to above and from the as-deposited surface. The intensity of carbon peaks was slightly lower in the zone A than in the as-deposited surface, which could indicate the presence of a thin MoSe₂ tribolayer. The zone B was clearly rich in MoSe₂ being the Raman peaks even more intense than those of carbon. Finally, molybdenum oxide was found in zone C.

Voevodin and Zabinski [9] deposited WS₂/WC/DLC composite coatings in order to provide self-adaptation friction to the environmental conditions (humid air, dry nitrogen and vacuum). When the environment was periodically switched during the sliding tests, the friction quickly stabilized in a level corresponding to the actual atmosphere (i.e. very low for dry nitrogen and higher for humid air). They showed that the DLC phase was used for lubrication (graphite-like transfer film) in humid environments whereas the WS₂ phase was responsible for the low friction in dry nitrogen and vacuum (hexagonal WS₂ plates). However, their interpretation cannot be applied in the present case. In fact, no significant graphitization or even carbon concentration was observed either in the wear track or in the counterpart. On the contrary, a TMD tribolayer was formed in all sliding tests regardless on the air humidity. Therefore, it is suggested that the formation of the thin TMD tribolayer is the dominant factor influencing the frictional properties of these TMD–C coatings.

Figs. 2 and 3 reported the average friction coefficient for the entire test. In fact, the friction slowly decreased with the number of laps, as shown in Fig. 8. Interestingly, this decrease persisted during the tests with the periodic change of air humidity (dry nitrogen/humid air), as documented in Fig. 9 showing the evolution of the friction coefficient with increasing number of cycles (W–S–C T, load 300 N). The friction in dry nitrogen slowly decreased from 0.035 to 0.02 and, then, increased to 0.055, when the humidity went up to ~25% RH. Nevertheless, in these conditions it slightly decreased again down to 0.048 with a steep drop when the dry nitrogen was again applied. It is obvious that the change of the humidity level moves the friction curve down without changing the global decreasing trend. In other words, the parts of the friction curve taken at constant humidity level are following the same trend even when they are interrupted when the humidity is periodically changed, see Fig. 9. This behavior suggests that the sliding mechanisms (composition of the sliding contact interface) should be basically the same in both testing environments. Hence, it is probable that the final friction coefficient values are resulting from a synergetic effect of the same type of sliding TMD tribolayer and the typical environmental conditions.

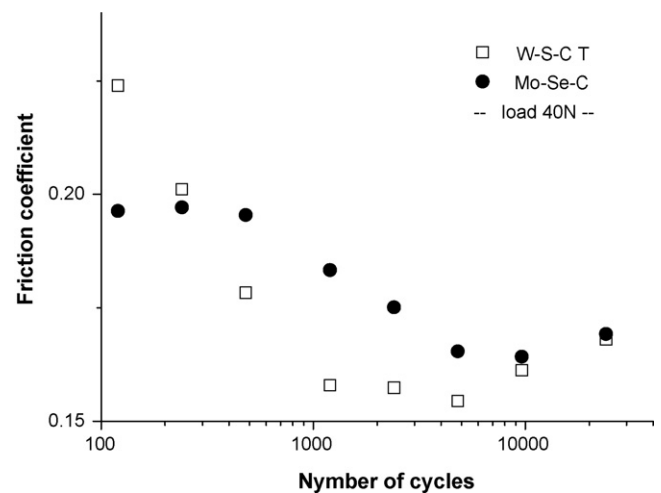


Fig. 8. Evolution of the average friction coefficient with the number of cycles, load 40 N, humid air.

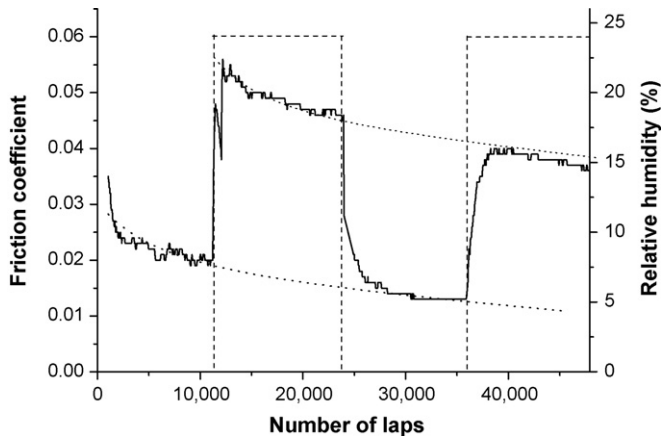


Fig. 9. Evolution of the friction with the number of laps and the periodic change of the atmosphere from dry nitrogen to humid air, W–S–C T coating, load 300 N. The dot lines represent the typical friction curves measured at dry nitrogen and humid air, i.e. tests at constant atmospheres.

The decrease of the friction during the test duration could not be considered as a typical running-in process, since the friction was not fully stabilized at steady state level even after 50,000 laps. It seems that the formation of the tribolayer is a long-term process, which is at least partially independent of the air humidity. Therefore, this is a matter of further research which is now being carried out based on the study of the tribolayer formation as a function of the tests duration.

4. Conclusions

Three self-lubricating coatings prepared by r.f. magnetron sputtering were tribologically tested under different atmospheres and loads: W–S–C T co-deposited from carbon and WS_2 targets, W–S–C P deposited from a carbon target with WS_2 pellets and Mo–Se–C deposited from a carbon target with $MoSe_2$ pellets. The deposition parameters were selected in order to prepared coatings with carbon contents in the range of 40–50 at.%. The W–S–C coatings could be described as $WS_2/WC/DLC$ nanocomposites, while the Mo–Se–C was nanostructured coating with $MoSe_2$ grains embedded into a

carbon matrix. The coatings exhibited friction coefficient decreasing with the applied load. The maximum load for the coatings deposited from composite targets was about 150 N, the W–S–C T coatings withstood tests with 1000 N without significant damage. The formation of a thin TMD tribolayer in the wear track dominated the sliding behavior of the tested TMD–C coatings, while the role of the carbon phases in the contact was probably only marginal.

Acknowledgements

This work was supported by the Czech Science Foundation through the project 106/07/P014, by the GAAV through the project KJB201240701, by the Ministry of Education of the Czech Republic (project MSM 6840770038) and by the Fundação para a Ciência e a Tecnologia through the project SFRH/BPD/34515/2006.

References

- [1] A.R. Lansdown, Molybdenum Disulphide Lubrication, Elsevier, 1999.
- [2] J.M. Martin, et al., Phys. Rev. B 48 (14) (1991) 2091.
- [3] A. Erdemir, J.M. Martin (Eds.), Superlubricity, Elsevier, Amsterdam, The Netherlands, 2007 (Chapter 13).
- [4] D.G. Teer, Wear 251 (2001) 1068.
- [5] K.J. Wahl, L.E. Seitzman, R.N. Bolster, I.L. Singer, Surf. Coat. Technol. 73 (1995) 152.
- [6] Y.L. Su, W.H. Kao, Tribol. Int. 36 (2003) 11.
- [7] M.C. Simmonds, A. Savan, E. Pfluger, H. Van Swygenhoven, Surf. Coat. Technol. 126 (2000) 15.
- [8] A.A. Voevodin, J.S. Zabinski, Compos. Sci. Technol. 65 (2005) 741.
- [9] A.A. Voevodin, J.S. Zabinski, Thin Solid Films 370 (2000) 223.
- [10] A. Nossa, A. Cavaleiro, J. Mater. Res. 19 (2004) 2356.
- [11] M. Evaristo, A. Nossa, A. Cavaleiro, Surf. Coat. Technol. 200 (2005) 1076.
- [12] A. Nossa, A. Cavaleiro, Surf. Coat. Technol. 142–144 (2001) 984.
- [13] A. Nossa, A. Cavaleiro, Surf. Coat. Technol. 163–164 (2003) 552.
- [14] M. Evaristo, T. Polcar, A. Cavaleiro, Int. J. Mech. Mater. Des. 4 (2008) 137.
- [15] T. Kubart, T. Polcar, L. Kopecký, R. Novák, D. Nováková, Surf. Coat. Technol. 193 (2005) 230.
- [16] T. Polcar, M. Evaristo, A. Cavaleiro, Surf. Coat. Technol. 202 (2008) 2418.
- [17] N.M. Renevier, V.C. Fox, D.G. Teer, J. Hampshire, Surf. Coat. Technol. 127 (2000) 24.
- [18] J.M. Antunes, A. Cavaleiro, L.F. Menezes, M.I. Simões, J.V. Fernandes, Surf. Coat. Technol. 149 (2002) 27.
- [19] T. Polcar, M. Evaristo, A. Cavaleiro, Vacuum 81 (2007) 1439–1442.
- [20] T. Polcar, M. Evaristo, A. Cavaleiro, Plasma Process. Polym. 4 (2007) S541–S546.
- [21] G. Weisse, N. Mattern, H. Hermann, A. Teresiak, I. Bacher, W. Bruckner, H.-D. Bauer, H. Vinzelberg, G. Reiss, U. Kreissig, M. Mader, P. Markschlager, Thin Solid Films 298 (1997) 98.
- [22] L.D. Towle, J. Appl. Phys. 42 (1971) 2368.
- [23] J.L. Grosseau-Poussard, P. Moine, M. Brendle, Thin Solid Films 307 (1997) 163.



Synthesis and properties of W–Se–C coatings deposited by PVD in reactive and non-reactive processes

Manuel Evaristo^{a,*}, Tomas Polcar^{a,b}, Albano Cavaleiro^a

^aSEG-CEMUC, Departamento de Engenharia Mecânica, Faculdade de Ciências e Tecnologia da Universidade de Coimbra, Rua Luís Reis Santos, 3030-788 Coimbra, Portugal

^bDepartment of Control Engineering, Faculty of Electrical Engineering, Czech Technical University in Prague, Technická 2, Prague 6, Czech Republic

A B S T R A C T

Keywords:

Transition metal dichalcogenides (TMD)
WSe₂
Carbon based coatings
Tribology

Transition metal dichalcogenides (TMD) are well known for their self lubricant properties, due to unique crystal structure, with low hardness which makes them inappropriate in applications requiring high load bearing capacity. Nevertheless, there is still a considerable potential for further improvements since other TMDs such as diselenides remain almost unknown. The WSeC coatings were deposited by either co-sputtering from WSe₂ and C targets or by working in reactive mode in an Ar + CH₄ atmosphere. Carbon content varied from 25 at.% up to 70 at.%, Se/W ratio of co-sputtered coatings was between 0.9 and 1.0, with no significant influence of the carbon content on their variations, while in the reactive process it reached values higher than 1.7. The hardness of the coatings was evaluated by nano-indentation, with values between 1.6 and 5.6 GPa. The structure of the coatings was analysed by X-ray diffraction in glancing mode, showing that the coatings have a quasi-amorphous structure. Finally, the selected samples were tested on pin-on-disc showing low friction properties of WSeC co-sputtered coatings.

© 2009 Elsevier Ltd. All rights reserved.

1. Introduction

Transition metal dichalcogenides (TMD—sulphides, selenides or tellurides of tungsten, molybdenum and niobium) are well known for their lubricating properties, being MoS₂ and WS₂ the most studied and applied as solid lubricants [1,2]. However, the application of these materials is limited to vacuum or dry environments since the presence of moisture in the atmosphere reduces dramatically their performance and endurance. In fact, the formation of strong chemical bonds, through the presence of oxygen, between the weakly bonded basal planes of those structures, makes harder their sliding and increases the friction coefficient. Furthermore, their low hardness makes them inappropriate for applications requiring high load bearing capacity. These major drawbacks have been partially overtaken by alloying TMD with other elements. In the case of MoS₂ titanium can be referred as a successful option [3], while for the WS_x many studies showed that carbon can be an alternative [4–6]. Despite significant improvement of the tribological performance of coatings by the addition of other elements, there is still place for further developments since the tribological behavior is always influenced by the environment, with increase of the friction as the relative humidity in the environment increases.

Selenides of molybdenum and tungsten are significantly less studied than sulphides. It was shown [7] that the friction of MoSe₂ and WSe₂ adhered transfer films was comparable to that of disulphides. Study focused on friction properties of sputtered dichalcogenide layers concluded that MoSe₂ exhibited similar friction as MoS₂ [8]; moreover, both referred coatings outperformed molybdenum ditelluride and niobium and tantalum diselenides. Our recent studies demonstrated that MoSe₂ [9] sputtered coatings could be good alternative for molybdenum sulphide due to their less sensitivity to the presence of moisture in the environment. MoSeC system deposited by magnetron sputtering exhibited unique tribological properties – high wear resistance, high load bearing capacity and limited sensitivity to humid atmosphere [10,11]. To our best knowledge, there are no reports describing in detail the tribological behavior of WSe₂ and WSeC coatings.

This study is targeted to widen the knowledge of TMD by the synthesis and study of structural and mechanical properties of W–Se–C coatings prepared by non-reactive magnetron sputtering from two individual targets (C+WSe₂) and by reactive magnetron sputtering of a WSe₂ target in an (Ar + CH₄) atmosphere.

2. Experimental details

The coatings were deposited on M2 (AISI), 100Cr6 steels (hardness close to 9 and 5 GPa respectively) and silicon wafers by r.f. magnetron sputtering from two individual targets WSe₂ (99.8%

* Corresponding author.

E-mail address: manuel.evaristo@dem.uc.pt (M. Evaristo).

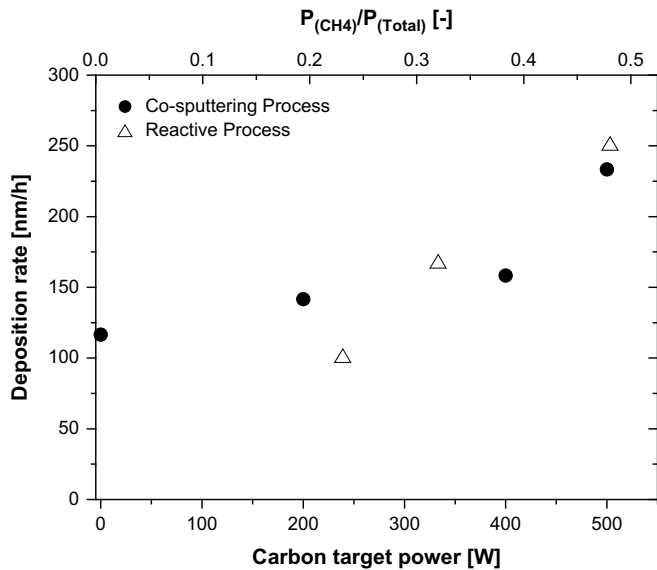


Fig. 1. Deposition rate as a function of the power applied on the carbon target for the co-sputtering process or as a function of the ratio of CH_4 partial pressure on the total pressure.

pure) and C (99.999% pure) in argon atmosphere with a pressure of $\sim 5 \times 10^{-1}$ Pa. The substrate holder was rotated with a speed high enough to avoid the formation of a multilayer structure. In order to vary the composition of the coatings, the power in both cathodes was changed. The W–Se–C system was also studied by sputtering from the WSe_2 target in a reactive atmosphere ($Ar + CH_4$) with different partial pressures of CH_4 in order to achieve coatings with different C contents. In this case, the substrates were stationary above the WSe_2 target and, prior to the deposition, a 270 nm thickness Ti interlayer was deposited for improving the final adhesion. To evaluate the chemical composition of the films, a Cameca SX 50 electron probe microanalysis (EPMA, Cameca, France) apparatus was used, being the final values an average of four different measurements. The structure was evaluated by X-ray diffraction (XRD) using a Philips diffractometer with $Co K\alpha$ radiation in glancing mode.

The hardness of the coatings was measured with a Micro Materials NanoTest system. Indentations were performed in load control with a maximum load of 5 mN, at a 0.1667 mN/s loading and unloading rate, with a 5 s hold period at maximum load and 60 s hold period at 90% unload for thermal drift correction. Over 30 indentations were performed for each coating. The contact depth was less than 10% of the coating thickness to avoid the influence of the substrate. The friction was measured on pin-on-disc equipment (CSM Instruments) at humid air. The sliding speed was 10 cm s^{-1} , number of laps 1000, applied load varied from 1 to 27 N. The 100Cr6 steel balls with a diameter of 6 mm were used as counterparts.

3. Results and discussion

3.1. Preliminary deposition of WSe_2 coatings and their chemical composition

Taking into account the limited information about sputtering W–Se coatings, to set up the conditions for achieving successful coating with the desired properties, preliminary runs were performed in non-reactive mode with only the WSe_2 target. Then, a power of 100 W ($\sim 0.8 \text{ W cm}^{-2}$) was applied to the WSe_2 target keeping the carbon target off. After a few minutes of deposition an

Table 1

Deposition parameters of selected coatings and their chemical compositions.

Sample	C target power (W)	WSe_2 target power (W)	CH_4 flow	Chemical composition measured by EPMA				
				O (at.%)	C (at.%)	W (at.%)	Se (at.%)	Se/W
WSe-2	0	40	–	23	8	26	43	1.6
WSe-3	0	40	–	25	7	38	30	0.8
WSe-4	500	40	–	11	66	9	14	1.4
WSe-5	400	40	–	9	70	11	10	0.9
WSe-6	200	40	–	10	62	16	12	0.8
WSe-7	400	51	–	9	63	14	14	1.0
WSe-8	400	74	–	8	56	18	18	1.0
WSe-9	300	91	–	8	52	20	20	1.0
WSe-10	100	110	–	10	33	30	27	0.9
WSe-12	–	123	3.5	2	25	22	51	2.3
WSe-13	–	91	6.4	5	66	7	22	3.0
WSe-14	–	91	5.1	6	64	11	19	1.7
WSe-15	–	91	4.3	Not measured				

intense brightness spot was observed moving randomly in the preferential erosion of the target, because of it after a couple of minutes the power was switched off. In this period an increase of the pressure and target potential was detected. The coating resulting from this trial presented an unexpected high thickness (more than $30 \mu\text{m}$) without any presence of tungsten or oxygen. In the next run, a much lower power was applied to the WSe_2 target, i.e. only 50 W. Even with these conditions, only after 8 minutes of deposition the same bright spot was detected moving in the erosion zone of the target. The target showed significant damage in the erosion zone, which was very rough with average depth about 1 mm, i.e. 1/6 of the target thickness. We suppose that evaporation from the target took place, which was confirmed by high coating thickness and absence of tungsten in the coating. Finally, a further reduction of the power down to 40 W allowed sputtering in apparent normal conditions during a total time of 6 hours. The measurement of the chemical composition of deposited $1.2 \mu\text{m}$ thick coating showed tungsten (37 at.%), selenium (31 at.%), oxygen (25 at.%) and carbon (7 at.%). The low Se/W ratio was probably caused by target damage during previous runs.

3.2. Deposition of W–Se–C coatings and their chemical composition

Prior $WSeC$ coatings depositions, the WSe_2 target was mechanically polished in order to remove top layer rich in tungsten. The first set of depositions of W–Se–C coatings was carried out with 40 W on WSe_2 target with different powers on the carbon target (0–500 W), Fig. 1 presents the evolution of the deposition rate with the variation of the power applied on the carbon target, where a linear increase of the deposition rate with the increase of the power applied on the carbon target is observed, in good agreement with the results found for W–S–C system deposited by co-sputtering from two targets ($WSe_2 + C$) [12]. Due to the low deposition rate achieved, a set of depositions with a slightly higher power applied on the WSe_2 target (co-sputtering with C allowed this increase without promoting the formation of the bright spot referred to above) was also performed, resulting on a slight increase of the deposition rate. Nevertheless, the deposition rate was still very low leading to long deposition times with increased coatings contamination from residual atmosphere.

Same trend, as for previous W–S–C coatings deposited in reactive mode [12], was achieved when sputtering the WSe_2 target in $Ar + CH_4$ atmosphere. Keeping constant the total pressure the increase in the CH_4 partial pressure gave rise to an approximate linear increase of the deposition rate (see Fig. 1).

As it would be expected the evolution of the C content in the films followed the increase in the source of the C species, i.e. the

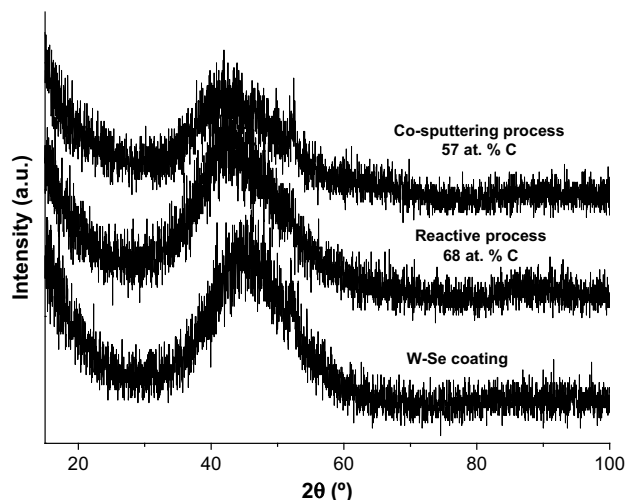


Fig. 2. XRD spectra of selected W–Se and WSeC coatings.

power applied to the C target or the CH_4 partial pressure. In both cases, C contents as high as 70 at.% were achieved (see Table 1). However, significantly different Se/W ratios were found in both cases. The co-sputtered coatings showed Se/W ratios between 0.9 and 1.0 with no significant dependence on the C content, the trend similar to that found previously for co-sputtered W–S–C coatings. However, unexpectedly the Se/W ratio was lower than the S/W ratio [12]. In fact, taking into account that the deficiency in Se (S) in relation to the stoichiometry could be attributed to their preferential re-sputtering by the high energy neutrals during the film growth, the re-sputtering rate should be lower for Se taking into account its higher atomic weight when compared to S. On the other hand, the coatings produced by co-sputtering exhibited relatively high oxygen content. It was suggested that oxygen directly replaces sulphur in MoS_2 structure forming $\text{MoS}_{2-x}\text{O}_x$ [13] and similar situation in case of WSeC system would lead to referred high Se deficiency.

Inversely, the reactive process produces Se/W ratios much closer to the stoichiometry. In fact, values higher than 1.7 could be achieved regardless of the C content. Since our previous study showed significantly lower S/W ratios in case of WSC system, which were attributed to the formation of volatile H_2S species, it can be

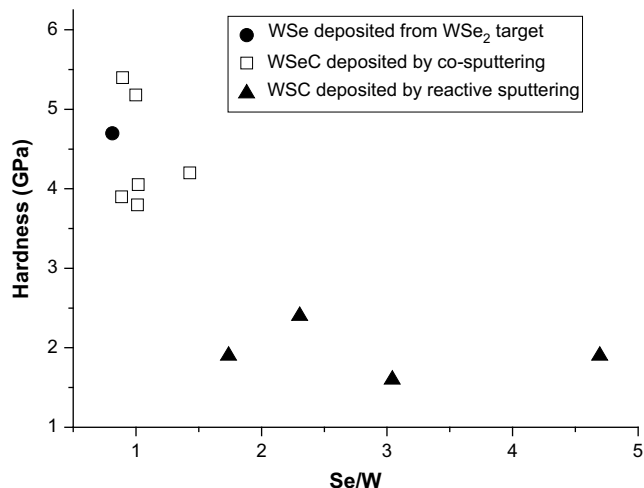


Fig. 3. Evolution of W–Se–C coatings hardness as a function of S/W ratio.

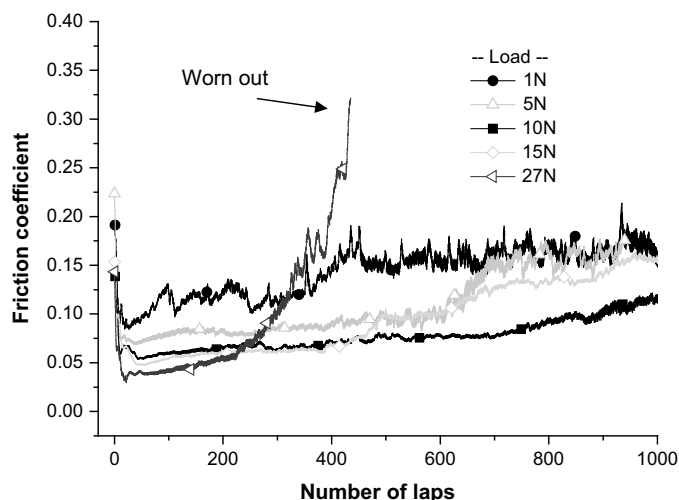


Fig. 4. Friction curves as a function of load, coating WSe-8 (see Table 1).

expected that the formation of gaseous H–Se species is less favorable.

3.3. Morphology and structure

SEM observations in all coatings revealed very compact featureless morphologies, regardless the C content or the deposition process. Fig. 2 shows typical diffraction spectra of deposited WSeC films. All coatings exhibited the broad peak placed at the position of the (10L) line of WSe_2 , giving rise to a similar pattern as those observed for quasi-amorphous W–S–C coatings deposited by co-sputtering from two individual targets [12].

3.4. Hardness and friction

The coatings deposited by co-sputtering from two individual targets presented an increase of the hardness with the increase of the carbon content, while the hardness of reactive sputtered films was almost independent. The hardness as well decreased with increasing Se/W ratio, when the co-sputtering process was used, see Fig. 3. The high hardness value for W–Se film could be explained by the high presence of oxygen, which can form relatively hard tungsten oxides [14] and increase the inter-crystalline slipping resistance of W–Se crystal by replacing Se atoms.

Preliminary tribological test showed that W–Se peeled off almost immediately after start of the pin-on-disc test. W–Se–C coatings deposited by co-sputtering exhibited more promising tribological behavior being tested with increasing applied load. In all cases, the friction decreased after couple of laps to the lowest value and then slowly increased with increasing number of cycles, see Fig. 4 as typical example. Furthermore, the friction was significantly lower for higher load (and thus higher contact pressures), the feature typical of TMD films. The coating wear was very high compared to previously studied WSC and MoSeC systems [10,11] and even loads higher than 20 N led to rapid destruction of the coatings. The low adhesion of the WSeC coatings deposited by reactive sputtering hindered completely the tribological testing.

4. Conclusions

The W–Se–C coatings were successfully deposited by r.f. magnetron sputtering from two targets (C + WSe_2) and by a reactive process from a WSe_2 target in a reactive atmosphere (Ar + CH_4), with carbon content in the range 25–70 at.%. Coatings

deposited by co-sputtering presented a Se/W ratio almost constant for all carbon contents with a value of ~ 1.0 , while in reactive process significant variations of the Se/W ratio were observed. The hardness of the coatings deposited by co-sputtering was significantly higher than that of reactive sputtered coatings deposited by co-sputtering. Preliminary tribological tests showed adhesion problems of reactively prepared coatings, while co-sputtered coating confirmed expect low friction behavior.

References

- [1] Lansdown AR. Molybdenum disulphide lubrication. Elsevier Science B.V.; 1999.
- [2] Zabinski JS, Donley MS, Prasad SV, McDevitt NT. *J Mater Sci* 1994;29:4834.
- [3] Rigato V, Maggioni G, Boscarino D, Sangaletti L, Depero L, Fox VC, et al. *Surf Coat Technol* 1999;116–119:176.
- [4] Nossa A, Cavaleiro A. *Surf Coat Technol* 2001;142:984.
- [5] Voevodin AA, O'Neill JP, Zabinski JS. *Surf Coat Technol* 1999;116–119:36–45.
- [6] Noshiro Junichi, Watanabe Shuichi, Sakurai Takahiko, Miyake Shojiro. *Surf Coat Technol* 2006;200:5849.
- [7] Jamison WE, Cosgrove SL. *ASLE Trans* 1971;14:62.
- [8] Bergmann E, Melet G, Muller C, Simon-Vermot A. *Tribol Int* 1981;14:329.
- [9] Kubart T, Polcar T, Kopecký L, Novák R, Nováková D. *Surf Coat Technol* 2005;193:230.
- [10] Polcar T, Evaristo M, Stueber M, Cavaleiro A. *Wear* 2009;266:393.
- [11] Polcar T, Evaristo M, Cavaleiro A. *Wear* 2009;266:388.
- [12] Evaristo M, Nossa A, Cavaleiro A. *Surf Coat Technol* 2005;200:1076.
- [13] Lince JR, Hilton MR, Bommannavar AS. *Surf Coat Technol* 1990;43–44:640.
- [14] Parreira NMG, Polcar T, Cavaleiro A. *Surf Coat Technol* 2007;201:5481.

Can W–Se–C Coatings Be Competitive to W–S–C Ones?

Manuel Evaristo,* Tomas Polcar, Albano Cavaleiro

W–Se–C coatings were deposited by co-sputtering from WSe₂ and C targets. Carbon content varied from 25 up to 70 at.%, Se/W ratio was between 0.9 and 1.0, with no significant influence of the carbon content on their variations. The hardness of the coatings was evaluated by nano-indentation with values between 3.8 and 5.6 GPa. The structure of the coatings analysed by X-ray diffraction in glancing mode could be defined as quasi-amorphous. The tribological properties were evaluated in an SRV machine using reciprocating ball-on-disk tests under increasing loads. In general, the friction gets decreased with increasing loads. The comparison with other transition metals, dichalcogenides alloyed with carbon, namely Mo–Se–C and W–S–C systems, showed that W–Se–C coatings could be a good alternative with almost identical friction properties.

Introduction

Compared to the widely used transition metal dichalcogenides (TMDs) based on disulphides, namely MoS₂ and WS₂, diselenides have not attracted so much attention as materials for reducing friction. Nevertheless, since many years, comparative studies have shown that diselenides could outperform disulphides.^[1] The entire family of TMDs shows similar drawbacks when used as self-lubricating films: low hardness and adhesion to the substrate and, consequently, low load bearing capacity, and both high wear rate and friction coefficient in humid air. Significant improvements have been achieved by alloying TMD with other elements, such as metals like Ti,^[2] Pb,^[3] Au^[4] or carbon.^[5–7]

It has been demonstrated^[1] that the friction of MoSe₂ and WSe₂ was ruled by the adhered transfer films and they were comparable to that of disulphides. Molybdenum diselenide

had been found comparable with disulphide considering friction coefficient^[8] and it was even less sensitive to humidity^[9]; moreover, both referred to the coatings outperformed by molybdenum ditelluride, niobium and tantalum diselenides. When carbon was added, the Mo–Se–C system showed better tribological properties than W–S–C.^[10,11] However, the MoSe₂-based coatings quickly deteriorate at elevated temperature exceeding 200 °C, while tungsten disulphide alloyed with carbon showed ability to work up to 400 °C.^[12] To the best of our knowledge, there were no reports described in detail the tribological behaviour of W–Se–C coatings, which might join the advantages of both tungsten disulphide and molybdenum diselenide. Therefore, it was decided to deposit and study the structural, mechanical and tribological properties of W–Se–C coatings prepared by non-reactive magnetron sputtering from two individual targets (C + WSe₂).

Experimental Part

The coatings were deposited on M2 (AISI), 100Cr6 steels (hardness close to 9 and 5 GPa, respectively; samples were polished to final $R_a < 30$ nm) and silicon wafers by r.f. magnetron sputtering from two individual targets WSe₂ (99.8% pure) and C (99.999% pure) in argon atmosphere with a pressure of $\sim 5 \times 10^{-1}$ Pa. The substrate holder was rotated with a high speed to avoid the formation of a

M. Evaristo, T. Polcar, A. Cavaleiro
SEG-CEMUC, Faculty of Sciences and Technology, Mechanical
Engineering Department, University of Coimbra, Rua Luís Reis
Santos, 3030-788 Coimbra, Portugal
E-mail: manuel.evaristo@dem.uc.pt
T. Polcar
Faculty of Electrical Engineering, Department of Control
Engineering, Czech Technical University in Prague, Technická 2,
Prague 6, Czech Republic

multilayer structure. In order to vary the composition of the coatings, the power in both the cathodes was changed. To evaluate the chemical composition of the films, a Cameca SX 50 electron probe microanalysis (EPMA, Cameca, France) apparatus was used, being the final values an average of, at least four different measurements. The structure was evaluated by X-ray diffraction (XRD) using a Phillips diffractometer with Co K α radiation in a glancing mode.

The hardness of the coatings was measured by a Micro Materials NanoTest system. The indentations were performed in load control mode with a maximum load of 5 mN, at a 0.1667 mN · s⁻¹ loading and unloading rate, with a 5 s hold period at maximum load and 60 s hold period at 90% unloading for thermal drift correction. Over 30 indentations were performed for each coating. The contact depth was less than 10% of the coating thickness to avoid the influence of the substrate. The friction was measured in a reciprocating machine (Optimol, SRV) in dry and humid air. The number of cycles was 10 000, while the applied load varied from 20 to 200 N and the stroke length was 1 mm. 100Cr6 steel balls with a diameter of 10 mm were used as counterparts. The wear tracks were analysed by scanning electron microscopy (SEM; Jeol) and by Raman spectroscopy (Ar⁺ laser; Renishaw).

Results and Discussion

Deposition Rate and Chemical Composition

Preliminary deposition of pure WSe₂ showed several problems when this material was used as magnetron target. The power applied to this target had to be limited to low values (about 40 W) in order to avoid a severe evaporation of the target material which led to a rapid destruction of the target. Therefore, the first set of depositions was carried out with a power of only 40 W applied to the WSe₂ target. However, it has been observed that when WSe₂ target was used simultaneously with the carbon one, the power could be increased without any detrimental effects up to 110 W. In these conditions, a second set of depositions was performed. As expected, the W–Se or the carbon contents depended almost linearly on the applied power to the targets. The chemical composition of the coatings is shown in Table 1. The deposition rate was

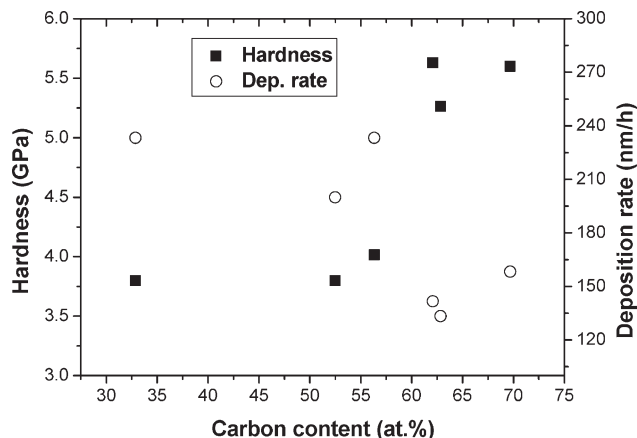


Figure 1. Evolution of the hardness and the deposition rate of W–Se–C coatings as a function of the carbon content.

still very low compared to similar W–S–C system^[13] leading to relatively long deposition times and high oxygen contents close to 10 at.% due to the contamination from the residual atmosphere. The Se/W ratio was close to 1, again lower than in the W–S–C and, particularly, Mo–Se–C systems.^[10,13] It is possible that oxygen can directly replace selenium in the WSe₂ structure as it was demonstrated in works dealing with the oxidation of MoS₂ structure.^[14] The sputtering yield was higher for tungsten diselenide than for carbon resulting in a higher deposition rate for coatings with the lowest carbon contents (see Figure 1).

Morphology and Structure

The cross-section of the coatings deposited on silicon wafers was observed in SEM. Whatever the carbon content was, the coatings presented were very compact and have featureless morphologies. Figure 2 shows the typical diffraction spectrum of the deposited W–Se–C films. All coatings exhibited a broad peak placed at the positions of the (10L) lines of the WSe₂ phase, giving rise to a similar pattern as

Table 1. Deposition parameters of selected coatings and their chemical compositions.

Deposition	Carbon target power (W)	WSe ₂ target power (W)	Thickness (μm)	O (at.%)	C (at.%)	W (at.%)	Se (at.%)	Se/W
WSeC-4	500	40	1.4	10.9	66.4	9.3	13.3	1.4
WSeC-5	400	40	1.0	9.0	69.7	11.3	10.1	0.9
WSeC-6	200	40	0.9	10.2	62.1	15.7	12.0	0.8
WSeC-7	400	51	0.8	9.1	62.8	14.1	14.0	1.0
WSeC-8	400	74	1.4	8.1	56.3	17.6	18.0	1.0
WSeC-9	300	91	1.2	8.0	52.5	19.7	19.9	1.0
WseC-10	100	110	1.4	9.6	32.9	30.5	27.0	0.9

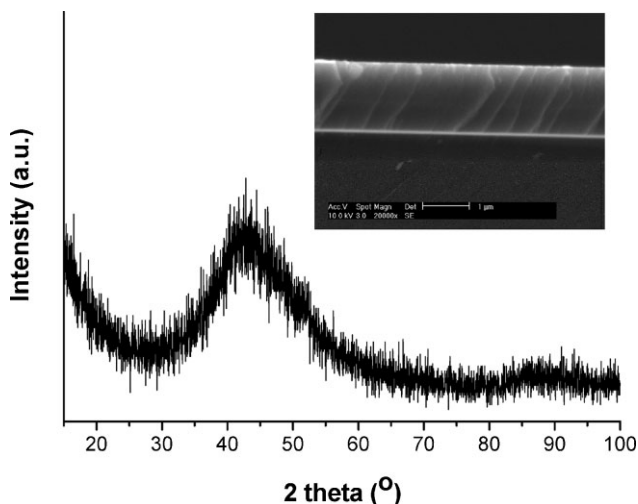


Figure 2. XRD spectrum of a typical W–Se–C coating. The inset shows the SEM micrograph of the cross-section of the coating

those observed for quasi-amorphous W–S–C coatings deposited by co-sputtering from two individual targets.^[13] Unfortunately, the XRD analysis in this case could not reveal any microstructural characteristics, such as the existence of tungsten carbide or the grain size of tungsten diselenide. Raman spectra shown in Figure 3 did not help with the characterisation of the coatings as well. The peak representing tungsten diselenide were located at low Raman shifts and their detection was difficult due to the optical filters used by the equipment. However, the D and G peaks of carbon showed, as expected, a significant decrease in intensity with decreasing carbon content.

Hardness and Tribological Properties

The coatings presented almost identical hardness values close to 3.5 GPa whatever the carbon content was in the range 33–56 at.%. A further increase of the carbon content led to higher hardness (see Figure 1). In our previous studies,^[10,11] the hardness increased almost linearly from a very low value typical for pure sputtered TMD to the highest value achieved for pure carbon coating. Therefore, the hardness value measured for the lowest carbon content could indicate the presence of hard tungsten carbide particles increasing the hardness. This hypothesis could be supported with Raman spectrum of this film, where the intensity of D and G carbon peaks is very low. However, further study will be carried out in order to prove or exclude the presence of tungsten carbide in the films.

The coatings with the highest carbon content (i.e. WSeC-4 to WSeC-7) showed unsatisfactory wear resistance being rapidly worn out. Therefore, the tests were focussed on the coatings with lower carbon content. All three tested films

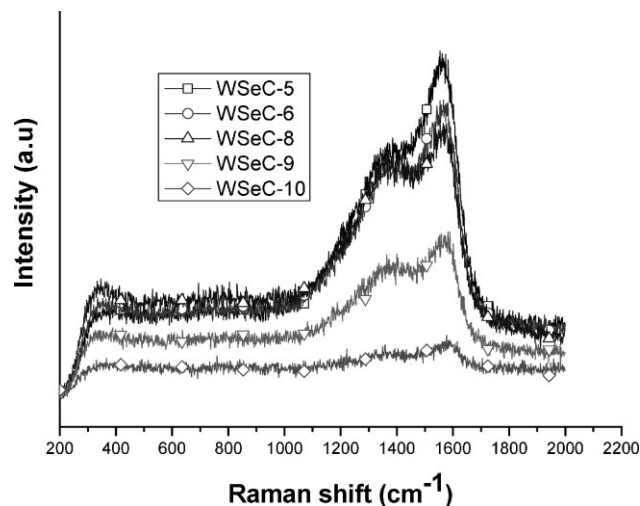


Figure 3. Raman spectra of selected W–Se–C coatings with increasing C contents.

(WSeC-8 to WSeC-10) exhibited significant decrease of the friction coefficient with increasing applied load and, thus, contact pressures. This behaviour is a clear deviation from the standard materials following the Amonton's law which considers the friction independent of the applied load. The decrease of the friction with the contact pressure is typical of pure TMDs^[15] and TMD alloyed with carbon.^[10,11,15] The friction curves showed three typical phenomena: (i) running-in represented by the rapid increase to the highest value and, then, a slower decrease, (ii) steady-state wear with stable and low friction and (iii) coating failure with the abrupt rise of the friction coefficient. As demonstrated in Figure 4 for WSeC-8 coating, the running-

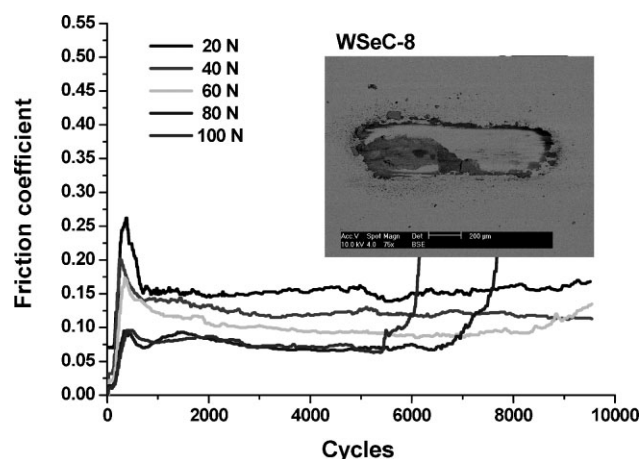


Figure 4. Friction curves of WSeC-8 coatings as a function of the load. The rapid increase of the friction coefficient (load 80 and 100 N) represents the coating failure. SEM micrograph (see inset) of the wear track obtained in BSE mode showed the adhesive failure of the coating.

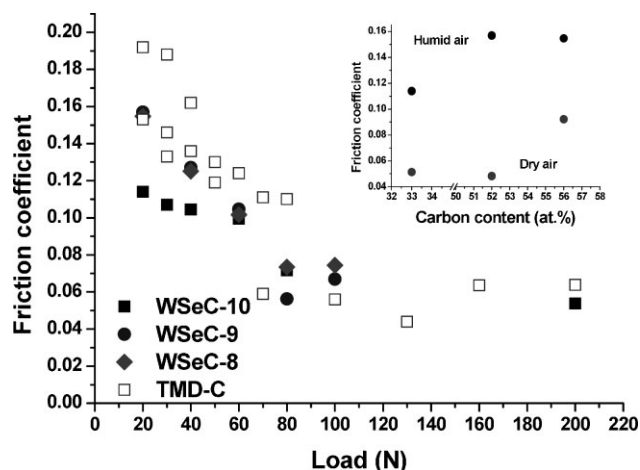


Figure 5. Steady-state friction versus load. The open points represent the results of similar Mo–Se–C and W–S–C coatings published in ref.^[11] The comparison of friction coefficient of W–Se–C films measured at dry and humid air is shown in the inset (applied load 20 N).

in length disappeared with increasing load, the coating did not withstand loads higher than 60 N. The coatings with lower carbon content, WSeC-9 and WSeC-10, were successfully tested at loads as high as 120 N and clearly demonstrated their potential as an alternative for similar W–S–C and Mo–Se–C systems^[10,11] (see Figure 5). The main wear mechanism leading to the coating failure was the adhesive wear. SEM micrographs of the wear track, in cases where an abrupt increase of the friction was observed, showed relatively shallow tracks, with zones in the centre where the coating is peeled off (Figure 4). The wear tracks, with no signs of failure, were analysed as well by Raman spectroscopy. The carbon peaks were identical with those of the as-deposited coatings; no signs of any graphite-based tribolayer were observed. The absence of graphite in the worn surfaces and the significant decrease of the friction with increasing contact pressures suggests that the friction of the W–Se–C coatings is determined by the formation of a self-lubricating tribolayer based on WSe₂, as demonstrated in similar MoSeC system.^[16] This was indirectly confirmed by the tribological tests carried out in dry air, where the friction dropped immediately after the start of the sliding to a very low level (0.05) almost identical for all the three tested coatings (see inset in Figure 5). Such behaviour is again typical for TMDs alloyed with carbon.^[10,11,15]

Conclusion

Coatings deposited by co-sputtering presented a Se/W ratio almost constant for all carbon contents with a value of ~ 1.0 . Tribological tests showed adhesion problems particularly for high C-content films. On the other cases, low friction behaviour was found with the friction coefficient decreasing with increasing applied load. Steady-state values as low as 0.05 in humid air could be measured, supporting the coating loads as high as 200 N. Generally, the tribological behaviour could be considered very close to other TMD + C systems, such as W–S–C and Mo–Se–C.

Acknowledgements: This work was supported by the *Czech Science Foundation* through the project 106/07/P014, by the *Ministry of Education of the Czech Republic* (project MSM 6840770038), by the *Fundação para a Ciência e a Tecnologia* through the project SFRH/BPD/34515/2006 and by project FOREMOST supported by *EU*. M. Stueber from FKZ centre is also acknowledged for the access to Raman analysis.

Received: September 29, 2008; Accepted: March 19, 2009; DOI: 10.1002/ppap.200930414

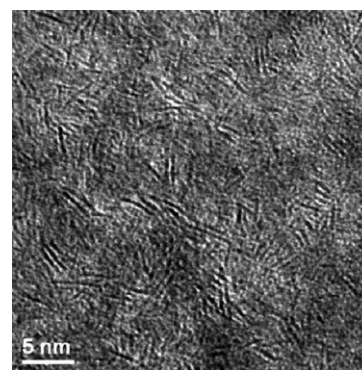
Keywords: C alloyed coatings; low friction coatings; transition metal dichalcogenides; W-Se-C

- [1] W. E. Jamison, S. L. Cosgrove, *ASLE Trans.* **1970**, *14*, 62.
- [2] V. Rigato, G. Maggioni, D. Boscarino, L. Sangaletti, L. Depero, V. C. Fox, D. Teer, C. Santini, *Surf. Coat. Technol.* **1999**, *116–119*, 176.
- [3] K. J. Wahl, L. E. Seitzman, R. N. Bolster, I. L. Singer, *Surf. Coat. Technol.* **1995**, *73*, 152.
- [4] M. C. Simmonds, A. Savan, E. Pfluger, H. Van Swygenhoven, *Surf. Coat. Technol.* **2000**, *126*, 15.
- [5] A. Nossa, A. Cavaleiro, *Surf. Coat. Technol.* **2001**, *142*, 984.
- [6] A. A. Voevodin, J. P. O'Neill, J. S. Zabinski, *Surf. Coat. Technol.* **1999**, *116–119*, 36.
- [7] J. Noshiro, S. Watanabe, T. Sakurai, S. Miyake, *Surf. Coat. Technol.* **2006**, *200*, 5849.
- [8] E. Bergmann, G. Melet, C. Muller, A. Simon-Vermot, *Tribol. Int.* **1981**, *14*, 329.
- [9] T. Kubart, T. Polcar, L. Kopecký, R. Novák, D. Nováková, *Surf. Coat. Technol.* **2005**, *193*, 230.
- [10] T. Polcar, M. Evaristo, M. Stueber, A. Cavaleiro, *Wear* **2009**, *266*, 393.
- [11] T. Polcar, M. Evaristo, A. Cavaleiro, *Wear* **2009**, *266*, 388.
- [12] T. Polcar, M. Evaristo, A. Cavaleiro, *Vacuum* **2007**, *81*, 1439.
- [13] M. Evaristo, A. Nossa, A. Cavaleiro, *Surf. Coat. Technol.* **2005**, *200*, 1076.
- [14] J. R. Lince, M. R. Hilton, A. S. Bommannavar, *Surf. Coat. Technol.* **1990**, *43–44*, 640.
- [15] B. J. Briscoe, A. C. Smith, *ASLE Trans.* **1982**, *25*, 349.
- [16] T. Polcar, M. Evaristo, R. Colaço, C. Silviu Sandu, A. Cavaleiro, *Acta Mater.* **2008**, *56*, 5101.

Self-Lubricating W–S–C Nanocomposite Coatings

Tomas Polcar,* Manuel Evaristo, Albano Cavaleiro

This paper is aimed on a perspective low-friction coatings, the W–S–C system deposited by magnetron sputtering, which exhibits extremely low-friction coefficient together with high-load-bearing capacity. Special attention has been paid to the analysis of the frictional and wear mechanisms under different operating conditions, such as the contact pressure, the air humidity, and the temperature. The formation of a thin self-lubricating WS₂ tribolayer, which was observed regardless on the sliding conditions, is the driving force for the promising frictional properties of the coatings.



Introduction

Transition metal dichalcogenides (TMD) have excellent self-lubricant properties in dry air or vacuum.^[1,2] Nevertheless, these films are easily rusted in the presence of moist environments and their reduced mechanical resistance makes them inappropriate for applications requiring high-load-bearing capacity. On the other hand, hard coatings are often employed to protect from abrasive and erosive wear; however, they do not have low friction and they are frequently brittle. Therefore, there is a need to design coatings combining low friction with high-load-bearing capacity; moreover, a good adhesion to the substrates is required. Voevodin et al.^[3,4] made use of the concept of nanocomposite structured coatings to reach very low-friction coefficients in a large range of environments. The idea was to join excellent frictional and wear properties of

hard DLC coatings at humid air with those of softer WS₂ in dry air and vacuum; the presence of tungsten carbide should increase the hardness. Thus, with a nanostructure consisting of nanocrystals of WS₂ and WC enclosed in an amorphous carbon matrix, friction coefficient lower than 0.1 was expected irrespective of the testing environment. They observed that the coatings kept very low friction at dry air and a much higher at humid air (about 0.2). When the humidity was periodically changed, the values of friction corresponded to that of dry and humid air, respectively. Raman analysis in the wear track indicated presence of WS₂ phase for sliding at dry air and combination of graphite and WS₂ phase when tests were carried out at humid air.

Our previous works^[5–10] showed that the synergetic effect of doping W–S films with carbon or nitrogen together with the deposition of a Ti interlayer could give rise to significant improvements of the mechanical properties and the tribological behavior, particularly in the case of films alloyed with carbon. The W–S–C coatings were deposited by reactive magnetron sputtering from a WS₂ target in an Ar + CH₄ atmosphere. To avoid the hydrogen contamination, a non-reactive process based on co-sputtering from C and WS₂ materials was also selected. With this approach, the most common procedure is co-sputtering from individual targets. However, there are some drawbacks such as, the non-homogeneity in the coatings composition when

T. Polcar

Faculty of Electrical Engineering, Department of Control Engineering, Czech Technical University in Prague, Technická 2, Prague 6, Czech Republic

Fax: (+420) 224 312 439; E-mail: tomas.polcar@dem.uc.pt

T. Polcar, M. Evaristo, A. Cavaleiro

SEG-CEMUC, Department of Mechanical Engineering, University of Coimbra, Rua Luís Reis Santos, P-3030 788 Coimbra, Portugal

stationary large substrates are used, or the formation of a multilayer structure if the substrates are rotated. Thus, it was decided to deposit the W–S–C coatings by non-reactive magnetron sputtering from a carbon target with pellets of WS₂ placed in its erosion zone. The high number and good distribution of the pellets assured the necessary homogeneity in the coatings chemical composition. Furthermore, the final chemical composition of the deposited coatings could also be easily controlled by changing the number of WS₂ pellets.^[11–13]

The objective of this paper is to describe the recent progress in the development of coatings with very low friction in environments with different temperatures and air humidity levels. Moreover, these coatings should withstand high contact pressures with minimum wear or adhesive damage. This study is focused on the structural, mechanical, and tribological properties of W–S–C coatings.

Experimental Part

All W–S–C coatings were deposited on steel 100Cr6 discs with a diameter of 36 mm and M2 polished steel samples with hardness close to 5 and 9 GPa, respectively.

The depositions were carried out in a radiofrequency (rf) magnetron sputtering Edwards ESM 100 unit, equipped with two cathodes ($\emptyset = 100$ mm). Prior to the depositions the substrates were sputter cleaned during 20 min by establishing the plasma close to the substrates electrode. Immediately, a Ti interlayer was deposited with an approximate thickness of 300 nm. The main sputtering target was pure carbon, partly covered by WS₂ pellets placed in the preferentially eroded zone. The dimensions of the pellets were 4.1 mm × 3.5 mm × 1.5 mm. The degree of target coverage determined the overall chemical composition of the sputtered film. The depositions were carried out with constant power density of 7.6 W · cm² in the carbon target.

To evaluate the chemical composition of the films, an electron probe microanalysis apparatus (EPMA) was used. The structure was analyzed by X-ray diffraction (XRD; Co K α radiation in glancing mode) and high-resolution transmission electron microscope (HRTEM), the morphology by scanning electron microscopy (SEM), the chemical bonding by X-ray photoelectron (XPS; Mg K α radiation), and Raman spectroscopies (Ar⁺ laser, 514.5 nm wavelength). The hardness was determined by depth-sensing indentation technique; the coatings deposited on M2 steel were used for these measurements. The load was increased in steps (60) until a nominal load of 20 mN was reached, following the procedure indicated elsewhere.^[14]

The tribological tests were carried out with a ball-on-disc tribometer on 100Cr6 samples. The linear speed was kept constant (20 mm · s⁻¹), while the diameter varied from 12 to 16 mm. The 100Cr6 steel balls with a diameter of 6 mm were used as sliding partners. The coatings tribological behavior was evaluated in air with different relative humidity (RH, 5–70%) or in dry nitrogen, at temperatures up to 400 °C and with loads in the range 5–48 N. High-load tests were performed using reciprocating SRV machine (ball-on-flat) with 10 mm 100Cr6 steel balls as counterparts. All

counterparts were cleaned in ethanol before the test. The friction coefficient reported in this study is the average value of the whole sliding test, unless stated otherwise. Each test was repeated three times; standard deviation of the average friction coefficient and the wear rate was lower than 10%. The number of laps is indicated in the test. The wear rate was calculated as worn volume per load and sliding distance. The worn volume was calculated from at least three independent profiles of the wear track measured by mechanical profilometer. The wear tracks and wear debris were analyzed by SEM coupled with energy dispersive X-ray spectroscopy (EDS), Raman spectroscopy, and Auger electron spectroscopy (AES).

Results

Coating Deposition, Chemical Composition, and Morphology

Different carbon contents were achieved in the coatings by varying the number of WS₂ pellets in the C target. As it was expected, the carbon content of the films decreased linearly with the increase of the total area of pellets (Table 1). A closer analysis of the arrangement of the experimental points allows estimating the reproducibility of the chemical composition. We deposited three times (always with a new re-distribution of the pellets) coatings with areas of pellets of 260 and 1 070 mm² (corresponding to the lowest and highest carbon contents), which allowed estimating the reproducibility of the chemical composition of the coatings. Considering the variation in the pellets distribution over the target erosion zone and the errors of the measurements, it can be concluded that the used deposition process is highly reproducible.

The oxygen content in the coatings decreased from 5 to 2 at.% with increasing carbon content. It is not surprising, since WS₂ pellets exhibited a high porosity affecting the residual atmosphere in the deposition chamber. The variation of S/W ratio was in the range 1.2–1.45 (Table 1); no dependency on carbon content was observed. The sulfur

Table 1. Parameters of selected W–S–C coatings.

Area of pellets	C	S/W	Deposition rate	Hardness
mm ²	at.%		nm · s ⁻¹	GPa
1 190	29	1.2	0.54	5.7
1 073	33	1.4	0.61	6.9
878	37	1.3	0.61	9.1
778	41	1.3	0.61	10.0
452	51	1.2	0.63	9.0
261	66	1.3	0.47	7.1

deficiency was probably caused by the re-sputtering of the sulfur atoms from the growing film and by the chemical reactions of sulfur with the residual atmosphere. Detailed information about the coatings deposition can be found elsewhere.^[11]

The cross-sections of fractured coated Si wafers observed by SEM and TEM showed more and more compact morphologies with increasing carbon content.^[11] Columnar structure and the presence of voids, typical feature of pure WS₂ coatings deposited by reactive sputtering from WS₂ target^[15] were not observed even for the lowest carbon content.

Structure, Chemical Bonding, and Hardness

With the increase of carbon in the coatings, a gradual loss of crystallinity was observed.^[8,9] The films with low-carbon content presented the typical XRD patterns of Me-S (Me – transition metal) sputtered films with prominent peak at $2\theta \approx 40^\circ$ showing an extended shoulder corresponding to a turbostrating stacking of (10L) planes ($L = 0, 1, 2, 3$). Peak at $2\theta \approx 70^\circ$ was indexed as the (110) plane. Wise et al.^[16] demonstrated that these XRD patterns could be explained by a 2D organization of the basal planes which could have several tens of unit cells dimension. With the progressive decrease of the lateral dimensions of the basal planes, either the broadening or the drop in the intensity of the (10L) plane occurred until a unique low intensity and broad peak typical of an amorphous structure was detected. This situation would arise when the lateral order of the basal planes did not exceed a couple of lattice parameters.

Three samples with different carbon content were analyzed by HRTEM confirming the short order of WS₂ basal planes. The coating with the lowest carbon content (27 at.%) exhibited WS₂ platelets preferentially oriented perpendicular to the coating surface (Figure 1a). The length of the platelets was typically 5–10 nm. Some platelets were curved with a maximum angle of about 30°. The medium carbon content (49 at.%) coatings could be described as a nanostructured material with randomly oriented WS₂ platelets with a typical length of 3 nm embedded into an amorphous carbon matrix (Figure 1b). The highest carbon content led to almost featureless HRTEM images revealing that the length of the WS₂ platelets was further reduced. Tungsten carbide grains were not observed in any case. The Raman spectra showed two groups of peaks belonging to the WS₂ phase (peaks at 325 and 416 cm⁻¹) and the carbon matrix (≈ 1390 and ≈ 1570 cm⁻¹ corresponding to D and G bands, respectively, see Figure 2). Comparing the sharp peaks from the WS₂ pellet with the broad ones of the W–S–C coatings, it can be concluded that the latter exhibited a significantly disordered material, again in agreement with

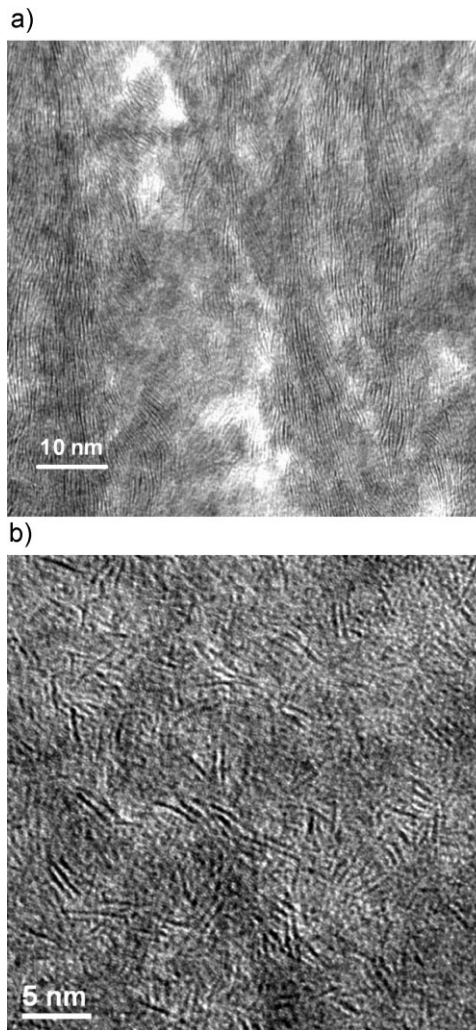


Figure 1. HRTEM images of W–S–C coatings with (a) 33 at.% C and (b) 51 at.% C.

the XRD and TEM analyses. XPS measurements did not reveal any evidence of tungsten carbides in the films.

The hardness of W–S–C films increased with decreasing number of pellets (i.e., with increasing carbon content), reaching a maximum of 10 GPa at ≈ 41 at.% of carbon.^[13] This trend can be related either to the increase of the compactness of the films or the changes in the coating microstructure, where the WS₂ platelets were losing, with increasing carbon content, the preferential orientation together with the shortening of the platelet length. With the addition of more carbon to the films, a slight decrease of the hardness was observed.^[11] It should be pointed out that the hardness of pure carbon coating deposited under identical conditions (i.e., sputtering from carbon target without WS₂ pellets) gave hardness close to 7 GPa. The hardness of W–S–C coatings is generally about one order of magnitude higher than that of pure tungsten disulfide.^[17]

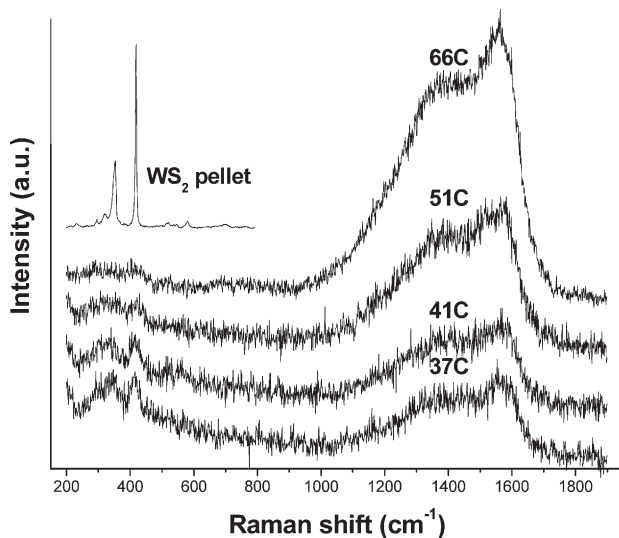


Figure 2. Raman spectra of as-deposited W-S-C coatings and a WS₂ pellet.

Influence of the Air Humidity

The friction coefficient and the wear rate of W-S-C coatings are summarized in Figure 3. The evolution of the friction coefficient was almost identical for all coatings up to a humidity level of 40%. The average friction coefficient in dry air (RH < 5%) was very low reaching values in the range of 0.03–0.06. The tests in humid air exhibited similar increase of the friction value of up to 0.2 for an RH of 40%. Above this value, a difference in the friction trends was observed. In general, the coatings with the highest carbon contents were much less sensitive to the high levels of humidity, being observed even a slight decrease of the friction coefficient. For the other carbon contents, the friction coefficients

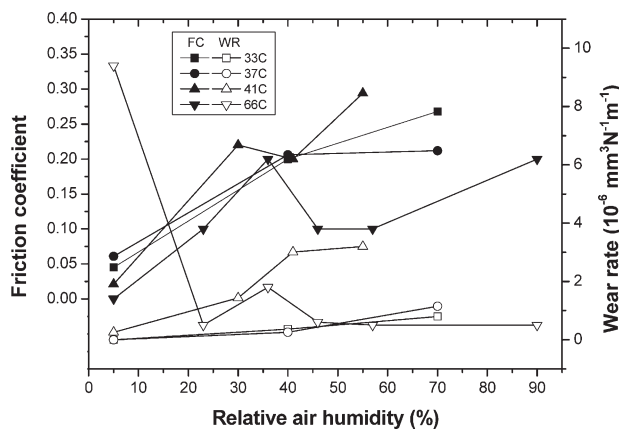


Figure 3. Average friction coefficient (full symbols) and wear rate (open symbols) of selected W-S-C coatings with different carbon content as a function of the relative air humidity (ball-on-disc, load 5 N, room temperature).

increased with increasing RH values. In contrast to the friction coefficient, the wear rate of the coating with the highest carbon content (66 at.% C) was significantly higher than the others when sliding in dry air. The coatings with 33 and 37 at.% C exhibited the best wear resistance, even in humid air, with wear rates slightly increasing with humidity. The hardest coating (41 at.% C) showed the highest wear in humid air.

The analysis of the friction and wear shows that the initial friction coefficient of the coating with 66 at.% C was very high during the first 25 turns and fell down abruptly to a steady-state regime at the lowest stabilized value. The wear track observed by SEM exhibited large cracks and delaminated parts.^[11] Nevertheless, the coating damage was only superficial, since EDS analysis and profilometry did not identify complete coating failure (i.e. penetration to substrate). A short test with 50 laps led to similar coating appearance and worn volume as those after 1500 laps. Thus, the high wear rate referred to above occurred exclusively during the first couple of turns. The coatings with lower carbon content reached the steady-state more slowly, only after approximately 250 laps; nevertheless, their maximum initial friction coefficient was only 0.15 compared to 0.65 obtained for the 66 at.% C coating. Such a different behavior for the high-carbon content coating can be understood by the limited self-lubricant WS₂ material available to form the tribolayer at the start of the tribological test which leads to a very high initial friction force causing severe damages to the coating surface. During this initial period a rapid release of a large quantity of debris for the sliding contact between the ball and the coating was expected facilitating the tribolayer formation and the subsequent significant decrease of the friction.^[11] The coatings with carbon content up to 51 at.% contained more self-lubricant material available since the beginning of the sliding test. Thus, its effect was exerted from the first moments of the contact but the formation of the tribolayer was slower and the steady-state wear regime with the low level of friction was reached later. The wear rate of the low-carbon coatings was as well higher during the initial part of the sliding tests, although the difference was not so evident compared to the high-carbon coating. The values of the wear rates of the coatings with low- and high-carbon content sliding in humid air were almost equal; contrary to the friction, the wear rate of W-S-C coatings was almost independent of the air humidity.

Effect of Testing Temperature

The value of friction coefficient at room temperature was close to 0.2, with the exception of the coating with 29 at.% C, which exhibited a rather higher value of 0.3. However, the

friction rapidly fell down with the increase in temperature.^[13] It is well known that TMD exhibit excellent friction properties in vacuum or in dry atmosphere, while a humidity-containing environment has, as above presented, a detrimental effect leading to the increase of the friction and the wear.^[18] Therefore, the low friction at 100 °C could be attributed to the drying of the atmosphere. However, comparative sliding tests in dry nitrogen showed that the friction coefficient was about 0.02 higher than that measured at 100 °C irrespective of the coating. It is supposed that the increase of the testing temperature can further facilitate the crystalline slipping of the weakly bonded basal planes and, therefore, contribute for diminishing the friction. Qualitative identical results were obtained for pure MoS₂ and MoSe₂ coatings also belonging to the TMD family, which showed higher friction in dry nitrogen than at a temperature of 80 or 100 °C.^[19] It should be pointed out that no structural or chemical changes of W–S–C were expected at 100 °C; in fact, XRD, EPMA, and Raman spectroscopy did not detect any difference in the annealed compared to the as-deposited coatings. When the temperature was further increased, the friction coefficient reached a maximum at 300 °C in both coatings with the highest and the lowest studied carbon contents, while for 41 and 51 at.% C films almost a constant friction, regardless on the temperature, was observed. Again, no structural or chemical changes in the coatings were detected.

Up to 300 °C, the wear rate was very low not exceeding $2.5 \times 10^{-6} \text{ mm}^3 \cdot \text{N}^{-1} \cdot \text{m}^{-1}$. The only exception was the coating with the highest carbon content exhibiting a steady increase of the wear rate in this temperature range. This coating presented a high friction (≈ 0.35), during the running-in period, which lasted for about 25 revolutions to reach the steady state. On the contrary, a rapid decrease in the friction, from a value of 0.1 down to the low steady-state value, was observed for the coatings with lower carbon. The wear tracks looked like polished for almost all the coatings, while large delaminated areas were observed for the one with 66 at.% C. This is a similar behavior to that found for tests in dry nitrogen and, as referred to above, in dry air at room temperature. Again, sliding tests performed with a short number of cycles (250) showed a very large worn volume of the coating material, comparable to the one after 1000 cycles. As the steady-state wear regime only takes place when a tribolayer of self-lubricant material is formed in the contact,^[19] the limited amount of WS₂ phase available in the high-carbon coating, delays the formation of the third body and leads to a high initial friction force. In this initial sliding phase, a severe damage of the coating surface is caused. The SEM analysis of the wear debris showed small wear particles (maximum 300 nm in diameter) for all coatings except of 66 at.% C film, where large and thin particles with sharp edges (up to 5 μm) were observed. Therefore, the delamination of the high-carbon

coating produced large particles causing further abrasive damage and high wear.

The temperature of 400 °C can be considered as the functional limit for the W–S–C coatings presented in this study. The coating with 29 at.% C was partially peeled off from the substrate whereas very deep (close to the titanium interlayer) wear tracks were achieved for the 51 and 66 at.% C samples; only the coating with 41 at.% C can be considered as an appropriate candidate for potential industrial applications, since the wear rate increased slightly at this temperature. The friction coefficient remained very low, even decreased in some cases, which supports the hypothesis that the sliding process is still driven by the self-lubricant mechanism typical of TMD, despite the partial oxidation of the coatings revealed by EDS measurements.

Influence of the Contact Pressure

Figure 4 shows that, as a general trend, the friction coefficient decreased with increasing load. The friction curves revealed two different typical aspects: (1) the coatings up to 51 at.% C exhibited high friction in the first hundreds of laps (running-in), which was followed by a drop in the friction to a lower level corresponding to the steady-state wear and (2) the coatings with the highest carbon contents showed almost constant friction during the entire test. As a consequence, the average friction for the low- and medium-carbon content coatings decreases with the number of laps (see Figure 4) while it remains the same in the case of high-carbon content. SRV tests carried out with the 51 at.% C coating showed a trend similar to that of ball-on-disc.

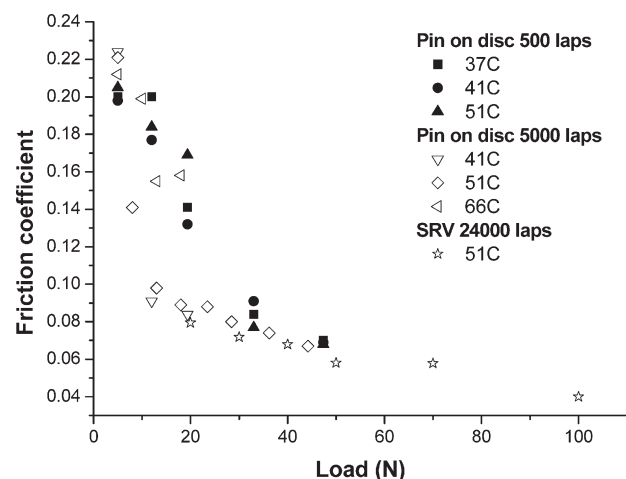


Figure 4. Friction coefficient of W–S–C coatings as a function of the load tested by pin-on-disc and SRV techniques. Tested at room temperature and RH 30%. The numbers indicate carbon content (e.g., 37 °C is the coating with 37 at.% of carbon).

The wear rate of the coatings was very small with values up to $1 \times 10^{-6} \text{ mm}^3 \cdot \text{N} \cdot \text{m}^{-1}$. The balls after the tests were covered by an adherent layer of the material transferred from the coating. When the adhered layer was removed, the optical observation revealed limited wear scar on the ball. Chemical maps of this layer showed an almost homogeneous distribution of W, S, C, and O. No vestiges of Fe originating from the steel were observed, which confirms that the ball wear rate was negligible. The wear tracks of the coatings with carbon contents up to 51 at.% observed by SEM were very smooth with no significant scratches even when the highest load was applied. The EDS analysis of the center of the wear tracks showed the same chemical composition as the unworn surface. However, at loads exceeding 20 N, the sides of the wear tracks were covered by adhered wear debris rich in tungsten and oxygen. The wear tracks produced by sliding with the high-carbon content coatings were covered by scratches with adhered isles of the wear debris on the worn surface.

Raman spectroscopy was proved to be an important tool in the wear track analysis. It was obvious that the intensity of the carbon peaks was lower inside the wear track than outside. Moreover, the ratio I_C/I_{WS_2} , calculated as the sum of the carbon peaks areas divided by the sum of the WS_2 peaks areas, decreased from the unworn surface toward the center of the wear track.^[12] This behavior was typical for all the coating compositions. The I_C/I_{WS_2} ratio obtained from the Raman spectra taken from the center of the wear tracks of a selected coating was lower in the cases of tests either with higher number of laps or with higher applied load. The Raman spectra of the wear debris accumulated at the borders of the wear track showed mainly graphitic carbon together with sharp peaks of the WS_2 phase.

The chemical analysis of the tribolayer was carried out by AES. Two wear tracks were selected, both produced with a load of 5 N but with a different number of laps, 500 and 5 000. To protect the tribolayer, the wear tracks were covered by a thin sputtered gold layer deposited immediately after the sliding test. The center of the wear track (an area less than $10 \mu\text{m}$ wide compared to the $120 \mu\text{m}$ width of the wear track) was bombarded by Ar ions and then an AES spectrum was obtained; the repetition of such a procedure gave rise to a detailed depth profile of the chemical composition in the center of the wear track. Despite the fact that the depth profile was only qualitative, since the sputtering yield of the tribolayer was unknown, its thickness could be estimated as less than 10 nm by comparing the sputtering yields of tungsten and a:C coatings. The results clearly illustrated an absence of carbon and oxygen in the first couple of layers suggesting an enrichment of W–S material in the top of the worn track (see Figure 5). The evolution of the S/W ratio in the top zone was probably only an artificial effect caused by the preferential re-sputtering of the lighter sulfur atoms during the erosion procedure.

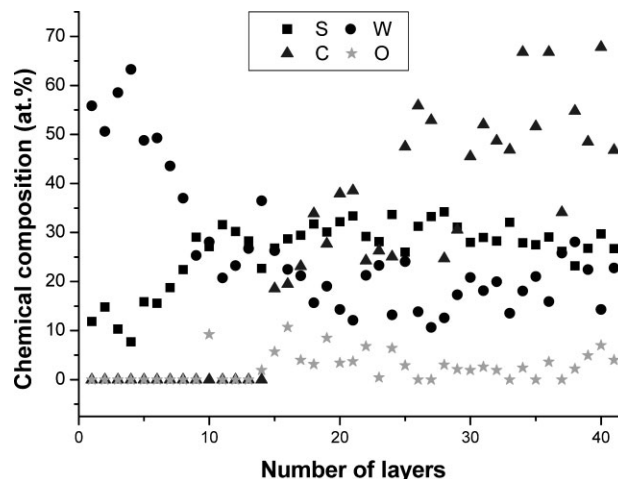


Figure 5. AES chemical composition depth profile in the center of the wear track of a W–S–C coating with 55 at.% C (ball-on-disc, load 5 N, 5 000 laps, room temperature, RH 30%). Each layer represents constant etching time.

Discussion

Structure

In our previous work on W–S–C system the coatings were deposited by reactive magnetron sputtering from a WS_2 target in Ar/CH_4 atmosphere, being the carbon content controlled by the flow of methane. Both XRD and XPS analysis proved the existence of tungsten carbide in some of the coatings.^[15] HRTEM observations showed WC nanograins with size lower than 10 nm,^[6] particularly in the case of the highest carbon content (68 at.%). It was possible to identify agglomeration of atoms of different atomic weight, being the lighter zones attributed to C-rich phases, whereas the darker ones to either tungsten carbide or tungsten disulfide.

In the present study, the coatings deposited by a non-reactive sputtering process show a fundamentally different microstructure. There is no evidence of tungsten carbides. In all cases, the gray parts in HRTEM images (see Figure 1) indicate the presence of carbon-based phases. Two types of microstructure could be defined in these W–S–C coatings co-sputtered in argon atmosphere from a carbon target with WS_2 pellets. The first one for the lowest carbon content films (up to ≈ 35 at.%) exhibits groups of parallel WS_2 platelets with the basal planes mainly perpendicular to the coating surface. The second one, for the films with higher carbon content (≈ 40 –68 at.%), shows clearly separated WS_2 platelets, which are randomly oriented and embedded into a (probably amorphous) carbon matrix.

Friction and Wear Mechanisms

Voevodin et al.^[3] developed the first pioneering concept of WC/DLC/ WS_2 coatings, where the hard WC and the self-

lubricant WS_2 grains were embedded into a carbon matrix. The matrix protected the WS_2 against the detrimental effect of the atmosphere, mainly the air humidity, and the tungsten carbide improved the hardness. The WC/DLC/ WS_2 coatings exhibited extremely low friction in vacuum and dry air (about 0.02) and moderate friction in humid air (about 0.2). When the atmosphere was cyclically changed from dry nitrogen to humid air during the sliding tests, the friction coefficient followed values typical of dry nitrogen and humid air, respectively. The wear track analysis showed that the tribolayer was formed exclusively of WS_2 material in dry nitrogen, whereas both WS_2 and graphite were observed in the tribolayer formed in humid air. It was proposed that the sliding process was dominated by the WS_2 in vacuum and the graphite in humid air.^[3] This adaptation of the wear mechanism to the environmental conditions was denominated as “chameleon” behavior.^[4]

We will show here that, in the W–S–C coatings presented in this study, the dominant feature influencing the friction and the wear properties is the formation of a tribolayer consisting exclusively of tungsten disulfide regardless on the sliding conditions (dry air, nitrogen, humid air, and elevated temperature).

The results of Raman analysis clearly indicate the existence of a WS_2 enriched top surface, whatever the sliding conditions are. The decrease of the I_C/I_{WS_2} ratio when analyzing toward the center of the wear track as well as when the applied load was increased reveals that the formation of the tribofilm rich in tungsten disulfide film on the worn surface is enhanced when the contact pressure is higher. Furthermore, the formation of the tribofilm is more evident when the number of laps increases, since in this situation the I_C/I_{WS_2} ratio is also decreasing. The evolution of the friction curves supports the Raman analyses, since the friction decreases with increasing load and number of laps. No visible changes in the characteristics of Raman carbon peaks, such as the position or the intensity ratio of D and G peaks, were observed when the spectra taken from the wear track (for all tested conditions) were compared to those of as-deposited material. The only significant difference was the lower intensity of the carbon peaks and the lower I_C/I_{WS_2} ratio for the analysis taken in the worn track.

The second indirect confirmation of the WS_2 predominance in the tribolayer is the frictional behavior of W–S–C coatings under different loads. The decrease of the friction with increasing load is typical of pure transition metal dichalcogenide coatings^[20–22] or metal doped TMD.^[23] It can be attributed to the coating material changes and tribolayer formation. However, the heating of the W–S–C surface as a consequence of the sliding would dry the air and, consequently, decrease the friction. Therefore, if the increase of the contact pressure causes an increase of the

temperature of the coating surface, the friction should diminish. The question is whether there is an increase of the coating surface temperature when contact load is increased. When the load increases, a higher rate of the frictional heating is spread over a larger contact area. Calculating the contact area from the static Hertzian contact pressure and considering the rate of frictional heating proportional to load, friction coefficient, and sliding speed, as shown in detail in previous work,^[12] it can be concluded that there is no increase of the frictional heating with increasing contact pressure in the studied range. It should be pointed out that if the sliding speed increases, the load and the contact area remains constant, a decrease of the friction should be observed due to the increase of the frictional heating. To prove this hypothesis, tests with loads of 5 and 15 N in the sliding speed range $0.01–0.9 \text{ m} \cdot \text{s}^{-1}$ were carried out and, indeed, an almost linear decrease of the friction coefficient from 0.19 to 0.13 (5 N) and from 0.14 to 0.07 (15 N) was observed (see Figure 6). Despite the high number of published papers dealing with the frictional analysis of non-hydrogenated DLC coatings, no persuasive evidence showing the decrease of the friction of DLC coatings with contact pressure could be found. Furthermore, identical sliding tests carried out in this work on pure carbon coatings deposited under identical conditions as for W–S–C system (i.e., sputtering from the carbon target without pellets) showed that the friction was higher when the load increased (Figure 6). Therefore, the decrease of the friction with the load observed in the sputtered W–S–C coatings cannot be attributed to the frictional heating and the sliding process should be related exclusively to the properties of the materials in contact.

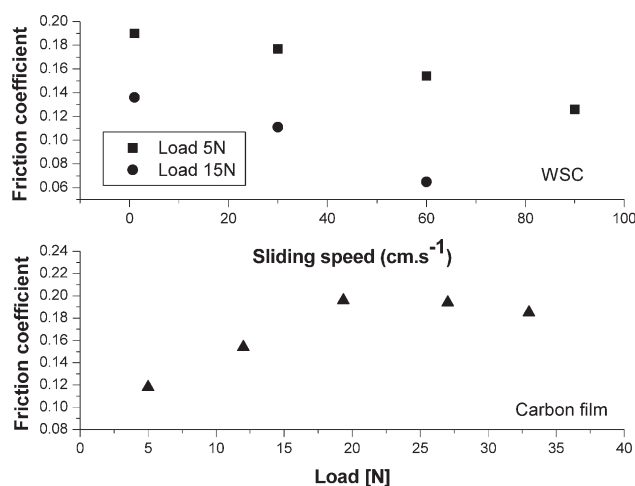


Figure 6. Influence of the sliding speed on the friction coefficient of a W–S–C coating with 51 at.% of C (upper) and evolution of the friction coefficient as a function of the applied load for a pure carbon film deposited without WS_2 pellets (lower).

Finally, the direct analysis of the tribolayer carried out by AES showed the striking evidence of the absence of carbon in the top layer of the wear track. It was clear that the tribolayer was formed exclusively by tungsten disulfide. Moreover, the extremely low-oxygen content in the tribolayer, very atypical in a sliding process, confirms that the friction of W–S–C coatings depends mainly on the properties of the WS₂ tribolayer formed on the worn surfaces. The improvement of the friction and the wear properties in different sliding environments cannot, thus, be attributed in our case to a “chameleon” behavior,^[3] i.e., changing of the dominant wear mechanisms. The role of the carbon matrix should be related to the increase of the overall hardness of the W–S–C coating and the protection of the tungsten disulfide against detrimental effects of the hostile atmosphere. When the carbon matrix is in contact with the counterpart, it is easily worn away, as confirmed by the wear debris which is rich in carbon on the sides of the wear tracks.^[24] On the other hand, the tungsten disulfide platelets form the low-friction tribolayer with, probably, the basal planes arranged parallel to the coating surface, similarly to that demonstrated for the Mo–Se–C system.^[25]

Conclusion

W–S–C coatings were deposited by rf magnetron sputtering from a carbon target with WS₂ pellets in order to achieve final carbon contents in the range 27–70 at.%. The coatings could be defined as nanostructured material with separated randomly oriented WS₂ platelets localized in the carbon matrix. The hardness of the coatings increased with the carbon content reaching a maximum close to 10 GPa for 40 at.%; further reduction of the WS₂ content caused a slight decrease of the hardness. The tribological analysis showed that the friction at 100 °C was even lower than measured at dry nitrogen. Due to high wear, 400 °C could be considered as limiting temperature for the W–S–C coatings; however, the coatings oxidation was still limited at this temperature. Immediate coating failure was observed when the temperature was further increased. Unlike the friction, which increased from ≈0.05 to ≈0.2, the wear rate was not affected by increase of air humidity from 5 to 40%. When contact pressure was increased, significant reduction of the friction was observed.

The friction and wear behavior at dry and humid air, elevated temperature and under different contact pressure was attributed to the formation of a thin tribolayer exclusively formed by WS₂, as confirmed by the analyses of the wear tracks with surface sensitive techniques.

Acknowledgements: This work was supported by the *Czech Science Foundation* through the project 106/07/P014, by the *Ministry of Education of the Czech Republic* (project MSM 6840770038), by *Fundação para a Ciência e a Tecnologia* through the project SFRH/BPD/34515/2006, and by FOREMOST project from EU.

Received: September 16, 2008; Revised: December 25, 2008; Accepted: January 7, 2009; DOI: 10.1002/ppap.200930005

Keywords: low friction; nanocomposite; self-lubrication; wear behavior; WS₂

- [1] J. M. Martin, C. Donnet, T. Le Mogne, *Phys. Rev. B* **1993**, *48*, 10583.
- [2] A. R. Lansdown, “*Molybdenum Disulphide Lubrication*”, Elsevier, 1999.
- [3] A. A. Voevodin, J. P. O’Neill, J. S. Zabinski, *Surf. Coat. Technol.* **1999**, *36*, 116.
- [4] A. A. Voevodin, J. S. Zabinski, *Thin Solid Films* **2000**, *370*, 223.
- [5] A. Nossa, A. Cavaleiro, *Surf. Coat. Technol.* **2001**, *984*, 142.
- [6] A. Nossa, A. Cavaleiro, N. J. M. Carvalho, B. J. Kooi, J. Th. M. De Hosson, *Thin Solid Films* **2005**, *484*, 389.
- [7] A. Nossa, A. Cavaleiro, *Surf. Coat. Technol.* **2003**, *552*, 163.
- [8] M. Evaristo, A. Nossa, A. Cavaleiro, *Surf. Coat. Technol.* **2005**, *200*, 1076.
- [9] A. Nossa, A. Cavaleiro, *Tribol. Lett.* **2007**, *28*, 59.
- [10] T. Polcar, M. Evaristo, A. Nossa, A. Cavaleiro, *Rev. Adv. Mater. Sci.* **2007**, *15*, 118.
- [11] M. Evaristo, T. Polcar, A. Cavaleiro, *Int. J. Mech. Mater. Des.* **2008**, *4*, 137.
- [12] T. Polcar, M. Evaristo, A. Cavaleiro, *Plasma Process. Polym.* **2007**, *4*, S541.
- [13] T. Polcar, M. Evaristo, A. Cavaleiro, *Vacuum* **2007**, *81*, 1439.
- [14] J. M. Antunes, A. Cavaleiro, L. F. Menezes, M. I. Simões, J. V. Fernandes, *Surf. Coat. Technol.* **2002**, *149*, 27.
- [15] A. Nossa, A. Cavaleiro, *J. Mater. Res.* **2008**, *19*, 2356.
- [16] G. Wise, N. Mattern, H. Herman, A. Teresiak, I. Bascher, W. Bruckner, H.-D. Bauer, H. Vinzelberg, G. Reiss, U. Kreissig, M. Mader, P. Markschlager, *Thin Solid Films* **1997**, *298*, 98.
- [17] S. Watanabe, J. Noshiro, S. Miyake, *Surf. Coat. Technol.* **2004**, *183*, 347.
- [18] S. R. Cohen, L. Rapport, E. A. Ponomarev, H. Cohen, T. Tsirlina, R. Tenne, C. Lévy-Clément, *Thin Solid Films* **1998**, *324*, 190.
- [19] T. Kubart, T. Polcar, L. Kopecky, R. Novak, D. Novakova, *Surf. Coat. Technol.* **2005**, *193*, 230.
- [20] B. J. Briscoe, A. C. Smith, *ASLE Trans.* **1982**, *25*, 349.
- [21] I. L. Singer, R. N. Bolster, J. Wegand, S. Fayeulle, B. C. Stupp, *Appl. Phys. Lett.* **1990**, *57*, 995.
- [22] A. K. Kohli, B. Prakash, *Tribol. Trans.* **2001**, *44*, 147.
- [23] J. A. Picas, A. Forn, M. Baile, E. Martin, *Surf. Eng.* **2006**, *22*, 314.
- [24] T. Polcar, N. M. G. Parreira, A. Cavaleiro, *Wear* **2008**, *265*, 319.
- [25] T. Polcar, M. Evaristo, R. Colaco, C. S. Sandu, A. Cavaleiro, *Acta Mater.* **2008**, *56*, 5101.

Nanoscale triboactivity: The response of Mo–Se–C coatings to sliding

T. Polcar^{a,b,*}, M. Evaristo^b, R. Colaço^c, C. Silviu Sandu^d, A. Cavaleiro^b

^a Department of Control Engineering, Faculty of Electrical Engineering, Czech Technical University in Prague, Technická 2, 16000 Prague 6, Czech Republic

^b SEG-CEMUC – Department of Mechanical Engineering, University of Coimbra, Rua Luís Reis Santos, P-3030 788 Coimbra, Portugal

^c Instituto Superior Tecnico, Technical University of Lisbon, Department of Materials Engineering, Av. Rovisco Pais, 1049-001 Lisbon, Portugal

^d EPFL – Ecole Polytechnique Federale de Lausanne, CH-1015 Lausanne, Switzerland

Received 15 May 2008; received in revised form 19 June 2008; accepted 27 June 2008

Available online 28 July 2008

Abstract

Mo–Se–C films were deposited by sputtering from a carbon target with pellets of MoSe₂. In addition to the standard evaluation of their chemical composition, structure, morphology, hardness and cohesion/adhesion, the core objective of this paper was to analyze the tribological behavior of these films, particularly in the high-load regime. The carbon content varied from 29 to 68 at.% which led to a progressive increase of the Se/Mo ratio and the hardness. The friction coefficient of Mo–Se–C coatings clearly decreased with load from ~0.15 to ~0.05. The excellent friction properties were attributed to the formation of a thin molybdenum diselenide film on the top of the wear track of the coating and on the counterpart surface, while the role of the carbon in the sliding process is only secondary by increasing the coating hardness and thus its wear resistance.

© 2008 Acta Materialia Inc. Published by Elsevier Ltd. All rights reserved.

Keywords: Sputtering; Wear; Coatings; Self-lubricant

1. Introduction

Transition metal dichalcogenides (TMDs) exhibit a unique sandwich lamellar structure with weak interlayer bonding. The TMDs family covers disulfides, diselenides and ditellurides of molybdenum, tungsten or niobium. The physical and tribological properties of TMDs, particularly MoS₂ and WS₂, have been intensively studied for more than five decades. Nowadays, they are used mainly as oil additives or low-friction thin films. Fullerene-like [1–3] and nanotube [4–6] TMDs structures have been considered as very promising materials for tribological applications; however, their industrial applicability is still very limited.

Magnetron sputtering is considered as one of the most effective methods for depositing thin TMDs films [7].

Nevertheless, pure sputtered TMDs exhibit low adhesion on standard substrate materials and high porosity. Since the friction and the wear resistance significantly increase in the presence of oxygen, and, particularly, air humidity, porosity is a significant drawback of such films, as it renders them vulnerable to environmental attack. Moreover, the hardness is usually very low, leading (together with the above-mentioned adhesion problems) to a very low load-bearing capacity. Pure sputtered TMDs are limited mainly to vacuum applications, where they could act even as “superlubricants” [8]. There are many different ways to improve the tribological behavior of these coatings. One of the most successful approaches is to deposit a composite material combining high strength with self-lubricant material, i.e. doping the TMDs films with other metals, such as Ti [9], Pb [10], Cr [11,12], Au [12], etc.

In the late 1990s, a new concept of coatings based on the alloying of TMDs with carbon started to attract the attention of several research groups. The original idea was to join the excellent frictional behavior of TMDs in vacuum and dry air with the tribological properties of DLC

* Corresponding author. Address: Department of Control Engineering, Faculty of Electrical Engineering, Czech Technical University in Prague, Technická 2, 16000 Prague 6, Czech Republic. Tel./fax: +420 224352439.
E-mail address: tomas.polcar@dem.uc.pt (T. Polcar).

coatings. Moreover, an increase in coating compactness in relation to TMDs and an improvement in the mechanical properties, particularly the hardness, was expected. Voevodin and Zabinski [13] prepared W–S–C coatings either by magnetron-assisted pulsed laser deposition (MSPLD, with a WS₂ target) or by laser ablation of a composite target made of graphite and WS₂ sectors. The friction coefficient in dry air was lower than that measured in humid air (0.02 and 0.15, respectively), and the so-called “chameleon behavior” observed during environmental cycling was considered the most interesting feature. The low friction in dry air increased in the presence of humid air but fell back down when the atmosphere was dried again.

Cavaleiro et al. [14,15] deposited W–S–C coatings by magnetron sputtering from a carbon target embedded with WS₂ pellets. The maximum coating hardness was around 10 GPa, i.e. about one order of magnitude higher than that of WS₂. The tribological behavior of the coatings was tested under different conditions, such as temperature, air humidity and load. The friction in humid air decreased significantly from 0.2 to 0.07 for loads varying in the range 5–48 N; the cyclic change of the air humidity showed the same “chameleon” features referred to above.

Both these W–S–C systems still show relatively high wear and friction coefficients in humid environments. To remedy this deficiency, it was decided to select another member of the TMDs family, molybdenum diselenide, which showed low friction that was almost independent of air humidity [16], and to study the mechanical and tribological properties of Mo–Se–C coatings prepared by non-reactive magnetron sputtering from a carbon target with MoSe₂ pellets.

2. Materials and methods

The coatings were deposited both on silicon wafers and on steel substrates (chromium steel, quenched and tempered with a final hardness of 62 HRC) polished to a final roughness, Ra ≤ 30 nm. A two-planar-cathode Edwards E306 machine with a 20 dm³ chamber was used for the deposition process. A rotating substrate holder placed 60 mm from the cathodes allowed the substrates to be placed over one or another cathode to deposit the titanium interlayer or the Mo–Se–C films, respectively. A Ti thin interlayer (~300 nm) was deposited in order to improve the adhesion of the coatings to the substrate. The coatings were deposited by radiofrequency magnetron sputtering in an argon atmosphere from a graphite (99.999% purity) target with pellets of MoSe₂. The pellets (99.8% pure) were positioned in the erosion zone of the 100 mm diameter graphite target. The dimensions of the pellets were 1.5 × 3 × 4 mm and their number varied between 16 and 72. The discharge pressure and the power density were 0.75 Pa and 8 W cm⁻², respectively. No bias was applied to the substrate holder during the deposition. The deposition time was 1 h.

The coating microstructure was studied by X-ray diffraction (XRD) in glancing mode (Co K_α radiation) and

by high-resolution transmission electron microscope (HR-TEM); the chemical composition was determined by electron probe microanalysis (EPMA), whereas the chemical bonding was investigated by Raman (Ar⁺ laser, 514.5 nm wavelength) and X-ray photoelectron spectroscopy (XPS; Mg K_α radiation). The hardness (H) and Young's modulus (E) of the coatings were evaluated by depth-sensing indentation (60 steps up to a maximum indentation load of 50 mN). To facilitate reading, the coatings are named according to their carbon content, which was calculated on the basis of at.% of C + Se + Mo = 100%.

Wear testing was performed using a pin-on-disc tribometer adapted to work in a controlled atmosphere; the sliding partners were 100Cr6 steel balls with a diameter of 6 mm. The air humidity (RH), measured by an accurate hygrometer, was 35 ± 2%. The number of laps is stated in the text. The morphology of the coating surface, the ball scars, the wear tracks and the wear debris were examined by scanning electron microscopy (SEM) and Raman spectroscopy; chemical analysis of the wear tracks and the wear debris was performed by energy-dispersive X-ray analysis (EDS). The chemical depth profiles in the wear track were obtained by Auger electron spectroscopy (AES). The profiles of the wear tracks were measured by a mechanical profilometer. The wear rate of the coating was calculated as the worn material volume per sliding distance and normal load. The average value of three profiles measured on the same wear track was used to calculate the coating wear rate.

Topographic and tribological characterization of the surfaces was performed by atomic force microscopy (AFM) in contact and lateral force mode (LFM: trace–retrace signal). The tests were carried out in ambient conditions with commercial etched silicon probes ($k = 0.9 \text{ N m}^{-1}$, tip radius ≈ 15 nm) with a normal load of 250 nN being the friction an average signal of, at least, four 2 × 2 μm² images.

3. Results

3.1. Fundamental characterization of Mo–Se–C coatings

With increasing number of pellets, the carbon content in the coatings decreased linearly, while the deposition rate showed an inverse trend from 0.6 to 1.1 nm s⁻¹ due to the higher sputtering rate of MoSe₂ compared to carbon. The coating thickness also increased, from 2.2 (68 at.% C) to 4.0 μm (29 at.% C). The Se/Mo ratio was very high, 2.0 for 68 at.% C, and slowly decreased to 1.7 with the decrease in the carbon content (see Fig. 1). The oxygen content decreased from 5 to 2 at.% for lower numbers of porous pellets, which were responsible for the contamination of the residual atmosphere in the chamber. Furthermore, as will be shown later, the coatings became denser for higher carbon contents, with a lower number of pores and a lower superficial area where oxygen can be adsorbed. Nevertheless, considering the deposition method and the

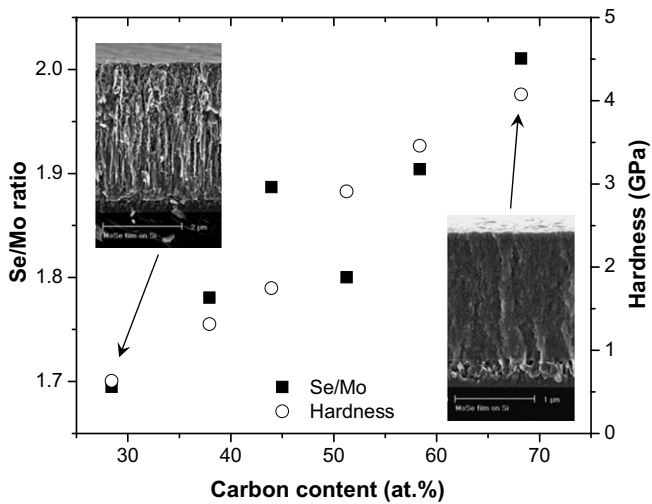


Fig. 1. Carbon content and deposition rate as a function of the number of MoSe_2 pellets embedded into the carbon target. The insets show SEM micrographs of the coatings cross-sections.

type of deposited material, the oxygen content could be regarded as low.

The XRD diffractograms of Mo–Se–C coatings were almost identical to those of the W–S–C system discussed in

detail elsewhere [17]. The well-defined peak at $\sim 37^\circ$ corresponding to the (100) orientation was followed by a peak at $\sim 43^\circ$ with a long tail representing a turbostratic stacking, i.e. the presence of (10L) orientations of MoSe_2 phase. The peak at $\sim 67^\circ$ was attributed to the (110) orientation. A loss of intensity and a broadening of the main peak could be detected with increasing carbon content. Details of the XRD analysis and diffractograms of the studied Mo–Se–C coatings are described in Ref. [18]. The hardness of the coatings linearly increased with carbon content from 0.6 to 4.1 GPa. It should be pointed out that the hardness of pure TMDs deposited by standard magnetron sputtering is in general lower than 1 GPa due to the very porous columnar structure [17]; in other words, alloying with carbon increased the hardness significantly. The hardness of pure carbon film deposited under identical conditions (i.e. from the same carbon target without MoSe_2 pellets) was 6.8 GPa.

TEM micrographs showed that the film with the lowest carbon content exhibited a columnar structure typical for pure TMDs [7], while the increase in carbon content led to homogeneous, amorphous-like morphology (Fig. 2). The film porosity decreased with increasing carbon content, which could promote the increase in the hardness referred to above. The basal planes of the MoSe_2 phase form platelets which, in contrast images, have the appearance of wires

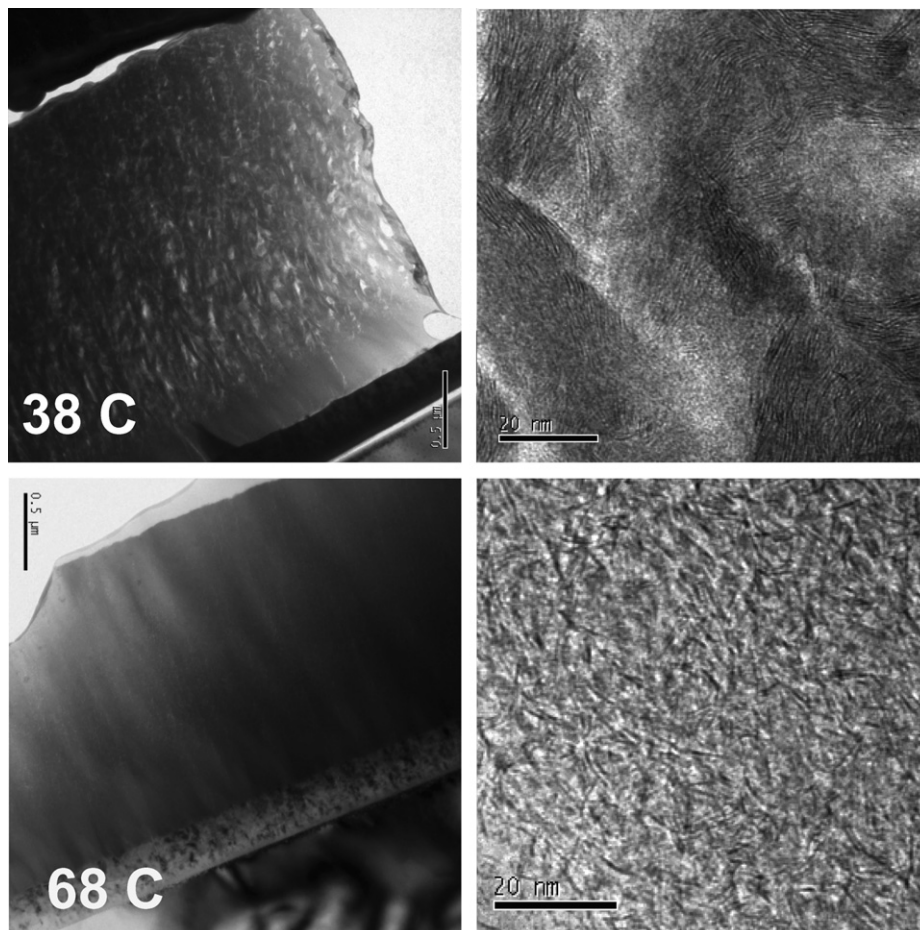


Fig. 2. TEM overall (left) and detailed images of Mo–Se–C coatings with 38 and 68 at.% carbon content.

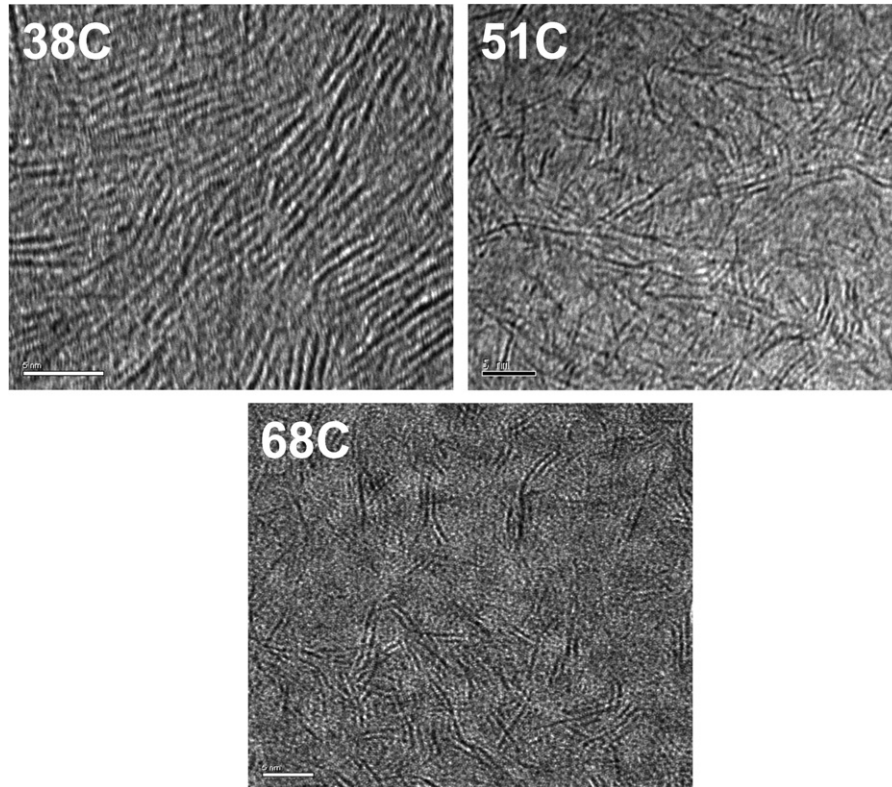


Fig. 3. HR-TEM images of as-deposited Mo–Se–C coatings with different carbon content.

(Figs. 2 and 3). The increase of carbon amount in the layer limited the development of the ordering of the basal MoSe₂ planes, decreasing the platelet dimensions, as can be concluded by the shortening of these apparent wires. Fig. 3a shows long, curved chains consisting of tens of parallel MoSe₂ basal planes, in contrast to Fig. 3c, where the platelets are clearly separated with a length of ~5 nm.

The XPS and Raman analyses of Mo–Se–C coatings have been published recently [18]. The XPS clearly showed the absence of Mo–C bonds. This result is in accordance with the hardness evolution, since the existence of hard carbide phases would increase the hardness, as documented in the similar case for W–S–C coatings [17]. The Raman spectra could be divided into three regions: (i) 200–700 cm⁻¹ with a group of peaks belonging to molybdenum diselenide phases; (ii) 700–900 cm⁻¹ corresponding to molybdenum oxide peaks; and (iii) 1100–1800 cm⁻¹ with peaks representing the D and G bands of carbon. The molybdenum oxide peaks identified at ~860 and ~950 cm⁻¹ were visible particularly for low carbon content, where the oxygen content was higher.

3.2. Friction and wear rate as a function of load

Figs. 4 and 5 show that the average friction coefficient and wear rate decreased as a function of the applied load. However, the coatings with carbon contents in the extremes of the studied range, i.e. 29 and 68 at.% C, were partially peeled off after the test and their friction was not evaluated. The wear

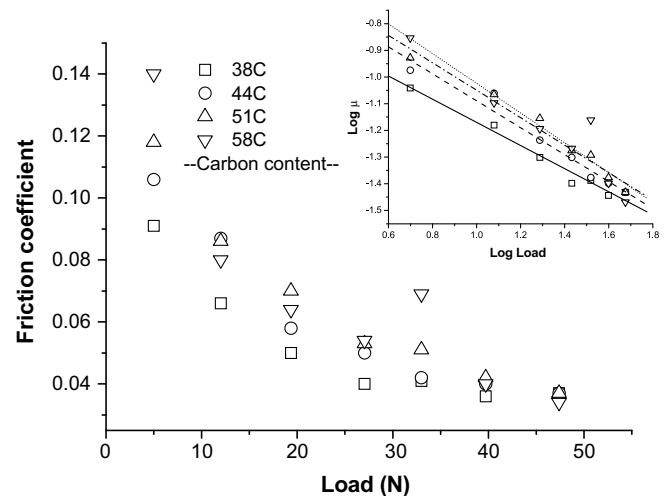


Fig. 4. Evolution of the friction coefficient of Mo–Se–C coatings vs. load (500 laps). Log (FC) vs. Log (Load) with the least-square fits is shown in the inset.

rate of the coatings with 58 at.% C was not calculated due to the presence of small cracks in the wear tracks. Therefore only three coatings are shown in Fig. 5.

The sliding process of the thin film could be usually divided into two main stages: running-in and steady-state sliding. As shown in Fig. 6, the running-in process was, for loads up to 20 N, longer than the test duration, since the friction coefficient monotonically decreased during

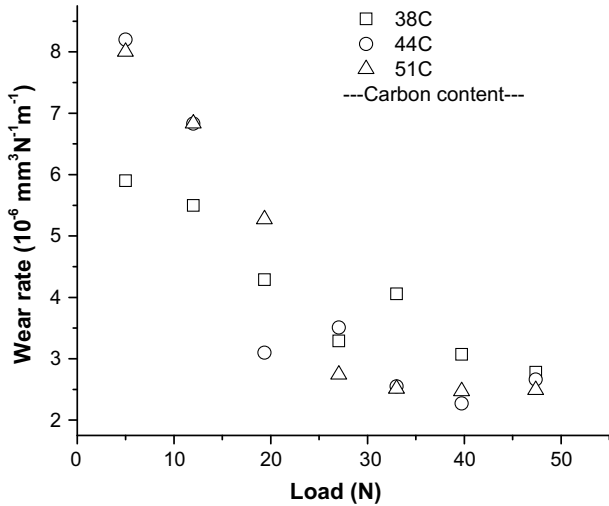


Fig. 5. Wear rate of Mo–Se–C coatings as a function of the load (500 laps).

the entire test. For higher loads, when the contact pressure was higher, the friction increased to a maximum value at about 30–50 laps, and then fell. The friction curves quickly reached a steady-state level and were less noisy than those of lower loads.

The coatings with the most promising friction and wear properties, i.e. 38, 44 and 51 at.% C, were submitted to tests with a higher number of cycles and a load of only 5 N. All three coatings showed almost identical behavior – a significant drop in the average friction and the wear rate down to very low levels (0.05 and $<10^{-6} \text{ mm}^3 \text{ N}^{-1} \text{ m}^{-1}$, respectively), which remained almost constant when the number of laps was further increased (Fig. 7). The running-in was a very long process; the friction very slowly decreased to the steady-state value, which was reached after $\sim 20,000$ laps. A final set of experiments was carried out with an increasing number of laps (500, 2000 and 20,000) and

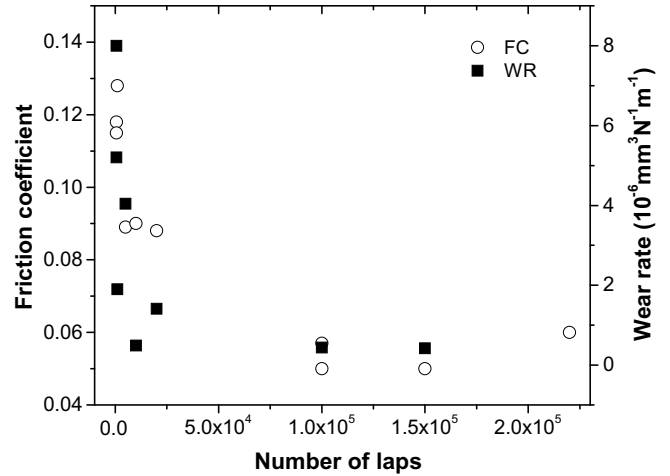


Fig. 7. Friction coefficients and wear rates of 44 at.% C coating, long-term tests (load 5N).

two loads (5 and 33 N). For these experiments, a new set of coatings was deposited with identical parameters and a number of pellets selected in order to reach a carbon content of 51 at.% C (i.e. the optimum carbon content from the tribological point of view). As expected, the friction and wear rate were considerably lower when the 33 N load was applied. The running-in was very short, about 50 laps, and no long-term decrease in the friction was observed. The wear rate was independent of the number of cycles as well (about $6.0 \times 10^{-7} \text{ mm}^3 \text{ N}^{-1} \text{ m}^{-1}$). The wear tracks were protected after the tests with a thin sputtered gold film in such way that only one-half of the surface of the samples (and of the wear tracks) was covered.

3.3. Analysis of the wear tracks

Optical microscopy and SEM were used to analyze the wear tracks of the coatings with carbon content in the

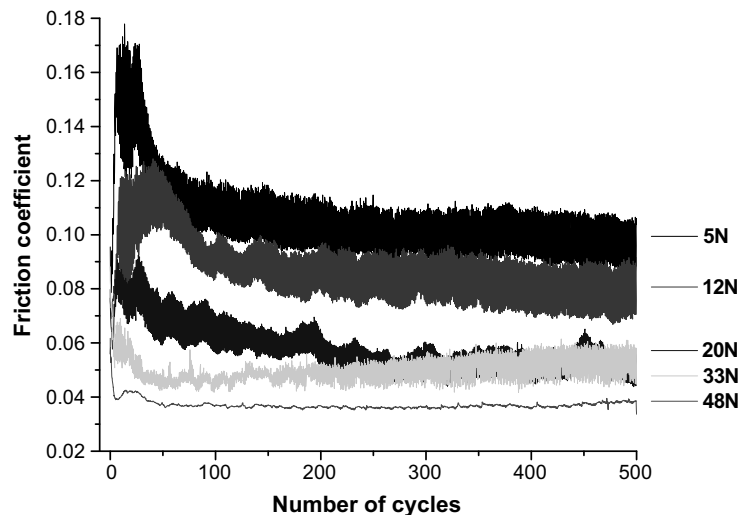


Fig. 6. Friction curves of Mo–Se–C coatings vs. load, coating with 44 at.% C.

range 38–51 at.%. As a general observation, the wear tracks were smooth, with only shallow scratches parallel to the direction of the ball movement. Lateral cracks or any distinguishable adhered layer were not observed. AFM observation of the worn tracks produced with the 33 N load revealed interesting features that could not be so clearly observed by SEM analysis. Sharp grooves with clean-cut edges were exhibited in the wear track after 500 laps of sliding, which demonstrated that the wear mechanism was essentially cutting in two-body abrasion conditions (Fig. 8a and b). Further increase of laps (5000 and 20,000) led to the polishing of the wear track with flat parallel grooves typical of abrasive wear (Fig. 8c and d). The average roughness (Ra) in the worn regions perpendicular to the relative ball movement was between 61 and 75 nm, a value approximately one order of magnitude higher than in the unworn surface of the film, which is similar to the one measured in parallel direction (about 5 nm). The existence of “negative” grooves parallel to the AFM measurement direction (see Fig. 8c and d) and, thus, perpendicular to the sliding direction, revealed the transfer of the material

from the wear track to the AFM tip when the test lasts for a high number of laps.

The counterparts were covered by an adhered layer; the ball coverage increased with the load and the number of cycles. The analyses of the ball surface after short tests (100 laps) did not reveal any traces of adhered material for loads lower than 20 N, while the contact spot on the ball was clearly covered for higher loads. All the counterparts were covered from 500 laps on, whatever the applied load was. EDS analysis showed in the transferred layer only elements related to the coating material (i.e. Mo, Se, C and O). The wear of the ball could not be detected even for the highest contact pressures.

Raman spectroscopy was often used for the analysis of the wear track and the wear debris in similar coating systems [14,19]. In previous work of the authors on the W–S–C system it was shown that the ratio of the integral intensities of the peaks related to WS_2 vs. those of carbon increased with load, when the analysis was performed in the centre of the wear track. Moreover, the increase in this ratio as a function of the contact pressure was confirmed

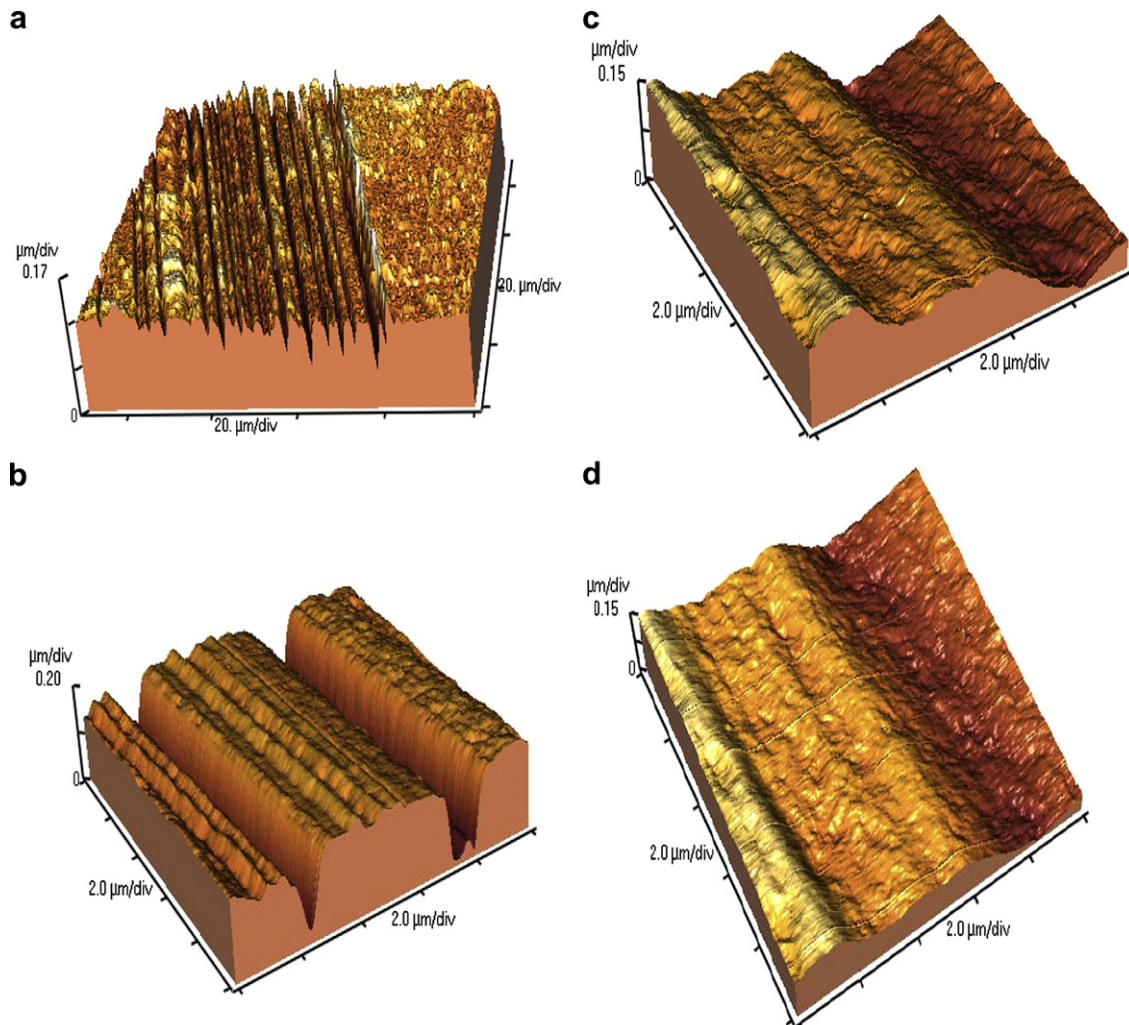


Fig. 8. The wear track analyzed by AFM (33 N, 51 at.% C), (a) – (b) 500 laps, (c) 5000 laps and (d) 20,000 laps.

since it was higher in the centre of the wear track than at the border [14]. The Mo–Se–C coatings exhibited similar behavior. The $I_{\text{MoSe}}/I_{\text{C}}$ ratio taken from the Raman spectra measured in the centre of the wear tracks, where I_{MoSe} is the area of MoSe₂ peak positioned at $\sim 240 \text{ cm}^{-1}$ and I_{C} is the sum of D and G carbon peaks areas, increased with either the applied load or the number of laps, as documented in Fig. 9. Since the optical mean free path for a selected laser wavelength should not exceed 100 nm [20], it can be concluded that there was an enrichment of MoSe₂ in the surface of the wear track. The molybdenum oxide peaks clearly visible on the as-deposited surface disappeared with increasing number of laps.

The free wear debris was agglomerated on the side of the wear tracks and ball scars. It was identified by Raman spectroscopy to be a mixture of graphitic carbon and MoSe₂ phase.

The wear tracks of the coatings, protected by a thin gold film sputtered immediately after the pin-on-disc test, were analyzed by AES. A selected spot in the center of the wear track was bombarded by Ar ion beam and an AES spectrum was obtained; then, this procedure was repeated until a steady-state value of the Auger intensity of the elements under analysis was reached. Therefore, a detailed depth profile of the chemical composition in the centre of the wear track could be achieved. Since the sputtering yield was not exactly known, the depth scale could not be calculated. Nevertheless, the obtained depth profiles closely characterize the main trends in the chemical composition variation. Fig. 10 shows the depth profile obtained (from the point where Au signal was not anymore detected) in the 51 at.% C coating after having been tested with 33 N and 500 laps; linear factors taken from EPMA measurements for bulk coating were used to calculate the chemical composition. Two main features emerge: (i) the increase of the carbon content from the surface down to approximately the seventh layer, and (ii) the low oxygen content of this surface layer. The depth profile measured on the wear track of the same sample with a higher number of laps

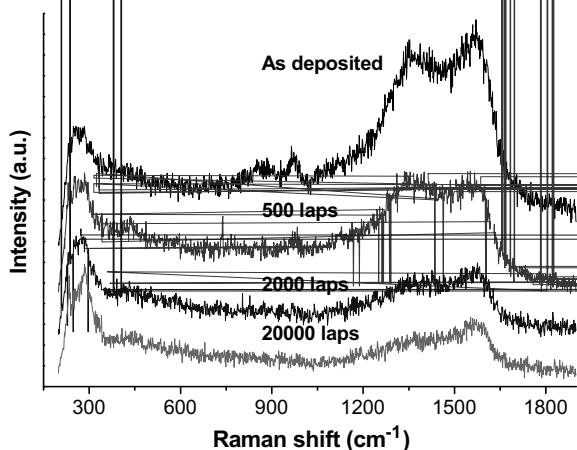


Fig. 9. Raman spectra taken in the centre of the wear track after different number of laps, load 33 N, coating 51 at.% C.

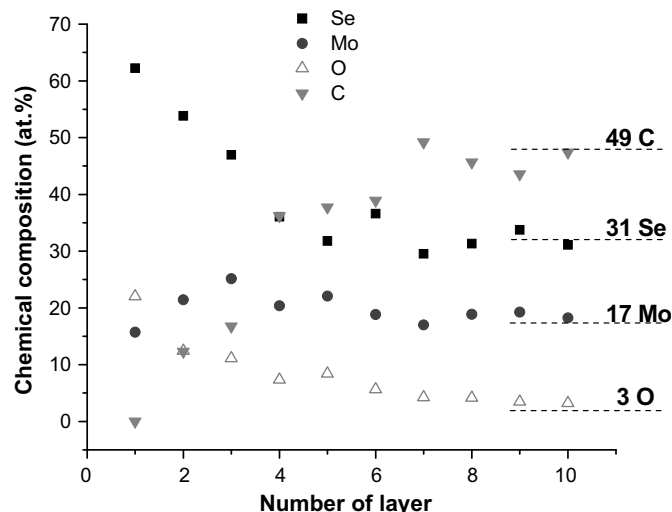


Fig. 10. Chemical composition depth profile of the wear track obtained by AES, coating with 51 at.% C, load 33 N, 500 laps. The chemical composition on the right corresponds to the as-deposited coating as measured by EPMA.

(51 at.% C coating, 33 N and 20,000 laps) exhibited a similar behavior (Fig. 11). However, carbon was not observed in the first five layers, and its content then increased very slowly for higher depths. Again, the oxygen content was low. Since the Ar⁺ bombardment time was constant, it is obvious that the tribolayer was much thicker when the number of laps increased.

Aiming to confirm whether the decrease in the friction coefficient was due to the formation of a tribolayer during the running-in period, two sets of lateral force measurements (LFMs) were taken in the wear tracks of the coatings which underwent AES testing (i.e. 51 at.% C, load 33 N): (i) one at the wear track covered by the thin gold

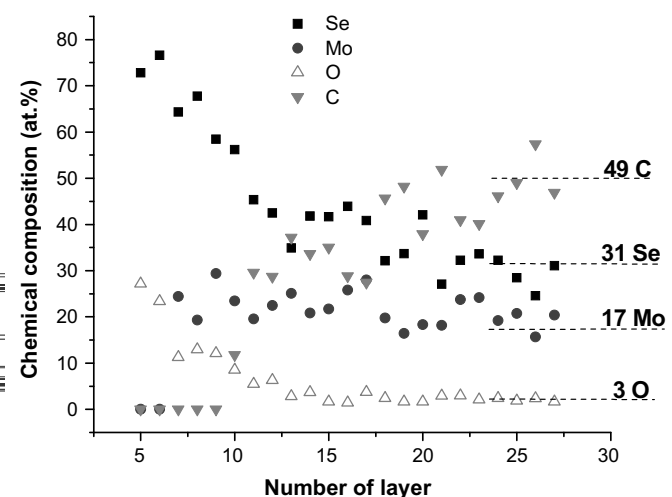


Fig. 11. Chemical composition depth profile of the wear track obtained by AES, coating with 51 at.% C, load 33 N, 20,000 laps. The chemical composition on the right corresponds to the as-deposited coating as measured by EPMA.

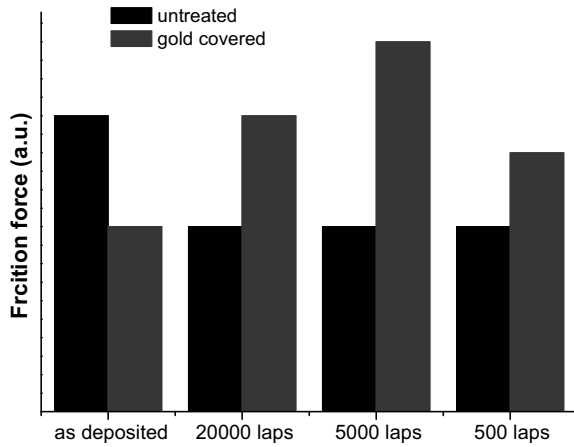


Fig. 12. Friction force measured on the as-deposited coating and the wear tracks before and after covering with a thin gold layer. Note that the friction force axis is in arbitrary units.

layer; and (ii) the second at the uncoated wear track. Since the morphology of the original and gold-covered wear tracks is identical, the torsional component of the

cantilever due to topographical features of the wear track surface is expected to be identical as well. It was observed that in the worn regions the friction force between the tip and the sample was approximately 30% smaller than in the unworn region, in spite of the much higher roughness in the wear track (Fig. 12). The analysis of the samples covered by the gold exhibited exactly the opposite trend, with friction forces higher in the wear tracks; therefore, it can be concluded that the friction in the wear track is significantly lower than at the as-deposited coating surface.

To confirm definitely the existence of a thin MoSe₂ tribolayer, HR-TEM of the gold-covered wear track (51 at.% C coating, load 33 N, 20,000 laps) was performed. The gold film protected the wear track from environmental attack and contamination and facilitated the TEM sample preparation by focused ion beam (FIB). Since the top part of the wear track was very probably inhomogeneous, 16 separate locations in the wear track were selected. The MoSe₂ tribolayer with basal planes parallel to the surface was clearly identified in 12 locations, as demonstrated in Fig. 13.

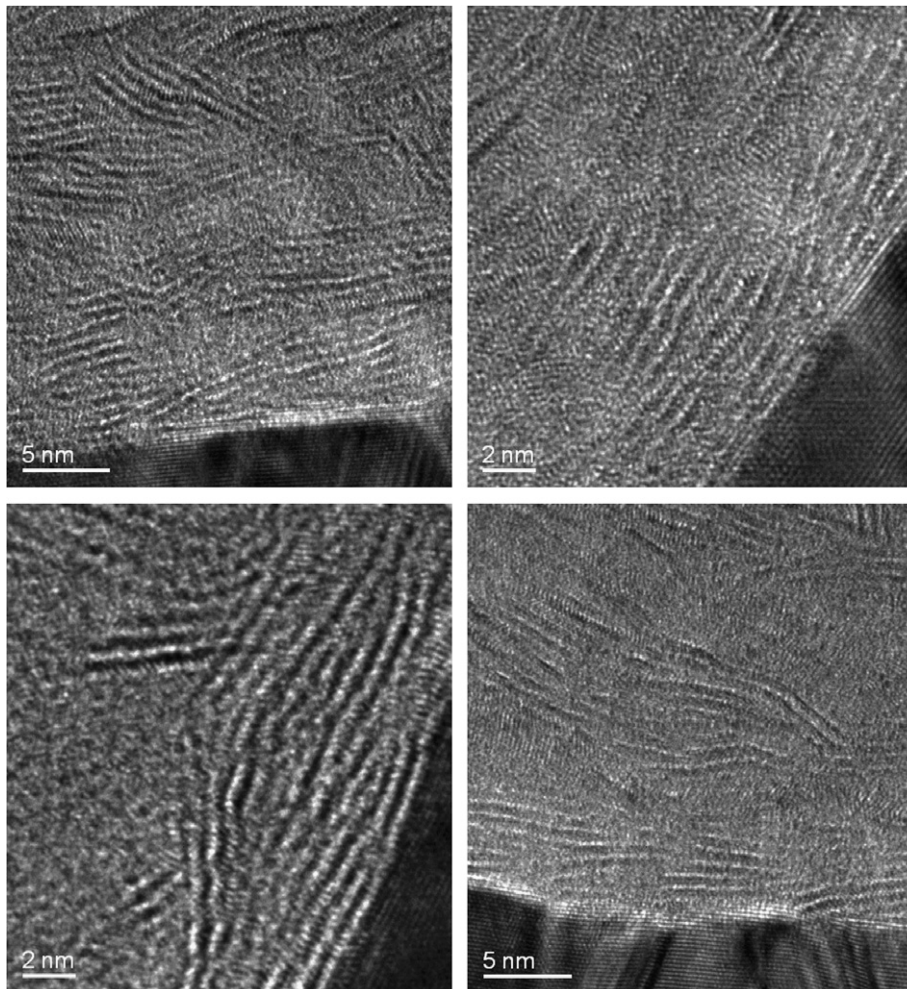


Fig. 13. Selected HR-TEM images of the wear track cross-sections prepared by FIB (33 N, 20,000 laps, 51 at.% C). The dark part of images corresponds to the sputtered gold covering the wear track.

4. Discussion

TMDs exhibit low friction thanks to their anisotropic layered structure, where the adjacent lamellae, with strong covalent bonding, interact through relatively weak van der Waals forces [7,21]. This structure allows the “easy” inter- and intracrystalline slipping, when the basal planes are oriented parallel to the surface in contact. When the basal planes are not oriented in such a direction (typically for magnetron sputtering deposited coatings), a reorientation, through the energy input induced by the mechanical action during sliding, is required to achieve the low friction. The thickness of such reoriented tribolayer is estimated to be lower than 5 nm [7,22]. In general, the presence of air humidity significantly increases the friction of all TMDs systems. On the contrary, non-hydrogenated DLC coatings exhibit low friction when sliding in humid air. The absence of the water vapour passivating the coating surface causes the interaction of the carbon atoms with the counterpart resulting in high friction and wear. Therefore, non-hydrogenated DLC coatings are not efficient as friction-reducing films at dry air or vacuum [23].

Zabinski et al. [13,24] have published several papers dealing with the tribological properties of the WS₂/DLC/WC nanocomposite coatings prepared either by MSPLD (with a WS₂ target) or by laser ablation of a composite target made of graphite and WS₂ sectors. The friction coefficient in dry air was significantly lower than the one measured in humid air (0.02 and 0.15, respectively). The low friction in dry air increased in the presence of humid air and fell when the atmosphere was dried again. They concluded that the friction and wear behaviors were driven by a WS₂-rich tribolayer at dry air, while the influence of a graphitic carbon was dominant in humid air.

The present study shows fundamentally different results. If the friction force measured with the AFM tip is the result of two additive terms, one due to the chemical interaction between surfaces and the other due to the mechanical deformation and interlocking [25], it can be assumed that it increases with increasing surface roughness [26]. Therefore, the results shown above could be interpreted as a strong indication of the existence of a lower friction layer in the surface of the wear track compared to the as-deposited coating. Since the mechanical interlocking term is much higher in the worn region, due to its higher roughness, the decrease in the measured friction force could be only attributed to a significant decrease in the chemical interaction component. When the coating is covered with gold, the adhesion component is virtually the same and the mechanical interlocking in the wear tracks enhanced by the higher roughness causes a significant increase in the friction force (compare the “gold-covered” results for as-deposited or wear-tested surfaces in Fig. 12). Thus, the AFM measurements indicated the existence of low friction in the wear tracks formed by the sliding process.

The AES depth profiles revealed the existence of a thin tribolayer in the top of the wear track rich in Mo and Se

elements with the carbon content slowly increasing with depth. The absence of the carbon in the contact layer was as well supported by Raman spectroscopy. Finally, the direct observation of the wear track by TEM revealed the existence of this thin tribolayer (up to 5 nm) exclusively formed by (002) oriented MoSe₂. As referred to above, the existence of such tribolayer has been shown in the case of pure TMDs.

The most surprising feature lay beneath the tribolayer. As described above, the MoSe₂ platelet orientation in the as-sputtered film is random. However, TEM images clearly show that the platelet orientation tended to be parallel or semi-parallel even in a significant depth of the coating (Fig. 13). If the zone close to the surface layer of the coating in the wear track is divided into three depth parts, i.e. (i) 0–5 nm, (ii) 5–10 nm, (iii) 10–20 nm, the orientation of the MoSe₂ platelets with respect to the coating surface can be calculated in each of them by analyzing all the 12 locations with evident formation of the tribolayer (basal planes parallel to the coating surface – see Fig. 13). Table 1 shows the average angle of the MoSe₂ platelet with (002) orientation expressed by the percentage of the number of specifically oriented platelets vs. the total number of platelets in each zone; the total number of the observed platelets in the 12 micrographs was 173, 141 and 121 for zones 0–5, 5–10 and 10–20 nm, respectively. Considering the accuracy in calculating the angle from the TEM micrographs, the case of platelets penetrating two zones and counting the total number of platelets, the estimated error of data set shown in Table 1 is about 10%. Comparing these data with the random platelet orientation calculated from the as-deposited coating shown in Fig. 3, it can be clearly observed that the orientation of the platelets is not limited to the very outermost surface of the wear track, but progressively decreases with depth beneath the worn coating surface.

In conclusion, it is suggested that the dominant factor influencing the sliding properties of Mo–Se–C coatings, regardless of the air humidity, is the formation of a thin MoSe₂ tribolayer both on the coating and on the counterpart surface. Carbon is gradually set aside from the wear track and has probably only a limited influence in the sliding process, contributing exclusively to improving the bulk

Table 1

The platelet orientation calculated from 12 selected HR-TEM images of the cross-section of the coating wear track

Depth	Platelets with angle higher than 20° (%)	Platelets with angle higher than 45° (%)	Platelets with angle higher than 60° (%)
0–5 nm	5	0	0
5–10 nm	17	8	2
10–20 nm	50	26	8
As-deposited	68	50	33

The total number of considered platelets in all three zones (i.e. 0–20 nm) was 227. The last line corresponds to the random orientation of the as-deposited coating.

characteristics of the Mo–Se–C films, such as density, hardness and, consequently, load-bearing capacity. Moreover, the depth orientation of MoSe₂ platelets under pressure should have a positive effect on the frictional properties as well. When a thin tribolayer (exclusively MoSe₂) is worn out, uncovered subsurface is “prepared” (i.e. MoSe₂ oriented predominantly with basal planes parallel to the coating surface) and the sliding process continues without any significant increase in the friction. The mechanism of platelet reorientation is not clear and will be further studied; however, it is enhanced when the contact pressure and/or the number of laps increased. In other words, if the load is low, a higher number of laps is needed to reach the steady-state wear regime.

The decrease in the friction coefficient with the applied load – a typical feature of pure TMDs coatings – deviates from the classical Amonton’s law, which can be well described using the formula approximating the shear stress of solids at high pressures and the Hertzian model for contact pressure [27–30]:

$$\mu = \tau_0 \cdot \pi \cdot \left(\frac{3R}{4E} \right)^{\frac{2}{3}} L^{-\frac{1}{3}} + \alpha, \quad (1)$$

where R is the radius of the ball, L is the normal load, τ_0 is the interfacial shear strength, α is a material constant representing the adhesive forces at zero load, and E is the composite modulus of the couple. A least-square fit was applied to the data set presented in Fig. 4 using Eq. (1), in order to obtain τ_0 and α parameters. The results were unrealistic for all the carbon contents, giving rise to negative values for α (about -0.03) and extremely high τ_0 (about 80–90 GPa) when compared to those achieved for sputtered MoS₂ [27,28] or WS₂ [31,32] films. In other words, the friction coefficient decreased with load more rapidly than in the case of pure TMDs and, thus, the contact pressure calculated by the Hertzian model is not valid. In fact, the decrease in the friction coefficient with increasing applied load can be expressed by a power law fit $\mu \approx L^b$, with $b = 0.43, 0.50, 0.51$ and 0.53 for carbon contents of 38, 44, 51 and 58 at.%, respectively. Mo–Se–C coatings thus follow the most widely accepted correction of the classical Amonton’s law: a power law between the frictional and normal forces [33]. It should be pointed out that the power law fit referred to above was calculated using the average friction coefficient taken from the first 500 laps. It was demonstrated that Mo–Se–C coatings exhibited unusually long running-in with steady-state process reached after more than 20,000 laps when a low (i.e. 5 N) load was used. However, the average friction coefficient in the range 20,000–50,000 laps for loads of 5, 33 and 48 N showed the same trend: power law between frictional and normal forces (coating with 51 at.% C).

Finally, the long-term tests revealed extremely high wear resistance of Mo–Se–C coatings with medium carbon content. The wear in the steady-state regime was extremely low with approximately 1000 laps required to

remove 1 nm of coating (in humid air), which makes Mo–Se–C coatings appropriate candidates for various industrial applications.

5. Conclusions

Mo–Se–C coatings deposited by radiofrequency magnetron sputtering from a carbon target with MoSe₂ pellets were tested by pin-on-disc under increasing load. The carbon content varied from 29 to 68 at.% as a function of the number of pellets, with a Se/Mo ratio close to MoSe₂ stoichiometry. Increasing carbon content led to a linear increase in the hardness and the coating density.

The friction coefficient and the wear rate decreased with the applied load. Long-term tests with constant load exhibited a sharp reduction in the wear rate within the first couple of thousand cycles to a constant level. The depth profile carried out by AES in the wear track revealed a deficiency of carbon in the tribolayer, particularly in the top layers, which was confirmed by Raman spectroscopy. AFM/LFM measurements indicated a lower friction in the wear track compared to the as-deposited surface. Finally, the existence of the tribolayer exclusively formed by MoSe₂ phase, with basal planes oriented parallel to the coating surface, was proven by TEM. Moreover, the randomly oriented MoSe₂ platelets in the as-deposited coatings tended to reorientate under contact pressure.

Acknowledgements

This work was supported by the Czech Science Foundation through the Project 106/07/P014, by the Ministry of Education of the Czech Republic (Project MSM 6840770038) and by the Fundação para a Ciência e a Tecnologia through the Project SFRH/BPD/34515/2006. M. Stueber from FKZ centre is also acknowledged for access to Raman analysis.

References

- [1] Rapoport L, Bilik Y, Feldman Y, Homyonfer M, Cohen SR, Tenne R. *Nature* 1997;387:791.
- [2] Chhowalla M, Amaratunga GAJ. *Nature* 2000;407:164–7.
- [3] Golan Y, Drummond C, Homyonfer M, Feldman Y, Tenne R, Israelachvili J. *Adv Mater* 1999;11:934.
- [4] Remskar M, Mrzel A, Skraba Z, Jesih A, Ceh M, Demsar J, et al. *Science* 2001;292:479.
- [5] Remskar M. *Adv Mater* 2004;16:149719.
- [6] Akbulut M, Belman N, Golan Y, Israelachvili J. *Adv Mater* 2006;18:2589.
- [7] Lansdown AR. *Molybdenum disulphide lubrication*. Amsterdam: Elsevier; 1999.
- [8] Martin JM, Donnet C, Le Mogne T. *Phys Rev B* 1993;48:10583.
- [9] Teer DG. *Wear* 2001;251:1068.
- [10] Wahl KJ, Seitzman LE, Bolster RN, Singer IL. *Surf Coat Technol* 1995;73:152.
- [11] Su YL, Kao WH. *Tribol Int* 2003;36:11.
- [12] Simmonds MC, Savan A, Pfluger E, Van Swygenhoven H. *Surf Coat Technol* 2000;126:15.
- [13] Voevodin AA, Zabinski JS. *Thin Solid Films* 2000;370:223.

- [14] Polcar T, Evaristo M, Cavaleiro A. *Plasma processes & polymers* 2007;4:S541.
- [15] Polcar T, Evaristo M, Cavaleiro A. *Vacuum* 2007;81:1439.
- [16] Kubart T, Polcar T, Kopecký L, Novák R, Nováková D. *Surf Coat Technol* 2005;193:230.
- [17] Nossa A, Cavaleiro A. *J Mater Res* 2004;19:2356.
- [18] Polcar T, Evaristo M, Cavaleiro A. *Surf Coat Technol* 2008;202:2418.
- [19] Wu J-H, Rigney DA, Falk ML, Sanders JH, Voevodin AA, Zabinski JS. *Surf Coat Technol* 2004;188–189:605.
- [20] Scharf TW, Singer IL. *Thin Solid Films* 2003;440:138–44.
- [21] Prasad S, Zabinski J. *Nature* 1997;387:761.
- [22] Takahashi N, Kashiwaya S. *Wear* 1997;206:8.
- [23] Jinang J, Zhang S, Arnell RD. *Surf Coat Technol* 2003;167:221.
- [24] Voevodin AA, O'Neil JP, Zabinski JS. *Surf Coat Technol* 1999;116–119:36.
- [25] Kopalinsky EM, Oxley PLB. *Wear* 1995;190:145–54.
- [26] Sung I-H, Lee H-S, Kim D-E. *Wear* 2003;254:1019–31.
- [27] Briscoe BJ, Smith AC. *ASLE Trans* 1982;25:349.
- [28] Singer IL, Bolster RN, Wegand J, Fayeulle S, Stupp BC. *Appl Phys Lett* 1990;57:995.
- [29] Towle LD. *J Appl Phys* 1971;42:2368.
- [30] Grosseau-Poussard JL, Moine P, Brendle M. *Thin Solid Films* 1997;307:163.
- [31] Prasad SV, McDevitt NT, Zabinski JS. *Wear* 1999;230:24.
- [32] Scharf TW, Prasad SV, Dugger MT, Kotula PG, Goeke RS, Grubbs RK. *Acta Mater* 2006;54:4731.
- [33] Bowden FP, Young JE. *Proc R Soc A* 1951;208:444.